# NOTE TO USERS

This reproduction is the best copy available.

UMI®

RICE UNIVERSITY

**The Cortical Mechanisms of Visual Stability**

By

**Erik Chihhung Chang**

A THESIS SUBMITTED IN PARTIAL FULFILLMENT
OF THE REQUIREMENT FOR THE DEGREE

**Doctor of Philosophy**

APPROVED, THESIS COMMITTEE:

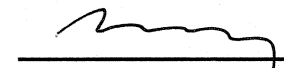

Tony Ro, Associate Professor, Chair
Psychology

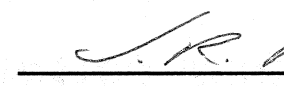

James Pomerantz, Professor
Psychology

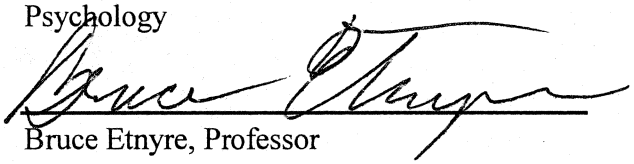

Bruce Etnyre, Professor
Kinesiology

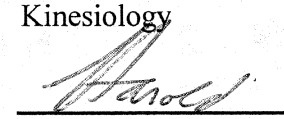

Harold Bedell, Professor
Optometry, University of Houston

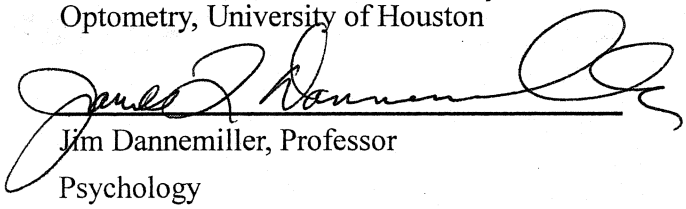

Jim Dannemiller, Professor
Psychology

HOUSTON, TEXAS
NOVEMBER 2004

UMI Number: 3168067

INFORMATION TO USERS

The quality of this reproduction is dependent upon the quality of the copy submitted. Broken or indistinct print, colored or poor quality illustrations and photographs, print bleed-through, substandard margins, and improper alignment can adversely affect reproduction.

In the unlikely event that the author did not send a complete manuscript and there are missing pages, these will be noted. Also, if unauthorized copyright material had to be removed, a note will indicate the deletion.

UMI®

UMI Microform 3168067

Copyright 2005 by ProQuest Information and Learning Company.

All rights reserved. This microform edition is protected against unauthorized copying under Title 17, United States Code.

ProQuest Information and Learning Company
300 North Zeeb Road
P.O. Box 1346
Ann Arbor, MI 48106-1346

November 2004

# ABSTRACT


The Cortical Mechanisms of Visual Stability

by

Erik Chihhung Chang

Visual stability refers to the apparent stability of the visual world given the displacement of retinal images induced by eye movements. Phenomenally visual stability involves both a stable representation of visual space and reduced sensitivities to perceptual changes at the temporal proximity of eye movements. While the psychophysics of the perisaccadic perceptual changes have been studied extensively, how visual stability is implemented in the human visual system remains to be explored. This dissertation examines the cortical mechanisms of perceptual stability in spatial vision with four series of experiments. Series 1 established a paradigm to induce saccadic suppression of displacement (SSD) and examined how the direction of saccades and displacements influence the strength of SSD. Series 2 examined the consequence of disrupting the posterior parietal cortex (PPC) with transcranial magnetic stimulation (TMS) in perceiving perisaccadic displacements. Series 3 examined psychophysical factors influencing perisaccadic mislocalization. Finally, series 4 explored how TMS on PPC impacts perisaccadic mislocalization. These experiments conjointly illustrate how the PPC contributes to a stable visuospatial perception during saccades.

ACKNOWLEDGEMENTS

I would like to express my sincere appreciation to all those who have helped me during the completion of this dissertation. I would especially like to thank my mentor, Dr. Tony Ro, for his guidance. I have learned a lot from his expertise and clear vision throughout my graduate study. I would also like to thank Dr. Harold Bedell, Dr. James Pomerantz, Dr. Jim Dannemiller, and Dr. Bruce Etnyre who served as members on the dissertation committee. Their invaluable feedbacks have not only improved the quality of the dissertation, but also broaden my vision on research. I am also grateful to Ashley Friggel, Sejal Shah, and Nancy Lin for their assistance in experiments. Finally, I would like to thank my parents and Denise Wu for their love and support.

Table of Contents

Abstract ..... ii

Acknowledgements ..... iii

Table of Contents ..... iv

List of Tables ..... viii

List of Figures ..... x

The cortical mechanisms of visual stability ..... 1

1. Introduction ..... 1

1.1. The Sources of Information ..... 1
1.2. The Processing of Information ..... 5
1.3. Summary ..... 7
1.4. Perceptual Changes Induced by Saccades ..... 8
1.4.1. Saccadic Suppression of Displacement ..... 9
1.4.2. Perisaccadic Mislocalization ..... 15
1.5. Neural Mechanisms of Visual Stability ..... 19
1.5.1. Primate single-unit recording ..... 21
1.5.2. Human patients' deficits in visuomotor coordination ..... 22
1.5.3. Application of TMS in the study of visual stability ..... 24

2. Overview ..... 27

2.1 General Methods ..... 30
2.1.1. Equipment ..... 30
2.2.2. Eye movement calibration and monitoring ..... 30

3. Factors Influencing the Strength of Saccadic Suppression of Displacement ..... 31

3.1. Experiment 1: Saccadic Suppression of Displacement in the Dimension Collinear with Saccades ..... 32

3.1.1. Participants ..... 32
3.1.2. Stimulus ..... 34
3.1.3. Procedures ..... 34
3.1.4. Data Analysis ..... 36

3.1.5. Results ..... 37
3.1.6. Discussion ..... 39
3.2. Experiment 2. Strength of SSD in Incongruent and Congruent Displacements 40
3.2.1 Participants ..... 41
3.2.2. Apparatus, Stimulus, and Procedures ..... 41
3.3.3. Results and Discussion ..... 41
3.3. Experiment 3. Saccadic Suppression of Displacement in the Dimension Orthogonal to Saccade Dimension ..... 42
3.3.1. Participants ..... 43
3.3.2. Stimulus ..... 43
3.3.3. Procedures ..... 45
3.3.4. Results of Horizontal Saccade/Vertical Displacement ..... 46
3.3.6 Discussion ..... 48
3.4. The Relationship between SSD and Perisaccadic Spatial Representation ..... 52
4. Locating the Cortical Areas Necessary for Perisaccadic Perceptual Changes with TMS ..... 58
4.1. Experiment 4: Influence of TMS on Saccadic Suppression of Displacement: the Round Coil ..... 59
4.1.1. Participants ..... 59
4.1.2. Apparatus ..... 60
4.1.3. Stimulus ..... 60
4.1.4. Procedures ..... 60
4.1.5. TMS administration ..... 61
4.1.6. Data Analysis ..... 64
4.1.7. Results ..... 64
4.1.8. Discussion ..... 67
4.2. Experiment 5: Influence of TMS on Saccadic Suppression of Displacement: the Figure-Eight Coil and MRI Guided Localization ..... 70
4.2.1. Participants ..... 70
4.2.2. Apparatus ..... 71
4.2.3. TMS administration ..... 71

4.2.4. Procedures ..... 73
4.2.5. Results ..... 76
4.2.6. Discussion ..... 76

5. Perisaccadic Mislocalization ..... 77

5.1 Experiment 6. Perisaccadic Mislocalization along the Saccade Direction ..... 77

5.1.1. Participants ..... 78
5.1.2. Apparatus and Stimulus ..... 78
5.1.3. Procedures ..... 80
5.1.4. Data Analysis ..... 81
5.1.5. Results of Horizontal saccades ..... 81
5.1.6. Results of Vertical Saccades ..... 82
5.1.7. Discussion ..... 85

5.2 Experiment 7. Perisaccadic Mislocalization of Low-contrast and High-Contrast Stimuli 87

5.2.1. Participants ..... 87
5.2.2. Apparatus and Stimulus ..... 87
5.2.3. Procedures ..... 89
5.2.4. Data Analysis ..... 90
5.2.5. Results ..... 92
5.2.6. Discussion ..... 94

6. Experiment 8. Influence of TMS on Perisaccadic Mislocalization ..... 95

6.1. Participants ..... 95
6.2. Apparatus, Stimulus, and Procedures ..... 96
6.3. Data Analysis ..... 97
6.4. Results ..... 97
6.5. Discussion ..... 101

7. General Discussion ..... 103

7.1. Contribution of the Current Dissertation ..... 103
7.2. Potential Neural Mechanisms Underlying Visual Stability in the PPC ..... 105
7.3. Future Directions ..... 107

References ..... 109

Appendix A. The Morrone et al. (1997) model of the relationship between real and

perceived spatial positions ..... 121

Appendix B. The normalized coordinates and compression index for perisaccadic localization ..... 124

Appendix C. The Precision of the Eye Tracker ..... 126

C.1. Precision measurement under with a model eye ..... 126

C.2. Precision measurement under experimental settings ..... 128

C.3. The Temporal Frequency Response and the Delay of the Eye Tracker .. 130

Appendix D. Mean Hit Rates and False Alarm Rates in Each Condition of Series 1 and 2 ..... 132

Appendix E. Mean Coordinates of Localization and Compression Index in Series 3 and 4 ..... 136

List of Tables


Table C1 The Output of the ASL 210 tracker and its Corresponding Values of Model Eye

Table C2 The Standard Deviation of Eye Position at Four Different Fixation Locations.

Table C3 The Mean of Eye Position at Four Different Fixation Locations

Table D1 Mean Hit Rates and False Alarms in Each Condition of Experiment 1.

Table D2 Mean Hit Rates and False Alarms in Each Condition of Experiment 2.

Table D3 Mean Hit Rates and False Alarms in Each Condition of Experiment 3.

Table D4 Mean Hit Rates and False Alarms in Each Condition of Experiment 4.

Table E1 Mean Coordinates of Perisaccadic Localization in Each Condition of Experiment 6 for Every Participant.

Table E2 Standard Deviation of Coordinates in Each Condition of Experiment 6 for Every Participant.

Table E3 Mean Compression Index in Each Condition of Experiment 6 for Every Participant.

Table E4 Mean Coordinates of Perisaccadic Localization in Each Condition of Experiment 7 for Every Participant.

Table E5 Standard Deviation of Coordinates in Each Condition of Experiment 7 for Every Participant.

Table E6 Mean Compression Index in Each Condition of Experiment 7 for Every Participant.

Table E7 Mean Response Coordinates of Perisaccadic Localization in Each

Condition of Experiment 8 for Every Participant.

Table E8 Standard Deviation of Response Coordinates in Each Condition of Experiment 8 for Every Participant.

Table E9 Mean Compression Index in Each Condition of Experiment 8 for Every Participant.

List of Figures


Figure 1 Configuration of stimuli and sequence of events in Experiment 1.

Figure 2 Corrected hit rates for congruent and incongruent displacements at each displacement onset in Experiment 1.

Figure 3 The configuration of stimuli in Experiment 3.

Figure 4 Corrected hit rates of vertical displacement detection during horizontal saccades in Experiment 3.

Figure 5 Corrected hit rates of different combinations of saccade and displacement dimensions from Experiment 1 and 3.

Figure 6 Ratio of congruent to incongruent displacement ($R_{CI}$) predicted by Morrone et al. (1997)'s model of perisaccadic mislocalization.

Figure 7 Illustration of the TMS round coil positions in Experiment 4.

Figure 8 The corrected hit rates for leftward and rightward saccades at each TMS onset time and stimulated site in Experiment 4.

Figure 9 The five landmarks used in 3D co-registration in Experiment 5.

Figure 10 Illustration of the TMS coil position and the lateral intraparietal sulcus in Experiment 5.

Figure 11 The 50% threshold of left/right discrimination in each condition of Experiment 5.

Figure 12 The sequence of events in a trial with rightward saccade in Experiment 6.

Figure 13 The mean normalized coordinates of localization responses in Experiment 6.

Figure 14 The compression index ($I_c$) at each probe position in Experiment 6.

Figure 15 Spatial arrangement of stimuli in Experiment 7.

Figure 16 The mean normalized coordinates of the localization responses in Experiment 7.

Figure 17 The mean compression index ($I_c$) at each probe position under different luminance conditions in Experiment 7.

Figure 18 The mean normalized coordinates of localization responses in Experiment 8.

Figure 19 The compression index at each TMS timing, probe position, and saccade direction in Experiment 8.

Figure 20 Illustration of the TMS-modulated strength of spatial compression in Experiment 8.

Figure A1 Ratio of the perceived size of congruent displacement to incongruent displacement ($R_{CI}$).

Figure B1 Definitions of the normalized distance ($N_r$) and the compression index ($I_c$).

Figure C1 Temporal response function of the ASL ET210 tracker.

# THE CORTICAL MECHANISMS OF VISUAL STABILITY

## 1. INTRODUCTION

Human eyes move frequently to bring the images of interesting targets into foveal vision, where the spatial resolution is the highest. These rapid eye movements, or saccades, shift retinal images without eliciting awareness of displacements. If the eyes were to remain still, the shift of retinal images would cause the perception of motion or displacement. This apparent stability of the visual world, which may be due to changes in perceptual sensitivities and unconscious transformation of spatial coordinates in the temporal vicinity of eye movements, has puzzled scientists for centuries. In the literature of visual stability, two essential questions have been identified: First, what are the differences between the information available during saccades and during fixation; Second, how is the available information processed by the visual system to maintain visual stability (Mackay, 1973; Bridgeman, Van der Hejiden, & Velichkovsky, 1994)?

### *1.1. The Sources of Information*

What are the differences between the information available to the visual system when only the external world moves and when only the eyes move? Since the late 19 century, scientists have considered two alternatives: retinal information (RI) and extraretinal eye position information (EEPI). Researchers supporting the RI theory of visual stability argue that structures in the retinal image are sufficient for differentiating passive from active image displacement (Gibson, 1966, pp. 256-259). Indeed, object movements in the surrounding environment do not cause the rigid displacement of the whole retinal image that occurs during every saccade. The displacement of the whole

retinal image, however, does not guarantee a stable percept of the visual world (von Helmholtz, 1866/1925). For example, pushing one's eye from the canthus displaces the eye and the whole retinal image passively, and one perceives image displacements *opposite from* the direction that the eye is pushed. Therefore, some sources of information outside the retina (i.e., EEPI) must be involved in forming stable perception of the spatial locations *only* when the eyes are voluntarily moved. Proponents of the EEPI argue that information about eye position in the orbit is used to counter the displacement of the retinal image during active changes of the eye position. Two sources of the EEPI have been suggested: the *inflow* from receptors in the extraocular muscles regarding the eye position in the orbit[1] (Sherrington, 1918; James, 1890/1950), and the *outflow* from the command ("effort of will") to turn the eyes (Helmholtz, 1925; von Holst & Mittelstaedt, 1971).

Some early observations not only make the EEPI theory more favorable than the RI theory, but also support the outflow version of the EEPI theory (Helmholtz, 1925; Bridgeman et al., 1994). First, when one's extraocular muscles are paralyzed and thus eye movements are almost impossible, attempts to shift gaze will not be successful; in this case one will experience the displacement of the visual world in the direction of the intended eye movement. Because theoretically the retinal image is stationary under this circumstance, the perception of displacement is unlikely due to the changes in retinal information. Furthermore, and again ideally, there should be no feedback from the proprioceptors in the extraocular muscles because the eyes cannot be turned. Thus the

---

[1] Receptors in the extraocular muscles include muscle spindles, Golgi tendon organs, and Palisade endings (Donaldson, 2000). Although there have been debates on whether receptors in extraocular muscles are indeed proprioceptors, accumulating evidence shows that they are used to provide information about the position about the position and movement of the eye in the orbit (Ono & Nakamizo, 1977; Gauthier, Nommay, & Vercher, 1990; Bridgeman & Stark, 1991; Donaldson, 2000).

inflow of information should not be the cause of the perceived displacement. In contrast, the outflow hypothesis accommodates the above observation quite well by assuming that the visual system compares the retinal image and the corollary discharge of the eye movement command to determine whether a displacement has occurred. When retinal images displace without the corresponding outflow signals from the eye movement command center, or when outflow signals are generated without the matching retinal image displacement, the visual stability of the world is disrupted.

Second, as mentioned in the example of pushing the eye, the visual world appears to displace against the direction of the passive movement. Now the retinal image is displaced, and there is feedback from the stretched muscles, but the displacement of the external world is perceived. This observation is against what the inflow hypothesis would predict: no displacement should have been perceived when both proprioceptive feedback and the displacement of retinal image exist. In contrast, the outflow hypothesis accounts for it easily, because the displacement of the retinal image cannot be corrected without the corollary discharge of the command to move the eyes.

Though the outflow model seems to appeal to scientists more than does the inflow model, the debate still continues with the reinterpretation of the classical observations and some new findings. The true picture may not only be a combined model of inflow and outflow information (e.g. Matin, 1982b), but also an integration of RI and EEPI.

The apparent displacement of the visual world in eye paralysis experiments may be due to the fact that only one eye is paralyzed (James, 1950/1890). When eye movements are attempted, the nonparalyzed eye, though occluded, can still move. The inflow signal from the nonparalyzed eye does not match the retinal image and could induce the unstable spatial perception reported by Helmholtz. Following the same logic, pushing one

eye does not produce inflowing signals from the other eye. The mismatch between the retinal image displacement in the pushed eye and the unchanged inflowing signal at the other eye might have led to the unstable spatial localization. It has been reported that the position of an occluded eye influences visual localization of a target viewed with the other eye (Ono & Nakamizo, 1977; Gauthier et al., 1990; Bridgeman & Stark, 1991). For example, Gauthier et al. (1990) showed that with one eye occluded and being pushed to offset 30 degree, the viewing eye made a 4-6 degree error in the pushed direction while localizing a visual target or judging "straight-ahead." Because the viewing eye did not move, and by Hering's law of equal innervation the efferent command should be equal (and zero in this situation) in both eyes, the biased localization perceived by the viewing eye must be attributed to the inflow information from the occluded eye.

Furthermore, when the extraocular musculatures are completely paralyzed so that no movement of the eyeball is possible, no visual movement or displacement of the visual field is perceived when the attempt is made to turn the eyes (e.g. Brindley, Goodwin, Kulikowski, & Leighton, 1976; Stevens et al., 1976). These observations, if valid, cast serious doubt on Helmholtz's outflow view because it relies heavily on the results of eye paresis. However, Matin (1986) raised the concern that these observations of totally paralyzed eye muscles were made without controlling the level of illumination or the presence of visual structure accompanying the stimuli. Studies on participants with their eye muscles partially paralyzed showed that whether the intention to move the eyes triggered the perception of displacement and bias perceived direction or not was largely influenced by the presence of a normally illuminated and structured visual environment (Matin, 1982b). It is very likely that in the studies of which participants' eye muscles were totally paralyzed, the lack of control in the level of illumination or the presence of

visual structure in the background gave participants visual cues to maintain visual stability. Therefore, it remains an empirical question whether people under total paresis of their eye muscles and in complete darkness can perceive the apparent displacement when attempting an eye movement, and surprisingly, this has not been reported.

Some researchers have suggested that both EEPI and RI are involved in maintaining visual stability (Volkmann, 1986; Bridgeman et al., 1994), and that the weight of contribution from each varies along the time course of the saccade. This conceptualization remains to be examined with behavioral and neurophysiological study.

### *1.2. The Processing of Information*

Independently of the source of information, another important issue is how the RI or EEPI are used to achieve visual stability. Theoretical approaches to this issue can be divided into three categories: the *cancellation* theory, the *take-into-account* theory, and the *saccadic target* theory. The three types of theories differ in their emphases on the importance of EEPI and in the ways pre- and post-saccadic retinal inputs are compared.

The cancellation theory assumes that the EEPI is subtracted from the retinal image displacements caused by eye movements, and that the effect of the retinal image displacement is "cancelled out" (Sperry, 1950; von Holst & Mittelstaedt, 1971). This is an intuitive solution to the processing of EEPI. Ideally, to achieve visual stability this way, the EEPI has to precisely match the displacement in RI during eye movements. In reality, the precision of saccades toward a visual target is much less effective than the precision of the spatial perception of that target (Mackay, 1973), which means the EEPI will not cancel the changes in RI perfectly, and visual stability cannot be maintained by cancellation alone. One possible way to maintain the cancellation hypothesis is to add the

assumption that the visual system will attribute the mismatch between RI and EEPI to errors in the oculomotor system when the error is not erratic. It has been shown that a 0.1 degree displacement of the whole visual field can be detected during fixation, whereas a 4 degree displacement of the visual field during a 12 degree saccade can go undetected (Beeler, 1967; Bridgeman, Hendry, & Stark, 1975; Stark, 1976 ). This phenomenon, *saccadic suppression of displacement* (SSD), might work together with the cancellation mechanism to maintain visual stability during eye movements. Matin (1974; 1982a) proposed a dual mechanisms of visual stability in which a primary mechanism uses saccade-contingent EEPI to compensate for the final displacement of the eye, and a second mechanism suppresses the perisaccadic visual perception. Beeler (1967) also postulated a cortical mechanism using the existence of efferent command signaling eye movements to discount the percept of retinal motion.

The take-into-account theories essentially argue that the visual system assumes the world is stable, unless the retinal input suggests otherwise. The postsaccadic retinal input is *evaluated* (Mackay, 1973) or *calibrated* (Bridgeman et al., 1994) with both the presaccadic retinal input and the extraretinal signals. Contrary to the precise EEPI required in the cancellation theories, evaluation and calibration involve flexible criteria in determining whether the visual world remains stable, which tolerates noisy EEPI. However, exactly how these processes are implemented is not clearly asserted in this type of theory.

The saccadic target theory contends that after the execution of a saccade, the visual system matches the pre- and postsaccadic scene within a limited spatiotemporal window (Deubel, Schneider, & Bridgeman, 1996; McConkie & Currie, 1996). Like the take-into-account theory, the saccadic target theory also assumes that the default of

spatial perception is set to be stable. If the saccadic target cannot be found within the local spatial area and shortly after the saccade, the assumption is not valid anymore and the displacement in the visual world is perceived. Currently this theory makes no use of EEPI, but the incorporation is possible (McConkie & Currie, 1996). Another important distinction between the saccadic target theory and the take-into-account theory is the scale of comparison between pre- and postsaccadic visual input. While the take-into-account theory suggests a *global* comparison that covers the whole retinal image, the saccadic target theory emphasizes a *local* comparison which is limited to regions adjacent to the saccadic target.

No matter what sources of information and mechanisms processing them are involved in visual stability, they are not perfect. For example, one can still notice the oscillation or "jump around" of the visual world when executing saccades of extremely large magnitude successively for a few seconds (i.e., voluntary oscillopsia, Enright, 1994b, a). The velocity of the extraretinal compensation is probably slower than the saccade velocity, as found in the studies of perisaccadic mislocalization (e.g., Honda, 1991b). However, the "displacement" observed in the circumstance of voluntary oscillopsia lack the vivid sensation elicited by the movement of external objects. Perhaps the duration between the displacement of retinal image and the subjective awareness of the displacement is long enough for the EEPI to function properly, or the post-saccadic clear view can mask the perceived displacement.

### *1.3. Summary*

Although the question of the sources of information and the question of the processing of information in achieving visual stability are theoretically independent of

each other, in practice "what is the process" is difficult to answer without first resolving "what is processed." This may be the reason why more empirical studies attempt to clarify whether EEPI or RI determines visual stability than to answer how the available information is used, and studies on the latter question are still at the level of speculation. With this background, the question regarding the source of information for visual stability is more suitable for investigation at the neurophysiological level. Perhaps when enough knowledge has been accumulated regarding where along the neural pathway visual stability occurs, researchers will have a better chance of determining what type of processing could take place in those identified neural networks. The following sections will concentrate on the behavioral tasks and neurophysiological studies that explored the sources of information available for visual stability.

### *1.4. Perceptual Changes Induced by Saccades*

Other than paralyzing the eye muscles or pushing the eye, the theoretical accounts for visual stability have also been evaluated by observing the perceptual consequences of saccades. Saccadic suppression and perisaccadic mislocalization are two extensively studied phenomena regarding saccade-induced perceptual changes. These two perisaccadic perceptual phenomena can be quantified with psychophysical methods, which is superior to the subjective reports in the eye paralysis and eye pushing studies. They also play an essential role in the experimental approach of this current dissertation. Over the past three decades, a number of studies have been carried out to specify the stimulus conditions inducing these two phenomena, and researchers have questioned whether saccades are necessary for mislocalization and suppression to occur. Studies addressing this question have also provided insights for the debate between the retinal

and extraretinal origin of visual stability.

### *1.4.1. Saccadic Suppression of Displacement*

In the temporal vicinity to a saccade, the visual system becomes less sensitive to some visual stimuli, especially to those defined by luminance or composed of low spatial frequency (Burr & Morrone, 2003; Ross, Morrone, Goldberg, & Burr, 2001a). *Saccadic suppression* refers to this saccade-induced threshold elevation. In the early 1960s, advances in techniques in eye tracking led to the first quantitative comparison of visual thresholds during saccades and during fixation (Volkmann, 1962) and the first measurement of the time-course of visual suppression during saccades (Latour, 1962). Researchers have observed elevation in thresholds of flash detection, contrast sensitivity, grating acuity, vernier acuity, recognition of color, recognition of words or letters, and stimulus displacement (see Volkmann, 1986; Matin, 1974 for reviews).

Saccadic suppression begins when visual stimuli are delivered approximately 100 ms prior to the onset of the saccade. For example, the sensitivity of detecting a light flash reaches its minimum at or a few milliseconds after the saccadic onset, and rises gradually back to the normal level approximately 100 ms beyond the end of the saccade. Human saccades larger than 5 degrees in amplitude normally take 20-30 ms plus about 2 ms for every degree of amplitude (Dodge & Cline, 1901; Robinson, 1964), whereas threshold luminance of detecting a light flash can be significantly affected for up to a total of 200 ms in the temporal vicinity of the saccade.

Among various types of saccade-induced threshold elevations, *saccadic suppression of displacement* (SSD) is distinct from all of the other types of suppression (i.e., saccadic suppression of visibility, SSV, Matin, 1974; Volkmann, 1986; Li & Matin,

1997; MacAskill, Jones, & Anderson, 2003). A vivid example of SSD is that one can not see his own eye movements in the mirror, but can easily perceive the saccade of another person's eyes while fixating upon them (Dodge, 1900). SSD reaches a level of 2.2 log unit (using data from Bridgeman et al., 1975 and )[2], whereas magnitudes of SSV are usually about 0.5 ~ 0.7 log units (Latour, 1962; Volkmann, Riggs, White, & Moore, 1978). SSD is stronger in darkness than in the well-lit environment, contrary to the effect of luminance on SSV (MacAskill et al., 2003).

Riggs, Merton, and Morton (1974) found reduction in sensitivity to electrically triggered visual phosphenes on the retina. Thus SSV cannot be attributed to optical or mechanical factors such as the Stile-Crawford effect (Castet, Sebastien, & Masson, 2001; Ross, Morrone, Goldberg, & Burr, 2001b). SSV may involved metacontrast masking (Deubel et al., 1996; Campbell & Wurtz, 1978; Breitmeyer, 1984; Breitmeyer & Ganz, 1976), whereas SSD may be primarily the manifestation of EEPI (Li & Matin, 1990b, 1997; Matin, 1982a). Bridgeman (1990) proposed that saccadic suppression of flashes is an epiphenomenon, resulting from the operation of the mechanisms in the visual system that suppress perception of image displacements during saccades. Although this view makes sense in the considerations of ecological optics because the physical change caused by saccades is a displacement rather than a flash, systematic testing of both SSD and SSV with comparable tasks is necessary to verify its validity.

The manifestation of SSD has been shown to depend on the visibility and duration of the visual target immediately after its displacement (Deubel et al., 1996; Li & Matin,

---

[2] Legge and Campbell showed that human displacement threshold is near 1.5 minutes (0.025 degree). Bridgeman et al. (1975) reported that displacements of 4 deg was detected at a chance level during saccades larger than 6 deg. Therefore, the threshold elevation during saccades is about 160-fold (2.2 log unit) to the threshold under fixation. It is thus unclear how Bridgeman and Fisher (1990) reached the estimation that SSD can reach a magnitude of 4 log unit.

1990b). Usually in the tasks examining SSD, a continuously visible target is abruptly displaced during a saccade, and remains in the displaced position afterwards either for a few hundred ms or until the judgment regarding the occurrence or direction of a displacement is made. To displace the target, it has to be erased from its original location and then presented in a new location. Between the erasure and reappearance of the visual target, a blanking duration ($T_{gap}$) can be inserted so that the target is hidden during $T_{gap}$. Interestingly, varying the length of $T_{gap}$ can modulate the threshold of displacement detection. It has been demonstrated that a $T_{gap}$ of 50 to 270 ms restores the sensitivity of displacement detection to near perfect level (Deubel et al., 1996). If the target is visible immediately after it is displaced (and also immediately after the end of the saccade), the sensitivity to displacement decreases and SSD is observed again.

Post-saccadic target blanking might restore the ability to detect displacement because the visual target in the pre-saccadic view was missing in the post-saccadic view, and the failure to find the visual target led the visual system to conclude that something must have changed (Deubel et al., 1996). After the displacement target reappears in a location, the longer it remains visible (up to 461 ms in their experiment), the better that displacement can be perceived (Li & Matin, 1990b). It could be that the detection of displacement is determined by a signal/noise ratio, with the EEPI contributing to the noise. The post-saccadic EEPI is less noisy than that during saccades, and prolonging the duration of the displacement target in the post-saccadic view allows the decision to be made according to the less noisy signals. Alternatively, a subject in the SSD task may be doing two very different tasks in the blanking vs. the no-blanking conditions. In the condition with post-saccadic blanking, because the displacement target is only seen for a short period of time, one may rely on the transient intrasaccadic percept to make the

judgment. On the contrary, in the condition where the target persists until the post-saccade period, the participant may judge by comparing presaccadic and postsaccadic direction of the target. Perhaps the poor accuracy in direction judgment results in the stronger SSD in the no-blanking condition.

An intriguing (but usually regarded as secondary) finding in the SSD literature is the relationship between the directions of saccades and target displacement. The majority of studies reported that suppression is omnidirectional (Beeler, 1967; Bridgeman et al., 1975; Mack, Fendrich, & Pleune, 1978; Stark, 1976). That is, target displacements orthogonal to the saccadic direction result in the same threshold increment as do those parallel to the saccadic direction. In addition, there seems to be some extent of agreement that displacements in the same direction (*congruent*) as the saccade result in the same magnitude of suppression as displacements in the opposite direction (*incongruent*) to the saccade (Bridgeman et al., 1975; Bridgeman, Lewis, Heit, & Nagle, 1979; Stark, 1976; Bridgeman & Fisher, 1990).

However, Whipple and Wallach (1978) reported that the sensitivity for detecting the displacement of a ring subtending 7° was greater when the displacement direction was parallel than when it was orthogonal to the saccadic direction. However, after reanalyzing the data by calculating the distance of displacement at the edge instead of the center of the ring, Bridgeman and Stark (1979) concluded that Whipple and Wallach's analysis overestimated the distance of orthogonal displacement and thus underestimated the threshold elevation under the orthogonal condition. After the correction for displacement distance, Bridgeman and Stark argued that Whipple and Wallach's results actually showed omnidirectional suppression of displacement.

There are other exceptions showing asymmetric suppression induced by

displacements congruent or incongruent with saccadic direction. McConkie and Currie (1996) examined the probability of detecting the displacement of natural, full-color pictures during saccades. Their analysis showed that congruent displacements had smaller threshold distance than incongruent displacements, with displacement length and saccade direction held constant. However, Macknik, Fisher, and Bridgeman (1991) showed just the opposite results with flickered stimuli: sensitivity to incongruent displacement was about twice as great as for congruent displacement (also see Anand & Bridgeman, 2002a for a similar directional effect revealed by chromatic stimuli). These inconsistent findings indicate that whether saccadic suppression is directional or not may depend on the characteristics of the stimuli. The task-dependent nature of the directional asymmetry could be due to differences in sensitivity or criterion. Thus, examining the conditions when the directional suppression can be found and in which way the suppression is asymmetric may be informative as to the origin of saccadic suppression.

Theories on the origin of saccadic suppression imply that it may be tightly linked to visual stability of the subjective perception of the visual world during saccades. The consensus on visual stability is that EEPI, whether originating from inflow or outflow, is integrated with the retinal signals to achieve a stable percept of space. Similarly, researchers have suggested that saccadic suppression cannot be accounted for purely by visual stimuli projected on the retina. Holt (1903) suggested that vision is "blanked out" during saccades due to a "central anesthesia" triggered by the neural impulses from the extraocular muscles. His view can be regarded as the "inflow" model of saccadic suppression. Dodge (1900; 1905) proposed that both a central inhibitory process and peripheral, retinally originating processes contribute to visual suppression during saccades. His idea can be regarded as a hybrid of the inflow and outflow model. The

retinal process Dodge proposed anticipated more recent explanations of saccadic suppression as the consequence of visual masking (Matin, 1974; Campbell & Wurtz, 1978; Matin, Clymer, & Matin, 1972). Woodworth (1906) offered the most parsimonious model, which attributed saccadic suppression purely to differences in retinal stimulation on the moving and the fixating eye. His view of the retinal origin is consistent with Gibson's ecological view of visual perception (Gibson, 1966), which proposed that perceptual cues in the external environment rather than the constructive processes in the brain are the building blocks of perception. It has also been suggested that the high velocities of saccades produced spatiotemporal contrasts below threshold so that sensitivity to various visual stimuli decreased during saccades (Kelly, 1979; but see Garcia Perez & Peli, 2001). However, this view does not reconcile with the finding that suppression induced by "simulated" saccades (moving the retinal image in a similar fashion as that during saccades with the aid of projection devices) was not as strong as the ordinary saccadic suppression, and suppression lasted for a shorter period for simulated saccades (Diamond, Ross, & Morrone, 2000). Differences between real and simulated saccades in the magnitude and time course of suppression indicate that saccadic suppression has an extraretinal component.

Studies presenting perisaccadic stimulus on a Ganzfeld also cast doubt on the masking account (Riggs et al., 1974; Volkmann et al., 1978; Manning & Riggs, 1984). A Ganzfeld is a background without any visual reference, such that no matter where the eyes fixate on the Ganzfeld, the view is always the same. Because saccadic suppression exists on a Ganzfield, no visual contours could have masked the perisaccadic stimulus and resulted in suppression.

From the discussion of visual stability, we know that EEPI is involved in

countering changes of retinal image induced by eye movements, which maintains the representation of the environmental spatial coordinate constant. Now we also know that EEPI is involved in perisaccadic changes of perceptual sensitivities, especially for detection of displacement. One would naturally ask if these two phenomena are related, and whether the EEPI involved in nullifying the changes in retinocentric coordinate is the same EEPI involved in modulating perceptual sensitivity.

### *1.4.2. Perisaccadic Mislocalization*

Another perceptual consequence of saccades, which may relate to the suppression of displacement, is the systematic bias in localizing visual stimuli (Matin, 1965; Matin, Matin, & Pearce, 1969; Matin, Matin, & Pola, 1970; Honda, 1989, 1991a, b, 1993; Ross, Morrone, & Burr, 1997; Lappe, Awater, & Krekelberg, 2000; Kaiser & Lappe, 2004). The time course of the change in apparent position of flashed targets is similar to that of saccadic suppression (e.g. Honda, 1991b; Ross et al., 1997). For example, Honda (1991b) showed that perceived location of a dot flash shifted in the saccade direction before the eye movement started; after the saccade onset, the bias reversed such that its perceived location shift opposite the saccade direction. This pattern holds for both vertical and horizontal eye movements, and the maximum bias is about half of the size of the saccade (cf. Bridgeman, 1995). The anticipatory shifts of the spatial localization seem to compensate for the displacement of the retinal image caused by saccades, and partially cancel the "lag behind" of the retinal image.

However, the perisaccadic mislocalization is not always biased in the saccadic direction. Burr and Morrone's group demonstrated a presaccadic "compression of space" *toward the saccadic target*, where flashes more eccentric than the saccadic target are

mislocalized *away from* the saccade direction, whereas flashes between the initial fixation point and the saccadic target are mislocalized *toward* the saccade direction (Morrone, Ross, & Burr, 1997; Ross et al., 1997). The compression is powerful enough to align two or four non-collinear vertical bars to a single vertical bar and/or misalign two collinear bars presented with a brief temporal separation (75 ms) before saccade onset.

Lappe, Awater, and Krekelberg (2000) examined how experimental settings such as illumination and the structure of the background influence the direction of mislocalization. They found that the locations in the visual space were compressed toward the saccade target only when visual references were available. In complete darkness, the mislocalization was always toward the saccadic direction (i.e., a location more eccentric than the saccadic target would be perceived as even more eccentric during a saccade). The same factors may contribute to the inconsistent directional effects in saccadic suppression of displacement. For example, when the target and background were complex pictures, target displacements congruent with the saccadic direction were detected more frequently (McConkie & Currie, 1996), but when the stimuli were small and simple and the background was featureless, displacements incongruent with the saccadic direction were detected more frequently (Macknik et al., 1991; Bridgeman & Macknik, 1995; Anand & Bridgeman, 2002a). Because the viewing conditions determine the available coordinate systems (e.g., allocentric[3] vs. egocentric), saccadic suppression of displacement under different viewing and stimuli conditions might be generated from different spatial representations.

Similar to the issue of visual stability and saccadic suppression, there is a debate

---

[3] An "allocentric" spatial coordinate refers to the spatial representation independent of the perceiver's perspective. It is sometimes used synonymously with "exocentric" or "geocentric."

whether the perisaccadic mislocalization has a central or retinal origin. By projecting images on the retina with a mirror system that can be rotated at the speed of saccades, it is possible to create a viewing condition similar to a saccade while the eyes remain still. When locating a position under these "simulated saccades," either the time course and magnitude of mislocalization were different from those in real saccades (Honda, 1995; Morrone et al., 1997), or the mislocalization was not observed (Cai, Pouget, Schlag Ray, & Schlag, 1997). More importantly, the spatial compression around the saccadic target is not evident under simulated saccades (Morrone et al., 1997). Apparently, the rapid movement of the retinal image itself is not sufficient to produce the perisaccadic spatial compression.

The mislocalization of briefly flashed targets is usually used to characterize the perisaccadic change of EEPI (Matin et al., 1969; Matin et al., 1970; Miller, 1996; Dassonville, Schlag, & Schlag Rey, 1992; Honda, 1991b). Changes in EEPI are estimated by subtracting localization response with the retinal position of the flash. However, this estimation is only accurate assuming the retinal responses to the flash are not delayed and do not extend over a relatively long period of time (like a few milliseconds). These two assumptions are hardly true (Pola & Wyatt, 2002; Pola, 2004), especially the latter one. The temporal impulse response to brief flash can persist for as long as several hundred milliseconds (Matin & Bowen, 1976; Bowen, Pola, & Matin, 1974). Accurate estimation of EEPI should consider the interaction between the persistence of the retinal response and the EEPI. Pola (2004) simulated perisaccadic mislocalization with models incorporating retinal persistence and found that the actual EEPI may only start changing after saccade onset and at a rate as quickly as the saccade. Conventional observations of anticipatory, slow changing EEPI could thus be an artifact of using target flash and

ignoring the temporal impulse response of the retina.

Another problem with the localization studies is how participants perceived and localized targets. In those studies, participants either located the position of the target flashed around the time of saccade by moving a visible landmark to indicate that location after they finished the saccade, or by reporting the number corresponding to their perceived location of the target on a ruler presented before and/or after the saccade (Ross et al., 1997; Morrone et al., 1997). Because perception of the peripheral positions is also compressed toward the fixation point (i.e., foveal bias, Muesseler, Van Der Heijden, Mahmud, Deubel, & Ertsey, 1999; Sheth & Shimojo, 2001; but see Mapp, Barbeito, Bedell, & Ono, 1989)[4], it is possible that the spatial compression toward the saccadic target may not only be caused by saccade, but also by the post-saccade visual perception when participants reported the location while maintaining fixation on the saccadic target. Furthermore, studies using manual pointing (Miller, 1996) or hammering (Hansen & Skavenski, 1985) as the localization response showed results different from studies using verbal reports or cursor. Miller (1996) showed that pointing errors were in the direction opposite the saccade direction and were maximal near the end of the saccade. Hansen and Skavenski (1985) found that striking the target with a hammer was fairly accurate near the time of saccades. The spatial compression toward the saccade target may thus result from the way perception was probed.

This criticism may be defended with two additional observations: First, the spatial compression only occurs for a target presented along the dimension of saccadic direction (Morrone et al., 1997). If the saccade-induced compression were due to the post-saccade

---

[4] Foveal bias is the tendency to estimate the position of a target as being closer to the foveal than its physical eccentricity. The magnitude of the bias is typically 10~30% of the target eccentricity (e.g. O'Regan, 1984; Sheth & Shimojo, 2001).

compression toward the fixation, targets along any dimension should be equally compressed. Second, the spatial compression toward the saccadic target does not occur for the simulated saccades (Morrone et al., 1997). In simulated saccades, the image of the whole stimulus display was shifted by rotating a mirror projecting the stimuli into the participant's field of view. The participant saw a saccade-like image displacement without making saccades. If the post-saccade compression toward the fixation accounted for the saccade-induced compression of space, the same pattern of compression would be observed regardless of whether the saccade is real or simulated.

Results from single-unit recording of neuronal activity in monkeys also support a central origin of mislocalization. Krekelberg, Kubischik, Hoffmann, and Bremmer (2003) showed that neurons in the medial temporal area (MT) and the medial superior temporal area (MST)[5] accurately represented the position of flashed bars retinotopically during fixation. However, this representation was disturbed perisaccadically and the alterations in these neurons' pattern of activity corresponded to the mislocalization found in human psychophysical studies. The fact that this disturbance starts *before* the saccade onset suggests that it is not caused by retinal signals.

### *1.5. Neural Mechanisms of Visual Stability*

Saccade-related activities occur in quite a few different brain regions such as frontal eye field (FEF) (Umeno & Goldberg, 1997), posterior parietal cortex (Duhamel, Colby, & Goldberg, 1992; Goldberg, Colby, & Duhamel, 1990; Batista, Buneo, Snyder, & Andersen, 1999), superior colliculus (Walker, Fitzgibbon, & Goldberg, 1995), and in

---

[5] Some neurons in the MT and MST of Rhesus monkeys have also been shown to change their preferred directions of motions during saccades, which is thought to suppress the motion percepts (Thiele, Henning, Kubischik, & Hoffmann, 2002).

earlier stages in the extrastriate cortex such as V4, V3, and V4 (Nakamura & Colby, 2002) and even V1 (Snodderly, Kagan, & Gur, 2001; Yu & Lee, 2000) or LGN (Reppas, Usrey, & Reid, 2002). Localizing the neural components that determine or correlated with perisaccadic perceptual changes, researchers may be able to distinguish the relative contributions of RI and EEPI in visual stability.

The neurophysiological implementation of the extraretinal signal can be conceptualized as the internal information generated as a correlate, or *corollary discharge*, of the neuronal movement command (Sperry, 1950; Sommer & Wurtz, 2002). The thalamus and cerebral cortex have been shown to be critical for using corollary discharge information (Duhamel, Goldberg, & Fitzgibbon, 1992; Gaymard, Rivaud, & Pierrotdeseilligny, 1994; Heide, Blankenburg, Zimmermann, & Kompf, 1995). Sommer and Wurtz (2002) demonstrated that a pathway going from the intermediate layer of the superior colliculus to the mediodorsal thalamus and finally reaching the frontal eye field (FEF)[6] carried corollary discharge. When experimenter inactivated the relay neurons in the mediodorsal thalamus by injecting muscimol (a γ-aminobutyric acid type A [$GABA_A$] agonist that inhibits neuron cell bodies) unilaterally in the mediodorsal thalamus, monkeys made the second saccade in a double-step paradigm as if the first saccade did not happen. This confirms the existence of EEPI in the visual system. The parietal cortex connects with both the frontal eye field and the superior colliculus (Schiller & Tehovnik, 2001), and may access the EEPI via these connections.

Other cortical neuronal recordings on monkeys (Duhamel, Colby et al., 1992; Kusunoki & Goldberg, 2003) and studies on normal human subjects (Donkelaar & Muri,

---

[6] Frontal eye field (FEF) locates at the medial bank of precentral gyrus and has been demonstrated to control voluntary saccades.

2001) or patients (Heide et al., 1995; Heide & Kompf, 1998) also pinpointed the *posterior parietal cortex* (PPC) as the site which maintained stable visuomotor coordinations by integrating retinal and extraretinal information around the time of saccades. Mechanisms maintaining stable visuomotor coordination may also contribute to the subjective stability of the visual world by modulating perisaccadic spatial perception (Sommer & Wurtz, 2002; Ross et al., 2001a).

### *1.5.1. Primate single-unit recording*

Given the crucial role of extraretinal information in maintaining visual stability, it is reasonable to assume that the neural substrate dealing with visual stability should have access to both retinal and extraretinal information. This kind of capacity has been found in the superior colliculus (Mays & Sparks, 1980), the FEFs (Goldberg & Bruce, 1990), the supplementary motor area (Schlag, Schlag-Rey, & Pigarev, 1990), and the posterior parietal cortex of monkeys (Andersen, Essick, & Siegel, 1985; Andersen & Gnadt, 1989; Goldberg et al., 1990). Of particular interest is the posterior parietal cortex, in which studies of both monkeys and humans have strongly suggested its possible role in visual stability.

From the recordings of neurons in the PPC, researchers have divided the PPC of macaque monkeys into several distinct but strongly interconnected cortical areas including area 7a, area 7b, the lateral intraparietal area (LIP), and the ventral intraparietal area (VIP). Among these subdivisions of the PPC, the LIP is one of the best understood areas. It receives strong direct projections from extrastriate visual areas and projects to areas in the cortex and brain stem which influence saccadic eye movements (Lynch, Graybiel, & Lobeck, 1985; Blatt, Anderson, & Stoner, 1990). The LIP also receives a

convergence of eye position and visual signals (Andersen & Mountcastle, 1983; Andersen et al., 1985). This convergence not only provides LIP cells with retinal receptive fields that have visual responses modulated by eye position, but also makes them capable of making predictive remapping of their post-saccadic receptive fields in the space *before* the saccade starts.

For example, Duhamel, Colby, and Goldberg (1992) demonstrated that some cells in the LIP of the macaque monkey started to respond to stimuli presented in the postsaccadic receptive fields 80 ms before the onset of the impending saccade. Presenting the stimuli at the same spatial location without making saccades or making saccades toward the same spatial location without presenting the stimuli there did not trigger these cells. These cells only responded when the monkey intended to make a saccade that would bring the stimulus into their fixation receptive fields (also see Kusunoki & Goldberg, 2003). The predictive remapping of these LIP cells suggested that the efferent copy is used to calculate the postsaccadic locations before the saccades are executed.

There is no way to know the monkey's subjective interpretation of the outputs from the remapping LIP cells. But a reasonable guess is that since these cells respond to both current and future receptive fields before the eye starts moving, the monkey may not have perceived the abrupt shift of position in the retinal image during a saccade.

### *1.5.2. Human patients' deficits in visuomotor coordination*

Patients with frontoparietal or parietal lesions show interesting patterns of *double-step saccades* that hint a parietal locus of processing extraretinal signals in the human brain. Duhamel, Goldberg, and Fitzgibbon (1992) tested a patient who had a lesion in the right frontal and parietal lobes with single and double-step saccade tasks.

The patient's lesions involved the right frontal eye field and a region of the right intraparietal sulcus. In the single saccade task, a target was flashed briefly either in the right or left hemifield, and the participant had to make one saccade to look at where the target was. In the double-step saccade task, two targets were flashed consecutively either in the same or in different hemifields but both disappeared before the initiation of saccades. The patient had to shift her gaze to look at where the targets were in the same order as how those two targets were presented. The patient's single saccades into the left (contralesional) hemifield had longer latencies and were hypometric relative to those into the right (ipsilateral) hemifield. The patient's performance in the double-step saccade task was normal when the two targets were presented in the right-left sequence, but she never succeeded in making the second saccade in the left-right sequence. Note that in the case of the left-right sequence, the second target was shown in her normal hemifield where she was capable of shifting her gaze in the single saccade task. Also, when the two targets were presented for 500 ms, allowing enough time for her to execute the first saccade before the onset of the second stimulus, the performance was normal. Although this study cannot exclude the possibility that when two stimuli were presented successively and disappeared before the first saccade started, the patient might have not perceived the second target in the left-right sequence due to some peculiar attentional deficit, the results still suggest that the fronto-parietal pathway was crucial for updating the spatial representations after making saccades into the contralateral space.

Heide, Blankenburg, Zimmermann, and Kömpf (1995) reported similar deficits in patients with lesions confined within the left or right posterior parietal cortex. In that study, the researchers compared performance in double-step saccade tasks among patients with unilateral lesions in the posterior parietal cortex, prefrontal cortex, right frontal eye

field, and the left somatosensory cortex. A group of normal control subjects was also tested. When there was retino-spatial dissonance (the second saccadic target had disappeared before the end of the first saccade), the parietal patients could not compensate for the second saccade in the ipsilesional direction after making a relatively normal first saccade in the contralesional direction. However, when there was no retino-spatial dissonance (i.e., the second target was still visible when the first saccade ended), the parietal patients performed normally on both the first and second saccades. In contrast, patients with lesions in the prefrontal cortex tended to abort the second saccade when it had to cross the vertical meridian, independent of the hemifield where the second target had appeared and independent of retino-spatial dissonance. Patients with lesions in the frontal eye field tended to make the double-step saccades in the wrong temporal order. In summary, the posterior parietal patients failed to update the target positions in the retinocentric coordinate, whereas the frontal patients had a problem maintaining the memory trace of the 2$^{nd}$ target during the processing time of the 1$^{st}$ saccade (Heide et al., 1995; see Funahashi, Bruce, & Goldman-Rakic, 1993, for the role of prefrontal cortex in spatial working memory).

### *1.5.3. Application of TMS in the study of visual stability*

From the anatomical connections of the parietal cortex with other brain regions, the predictive remapping in monkeys' LIP, and patients' deficits in the double-step saccade, it is reasonable to hypothesize that the PPC is involved in the processing of extraretinal information. Transcranial magnetic stimulation (TMS) is an ideal tool to test this hypothesis in the normal human population. TMS induces transient or repetitive electrical currents in the cortex, which can be regarded as introducing noise into the neural system

and thus disrupting the normal function of the stimulated region. The precise timing of single-pulse TMS also grants researchers the ability to map the time course of the neural processing of the behavior under investigation. With the appropriate design and control conditions, it is possible to derive a causal relationship between a brain region and a behavioral task with TMS that is not attainable with neuroimaging techniques (Robertson, Theoret, & Pascual-Leone, 2003; Walsh & Cowey, 2000).

A study testing normal human subjects on a double-step saccade task with single-pulse TMS applied to the PPC[7] supported the speculation that this region was involved in the processing of extraretinal information (Donkelaar & Muri, 2001). In saccade tasks, the magnitude of saccades always varied. When making double-step saccades, the magnitude of the second saccade typically compensates for the variation in the magnitude of the first saccade. For example, when the two saccades in the double-step paradigm are going in opposite directions and the first saccade undershoots the target, the magnitude of the second saccade should also be shorter than it would have been so that it lands on the second saccadic target. A linear relationship with a positive slope exists between the magnitudes of the two successive saccades if the spatial representation of the second saccadic target is updated after the execution of the first saccade. A slope of one indicates perfect updating of the head-centered spatial representation, and a slope of zero indicates the second saccade does not take the first saccade into account at all.

It was shown that when the TMS was administered to the right PPC 150 ms after the first saccade (i.e., immediately before the second saccade), the slope was significantly

---

[7] In this study and the majority of TMS studies on the PPC by Muri's group, the PPC is defined as 3 cm lateral and 3 cm posterior to the vertex, corresponding to the P4 location of the international 10-20 system.

reduced for saccades made in a left-right sequence, whereas when TMS was administered simultaneously with or 100 ms after the onset of the first saccade, the slope values were the same as those generated when no TMS was given, regardless of the sequence. The lack of compensation for the first saccade was most obvious when the TMS onset time was shorter than 116 ms before the onset of the second saccade. Therefore, TMS may disrupt the integration of retinal and extraretinal information and thus reduce the extent to which craniotopical (head-centered) coding of the target was possible (Donkelaar & Muri, 2001).

Given the PPC's role in the integration of retinal and extraretinal information for craniotopic coding, it is reasonable to speculate that the subjective stability of visual space may also be processed in the same area. This hypothesis can be examined by applying TMS to the PPC at various time points prior to saccade onset to determine how it influences performance on perisaccadic perceptual tasks (i.e., displacement detection and localization). Although TMS should interrupt processes for maintaining a stable percept of the visual world, it is not clear, whether the interruption enhances or compromises the abilities to localize targets and to detect displacement presented during saccades. If the perceptual stability is maintained by processes inhibiting cortical activities (Kleiser & Skrandies, 2000; Anagnostou, Kleiser, & Skrandies, 2000; Bodis-Wollner et al., 1997), abolishing the inhibition may result in higher sensitivity to displacement and precision of localization. Alternatively, if perceptual stability involves processes compensating image displacement with EEPI, introducing noises into those processes may disrupt spatial representation and thus result in compromised performance on displacement detection and localization.

# 2. OVERVIEW

In our subjective awareness, we do not usually perceive changes in spatial coordinates due to image displacement caused purely by saccades. This visual stability keeps our subjective interpretation of the visual environment from chaos. We are also able to make a saccade toward two target locations successively in the darkness, given that the viewing directions differ between the time of perceiving that target and the time of initiating the saccade toward it (Hallett & Lightstone, 1976; Honda, 1997)[8]. The precise motor programming and execution of double-step saccades in darkness shows that the oculomotor system utilizes extraretinal information to calculate where the eyes are going. It has been shown that failure to take the eye movement factor into account may result in false perception of object motion during eye movements (Haarmeier, Thier, Repnow, & Petersen, 1997). It is likely that oculomotor programming and the subjective stability of the visual world share the same information about eye position, and perhaps the same cortical mechanisms process this information.

The normal performance in the double-saccade task needs the updating of spatial coordinates after the execution of the first saccade. The PPC has been suggested to be necessary for this updating process (Duhamel, Goldberg et al., 1992; Heide et al., 1995; Heide & Kompf, 1998; Donkelaar & Muri, 2001). Though these neurophysiological studies demonstrated the importance of PPC for precise double-step saccades, they did not address whether the PPC is crucial for the subjective stability of the visual world in the temporal vicinity of saccades.

The primary goal of the current project is to explore the cortical mechanisms of

---

[8] The ability to carry out double-step saccade based on body-centered representation emerged as early as 6-month-old in human (Gilmore & Johnson, 1997a, b).

perisaccadic perceptual changes. With a "virtual lesion" induced by TMS, the perisaccadic perceptual changes can be observed in normal human subjects when the processing of the PPC or another cortical site is disrupted. If TMS on a given cortical site changes the sensitivity of displacement detection or the pattern of mislocalization during saccades, that site is likely to be involved in maintaining visual stability.

Another goal of this project is to investigate the potential linkage between mislocalization and SSD. It has been suggested that perisaccadic mislocalization is due to the remapping of the spatial representation in the proximity of saccades. If the detection of displacement is related to the representation of spatial locations, it may also be subject to the remapping process, and thus be related to perisaccadic mislocalization. Models describing the compression of space toward the saccadic target (Morrone et al., 1997; Kaiser & Lappe, 2004; Niemeier, Crawford, & Tweed, 2003) may also account for the patterns of SSD. More specifically, the extent of SSD may be predicted by the degree of spatial compression, with displacement occurring in the spatial locations that are more strongly compressed being detected less frequently. The rest of this section summarizes four series of experiments conducted to fulfill the purposes stated above.

The first series of experiments established the parameters for SSD. The spatial and temporal parameters of the stimulus inducing SSD optimally are systematically examined. Of particular interest is how the relationship between directions of saccades and displacements (i.e., congruent vs. incongruent) influences the sensitivity to displacement detection because of the inconsistent reports in the literature and its potential impact on theory of visual stability. In addition, the sensitivity to displacements orthogonal to the saccade direction was also examined to understand whether suppression of displacement is omnidirectional or not.

The second series of experiments examined the potential cortical sites of SSD, most likely the PPC, with single-pulse TMS. The PPC has been implicated in various attentional, perceptual, and motoric tasks that require transformation and integration of different reference frames of space. With respect to the double-step saccades, the PPC has been shown to be crucial for the precise metrics of the second saccades (Donkelaar & Muri, 2001; Heide et al., 1995; Heide & Kompf, 1998). In contrast, the frontal cortex has been shown to be necessary for memory and decision making. As for the double-step saccades, the frontal cortex is crucial for the correct order of the double-step saccade (Heide et al., 1995). In other words, the PPC could be in charge of updating the spatial representation which is the key to precise and successive saccades, whereas the frontal cortex is responsible for memorizing the order of executing a sequence of saccades. Because the central interest of this dissertation is whether the updating of spatial representation in the temporal vicinity of saccades also contributes to perisaccadic perceptual changes, it is reasonable to hold a working hypothesis that the PPC plays a more critical role than does the frontal cortex in modulating saccadic suppression of displacement and perisaccadic mislocalization.

The third series of experiments investigated perisaccadic mislocalization and its potential relationship to SSD (c.f. Matsumiya & Uchikawa, 2003). As mentioned in previous section, the perisaccadic compression of the space could truncate the perceived size of displacement during saccade and the "shrinkage" of displacement reduces the sensitivity. Magnetic stimulation was also applied when the participant performed a perisaccadic localization task to examine the cortical site of mislocalization.

## *2.1 General Methods*

The equipment and procedure common to all four series of experiments are described here, whereas those specific to an individual experiment will be introduced in its own 'Apparatus' or 'Procedure' sections.

### *2.1.1. Equipment*

Stimuli were generated by an IBM compatible personal computer and presented on a 17" Sony Trinitron Multiscan 220GS CRT monitor operating at a 60Hz or 120Hz vertical retrace rate. The CRT monitor was surrounded by a black cardboard to reduce the visual cues available. The viewing distance was either 57 or 28.5 cm. The responses were made by pressing buttons on a Microsoft compatible computer mouse and were registered by the same PC. The generation of stimuli and the control of experimental procedures were programmed with Borland C under the 16-bit MSDOS environment by the author.

An Applied Science Laboratories (Bedford, Massachusetts) Eye-Trac 210, which consists of one infrared emitting diode and two photo diodes, was used to measure the horizontal or vertical eye movements of the participant's left eye with precision of approximately 1 degree (see Appendix C for details of precision measurement).

### *2.2.2. Eye movement calibration and monitoring*

The eye-tracking device was calibrated at the beginning of every experimental session with three positions on the horizontal meridian located at the center, 10 deg in the left visual field, and 10 deg in the right visual field. A central fixation cross and two black squares (1 × 1 deg) symmetrically positioned in each visual field and on the horizontal meridian served as the calibration points. After the experiment started, the experimenter

paused the experiment to calibrate the eye tracker whenever the reading of the initial fixation deviated from the ideal value by more than 1 degree.

The signal from the eye tracker was recorded by the PC via the LPT port with a sampling rate of 1000Hz and a response delay of 4 ms (See Appendix C for its temporal response function). The trajectory of the eye was immediately resampled at a rate of 250 Hz to filter out the high frequency noise, and was then subjected to a 10-ms moving window to extract the eye velocity. The onset of a saccade was defined as the time when eye velocity just exceeded 30°/s. Thus, there was an approximately 14 ms delay between the detected and the real saccade onset. When the computer monitor operated at a 60Hz of vertical retrace rate (16.7 ms per frame), theoretically it took 22.4 (i.e., 14 + 16.7/2) ms averagely for a stimulus to be presented when it was time-locked to the saccade onset.

## 3. FACTORS INFLUENCING THE STRENGTH OF SACCADIC SUPPRESSION OF DISPLACEMENT

As discussed in the introduction, SSD is distinct from other types of altered visual sensitivities during saccades. In the literature it is clear that SSD is subject to the size of saccades (Stark, 1976; Bridgeman et al., 1975; Li & Matin, 1990a), the background luminance and configuration (MacAskill et al., 2003), the retinal eccentricity of the displacement (Bridgeman & Fisher, 1990), and post-saccadic duration of the displaced image . The mixed report on the relationship between saccade direction and displacement direction in SSD (Bridgeman & Stark, 1979; Mack, 1970; Stark, 1976; Whipple & Wallach, 1978; McConkie & Currie, 1996; Li & Matin, 1997), however, begs further investigation.

## 3.1. Experiment 1: Saccadic Suppression of Displacement in the Dimension Collinear with Saccades

The primary purpose of this experiment is to establish the paradigm for following experiments. Another purpose was to examine SSD in a well-illuminated environment where the visual cues were not removed from the visual field: the rim of the CRT, the sensor set of the eye tracker, and the participant's own nasal face contour were all visible. The visual cues can either serve as reference points to help displacement detection, or can serve as visual masks to impair the detection of displacement (Matin et al., 1972; Campbell & Wurtz, 1978; Mackay, 1970, 1973). The hit rate of displacement detection may be higher or lower than that obtained in the absence of visual cues (e.g., in the Ganzfeld or complete darkness).

### *3.1.1. Participants*

After informed consent, following the guidelines approved by the institutional review board of Rice University, twelve participants (3 males and 9 females) were recruited from the student population. Their mean age was 18.5 yrs (range: 18-20 yrs). The participants joined the experiment as part of their course requirements in psychology classes. All participants were right handed and had normal vision or wore soft contact lenses if they had corrected vision[9].

---

[9] Eye dominance of the participant was not established because none of the literature on SSD has shown eye dominance is a relevant factor. Because in all of the experiments examining horizontal saccades and displacements, the participant made both leftward and rightward saccades, and the displacement occurred in both direction, I think the reliance on a particular eye in detecting perisaccadic displacements should have been counterbalanced.

A

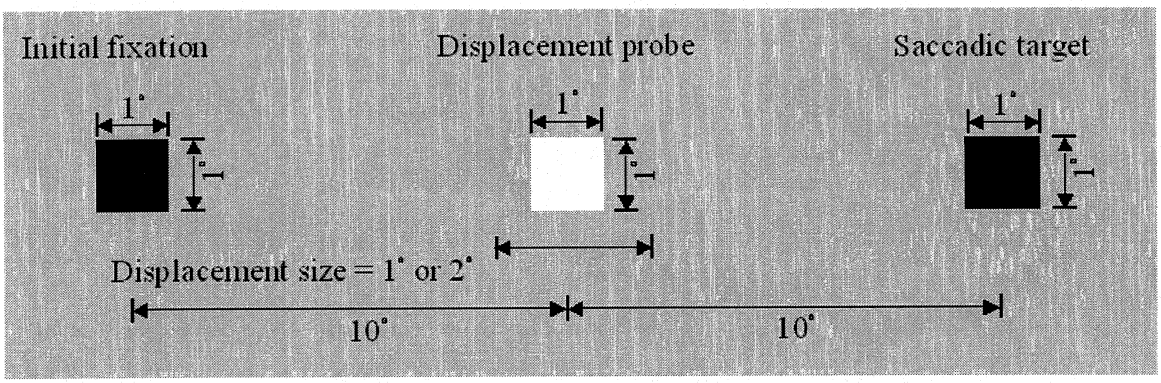


B

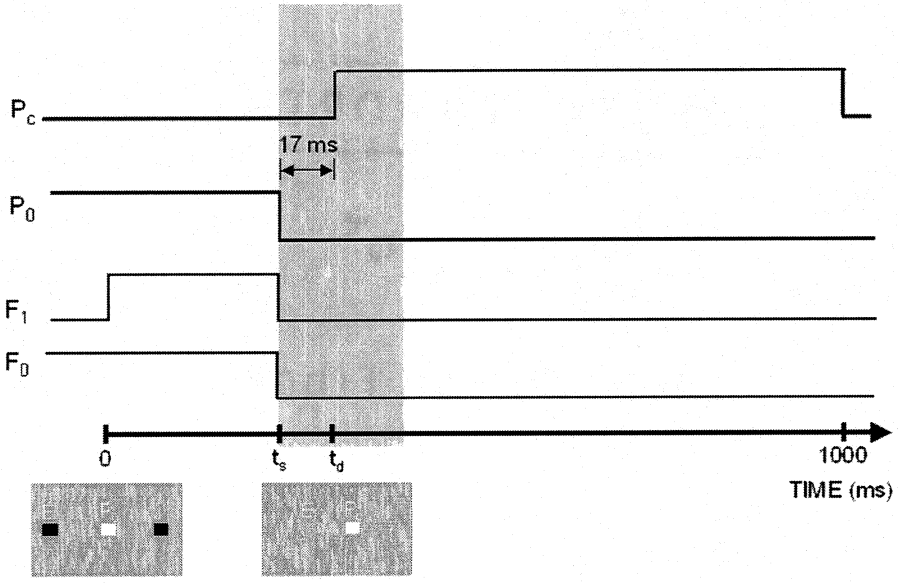


**Figure 1**. Configuration of stimuli and sequence of events in Experiment 1. A) Configuration of stimuli for a rightward saccade. For the purpose of depicting the spatial relationships among stimuli, all stimuli are shown in the figure. The white probe is located at the center of the display, whereas the initial fixation and the saccade target are located at the 10 degree eccentricity in the LVF or RVF, respectively. B) The sequence of events in a trial with a rightward saccade. The shaded area represents the duration of saccades. The raised portion of the line graph indicates the onset of that stimulus. Note the lines are not to scale in time. The two small windows at the bottom show what the participant saw when saccade target appeared and when the probe displaced to a new location. P: probe; $F_0$: initial fixation; $F_1$: saccade target; $t_s$: saccade onset; $t_d$: displacement onset; $P_0$: initial probe position; $P_c$: end probe position after a congruent displacement; E in the smaller windows at the bottom indicates eye position.

### *3.1.2. Stimulus*

Figure 1 shows the configuration of stimuli in a typical trial. The initial fixation and the saccadic target were two black squares (6.01 cd/$m^2$) whose centers were located at 10 deg eccentricity in the left or right visual field, respectively, and on the horizontal meridian. The displacement probe was a white square (69.68 cd/$m^2$) whose center was initially located at 10 deg to the left or right of initial fixation and on the horizontal meridian. The background was gray (15.29 cd/$m^2$). The position of the probe after displacement could be located at one of five different locations with a separation of 1 deg from each other. Thus, there was either no displacement (initial position = displaced position) or 1 or 2 deg displacement leftward or rightward in a given trial. All of the squares were 1 × 1 degree in size.

### *3.1.3. Procedures*

Figure 1B shows the sequence of events in a trial. At the beginning, the initial fixation target appeared at a 10-degree eccentricity in the left or right visual field simultaneously with the displacement probe in the center of the visual field. Participants were required to keep their gaze at the fixation target. After a duration randomly selected between 1500 and 2000 ms, the saccadic target appeared in the visual field opposite the initial fixation (the 0 ms on the timeline in Figure 1B). Participants made a saccade toward the saccadic target as soon as they detected the saccadic target, and kept their fixation at the ending location of their eye movements. At one of the three onset times (22/56/106 ms) after the eye speed exceeded 30°/s ($t_s$), the initial fixation and the saccadic

target were erased ($t_d$)[10]. The probe was erased together with the saccade target and then reappeared 8.3 ms later either at the same position (*no-displacement condition*) or at a new position 1 or 2 degree leftward or rightward (*displacement condition*). The displaced probe was not erased until 1000 ms after the appearance of the saccadic target, which made the post-saccadic probe duration approximately 650 ms, given that average saccade had 250 ms onset and 80 ms duration in this experiment. A tone reminded the participant to respond by pressing the button on the mouse after the disappearance of the probe. The participant hit the left mouse button to signal "YES" if they perceived the displacement, and the right button to signal "NO" otherwise. They were also instructed to randomly select a button when they could not decide whether or not a displacement had occurred.

Each displacement trial belongs to one of the combinations of three factors: direction of displacement (congruent/incongruent with the direction of the saccade), size of displacement (1/2 deg), and the onset of displacement (22/56/106 ms after the onset of saccades). There were 240 displacement trials, with 20 trials for each combination of conditions. As for the no-displacement trials, the probe was erased and redrawn at the same location at 22, 56 or 106 ms after the onset of saccades. There were 20 trials for each saccade-redrawn duration.

---

[10] By attaching a photocell to the region within a white square on the CRT and reading its output from an oscilloscope, the peak-to-peak duration is found to be 16.7 ms (i.e., 60Hz). The program could detect the saccade onset at any time point during a vertical retrace cycle. A reasonable and representative time point is half of the cycle, 8.3 ms. To test this a TTL pulse is triggered and sent to the oscilloscope immediately after a saccade onset is detected. The average peak to saccade-onset duration is 8.13 ms. It is also confirmed that the displacement probe reappears at the new location in the immediate next retrace cycle. In addition, the true saccade onset should occur 14 ms earlier than the time detected by the program. Therefore, in the current experiment the probe is erased averagely 22.3, 55.7, or 105.8 ms after the detection of the saccade onset, and reappears at 30.7, 64, or 114.1 ms after the true saccade onset.

### *3.1.4. Data Analysis*

The traces of eye movements were analyzed offline to determine whether a saccade was executed appropriately. That is, a saccade had to exceed the threshold velocity at some point along its course and must have a magnitude larger than 10 degrees to be included in the analysis. Two participants had more than 40% trials failing this criterion and thus their data were not included in further analyses. For the remaining ten participants, on average 23% of their trials were discarded. Most of these errors were due to double-step saccades in which the displacement probe distracted participants' saccades. The remaining participants' data were further screened by discarding trials with reaction times that deviated more than 2 standard deviation from the condition mean.

Hit rates for the displacement condition and false alarm rates for the no-displacement condition was arcsine-square-root transformed to avoid heterogeneity of variance across subjects in ANOVA[11]. The transformed hit rate was corrected by subtracting the arcsine-square-root transformed false alarm rates. The corrected, transformed hit rates were subjected to 3-way repeated-measures ANOVA (direction × displacement size × displacement time). The significance level was set at .05. The saccade magnitude, onset, and duration were also subject to the same ANOVA. For future reference, the untransformed hit rates and false alarms can be found in Table D1 (see Appendix D).

---

[11] For a sequence of yes/no responses, the outcome is a binominal distribution. Let y be the number of success and n be the total number of observation. The variance for the binomial distribution of the observed proportion, p=y/n, is a function of p: VAR(p) = (p)*(1-p)/(n-1). The fact that the variance of p depends on its value violates the homogeneity of variance assumption across subjects required for ANOVA. One approach to deal with this problem is to derive a mathematical function of p whose variance is essentially free of the value of p. It can be shown that for the binomial distribution the arcsine transformation serves this purpose (see Hogg & Craig, 1995)

### *3.1.5. Results*

*Corrected hit rates*. The effects of displacement size ($F$ [1, 9] = 29.58, $MSE$ = 0.06, $p$ < .001) and displacement time ($F$ [2, 18] = 7.33, $MSE$ = 0.35, $p$ < .0001) were both significant. Two-degree displacements (0.43) were detected more frequently than one-degree displacements (0.23). Displacements that occurred 100 ms after the saccade onset (0.54) were detected more frequently than those that took place at 22 or 56 ms (0.23 and 0.20, respectively; both $p$s < .05).

The displacement direction × size interaction was significant, $F$ (1, 9) = 5.29, $MSE$ = 0.02, $p$ < .02. A linear contrast revealed that the difference between congruent and incongruent displacement was larger for the 1-degree than the 2-degree condition (0.07 vs. 0; $p$ < .05).

The displacement direction × displacement time interaction was significant, $F$ (1, 9) = 12.33, $MSE$ = 0.02, $p$ < .001. For displacements that occurred at 22 or 56 ms after saccade onset, there was a statistically insignificant trend that incongruent displacements were detected more frequently than congruent displacements; however, when the displacement occurred at 100 ms, congruent displacement was detected more frequently than incongruent displacement (.59 vs. .50; $p$ < .01; also see Figure 2). No other effects approached significance.

*Saccade latency, duration, and magnitude.* The overall mean saccade latency was 250 ms, the mean saccade magnitude was 17 degrees, and the mean saccade duration was 81 ms. These dependent variables were subject to the same ANOVA as conducted on the corrected hit rates. No effect was significant for latency and magnitude. For the saccade duration, there was a significant effect of displacement direction, $F$ (1, 9) = 6.15, $MSE$ =

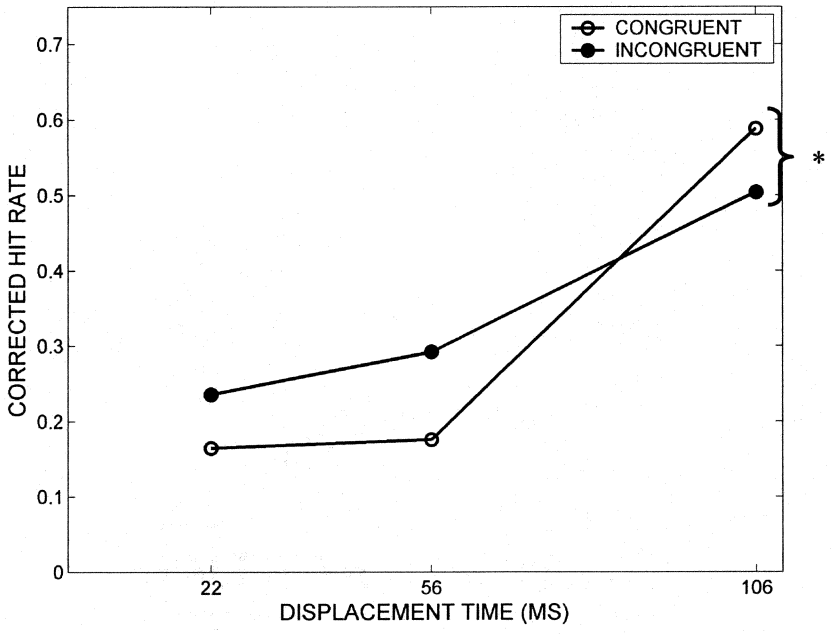


**Figure 2.** Corrected hit rates for congruent and incongruent displacements at each displacement onset in Experiment 1. Each data point was collapsed across the two displacement sizes. The asterisk indicates a significant difference.

78.7, $p < .05$. The saccade duration for the congruent displacement (79 ms) was shorter than the incongruent displacement (81 ms). No other effect was significant for the duration.

### *3.1.6. Discussion*

The current experiment basically replicated previous findings in SSD: stronger suppression for displacement occurred closer to saccade onset or with smaller size. The conventional rule-of-thumb is that the ratio of the intrasaccadic displacement distance to the saccade size (displacement ratio) should be no more than one third (Bridgeman et al., 1975). In that case the threshold distance for a 20-degree saccade would be 6 degrees. In this experiment, however, before the correction with subtracting false alarm rates, the hit rates for the 2-degree displacement were .48, .51, and .79 for the 22, 56, and 106 ms onset time, respectively. These hit rates were much higher than those reported by Bridgeman et al. A recent report by MacAskill, Muir, and Anderson (1999), using a signal detection paradigm in the SSD task, pointed out that the displacement ratio should be a value closer to 0.1, which is consistent with our observation.

The discrepancy in the estimation of threshold displacement ratio was probably because of the difference in stimulus configuration. In Bridgeman et al. (1975), an extended target was composed of a row of 13 fixation points spaced 1 degree apart. When the perisaccadic displacement occurred, the whole stimulus pattern was displaced. In MacAskill et al.'s and in the current study, a much smaller stimulus (.75 degree in MacAskill et al.'s study and 1 degree in the current) was displaced perisaccadically. It may be more difficult to detect the displacement of a huge pattern than a confined stimulus. Moreover, in Bridgeman et al. (1975), there was no well-defined boundary

between trials. The subjects were instructed to make eye movements from one fixation point to another in an irregular pattern, and the stimulus was moved either leftward or rightward at unpredictable times. In contrast, there were clear boundaries between trials in the current experiment, and the displacement always occurred after saccade onset. The reduced temporal and spatial uncertainty of the displacement may enhance the chance to detect it (but see Bridgeman & Fisher, 1990). With stimulus configurations more similar to this experiment, three other studies from Bridgeman's group also found stronger SSD for displacements congruent with saccade directions (Anand & Bridgeman, 2002b; Bridgeman & Macknik, 1995; Macknik et al., 1991).

The intriguing interaction between displacement direction and time deserves some attention. When the displacement occurred at the earlier phase of the saccade (22 or 56 ms), incongruent displacements tended to be perceived more frequently than congruent displacements, and vice versa for displacement occurred toward the end of the saccade. The reversal seemed to occur when the saccade had ended (Figure 2). When the displacement occurred at 106 ms, the advantage of the congruent displacement may have been because of a smaller retinal eccentricity: The displaced probe ended closer to the foveal vision in the congruent than in the incongruent condition. The 106 ms displacement served as a post saccadic baseline of displacement detection. To confirm whether intrasaccadic displacement favors incongruent direction, the next experiment will focus on displacements occurred during saccades.

### 3.2. Experiment 2. Strength of SSD in Incongruent and Congruent Displacements

In Experiment 1, the 106 ms displacement occurred when the saccade had ended.

The postsaccadic displacement was more visible, and may have complicated participants' judgment of whether a displacement occurred perisaccadically. For example, they may have only responded "YES" when displacements were seen as clearly as those at 100 ms after saccade onset. To examine the intrasaccadic SSD more accurately, the current experiment focused on displacements that occurred 22 ms after saccade onset.

### *3.2.1 Participants*

After informed consent, following the guidelines approved by the institutional review board of Rice University, eight participants (5 males and 3 females) were recruited from the student population. Their mean age was 23.8 yrs (range: 19-30 yrs). The participants joined the experiment as part of their course requirements. All participants were right handed and had normal vision or wore soft contact lenses if they had corrected vision.

### *3.2.2. Apparatus, Stimulus, and Procedures*

The paradigm of this experiment was the same as Experiment 1 except that displacements were presented only at 22 ms after saccade onset, and only 2-degree displacements were presented. In addition, a trial was discarded if its saccadic magnitude fell out of the range between 15 and 25 degrees, and the same condition was replaced in the pool of trials for later selection.

### *3.3.3. Results and Discussion*

The corrected hit rates were subject to one-way repeated-measures ANOVA, with displacement direction as the independent variable (uncorrected hit rates and false alarms

can be found in Table D2). The effect of displacement direction was significant, $F(1, 7) = 14.17$, $MSE = 0.06$, $p < .01$. The corrected hit rate of the incongruent condition (.43) was higher than the congruent condition (.04). The reader will find that the superiority of incongruent condition was also replicated in Experiment 4. Thus it should be clear that incongruent displacements are easier to detect than congruent displacements during saccades.

## 3.3. Experiment 3. Saccadic Suppression of Displacement in the Dimension Orthogonal to Saccade Dimension

The purpose of this experiment is to examine whether displacement detection along the dimension orthogonal to saccade direction was compromised. Though some early studies suggest that SSD is omnidirectional (Bridgeman & Fisher, 1990; Bridgeman & Stark, 1979), other studies did find weaker SSD for the orthogonal dimension (Heywood & Churcher, 1981; Mack, 1970). A difference between SSD in the collinear and orthogonal dimension can be expected from the extraretinal view of visual stability. The EEPI informs the visual system where the eye is in orbit. During saccades this information should vary more in the dimension collinear with saccade than in the orthogonal dimension. When the EEPI is involved in mechanisms maintaining visual stability, it should thus provide more information for countering perceptual changes along the collinear dimension than along the orthogonal dimension. Displacement in the orthogonal dimension may thus appear less stable. Alternatively, it is also possible that eye movements introduce noise into spatial representations through the remapping of

receptive fields or image smear, both noisier along the saccade dimension. Positions along the orthogonal dimension may be subject to less noisy representations or inputs, and are thus clearly discriminated (Li & Matin, 1997). Conversely, the visual masking account of SSD would predict an omnidirectional SSD because the post saccadic clear scene should mask everything that occurs during saccades.

### *3.3.1. Participants*

After informed consent, following the guidelines approved by the institutional review board of Rice University, twenty participants completed this experiment. Among them a group of eight subjects (4 males and 4 females; mean age: 19.1 yrs) completed the horizontal saccade/vertical displacement task, and the other group of twelve (4 females and 8 males; mean age: 19.3 yrs) performed the vertical saccades/horizontal displacement task. All subjects were right-handed and reported having normal or corrected vision. They were recruited from the Rice University campus for their fulfillment of course credits.

### *3.3.2. Stimulus*

Figure 3 shows the configuration of stimuli in the horizontal saccade/vertical displacement task. The configuration of vertical saccade/horizontal displacement was just the 90-degree rotation of Figure 3. The initial fixation and the saccadic target were two black squares whose centers were located at 10-degree eccentricity in the left or right visual field along the horizontal meridian. The displacement probe was a white square whose center was initially located at 0 deg in the horizontal dimension or 2, or –2 degrees on the vertical meridian. The size of displacement was 0.5, 1, or 2 degrees upward or downward.

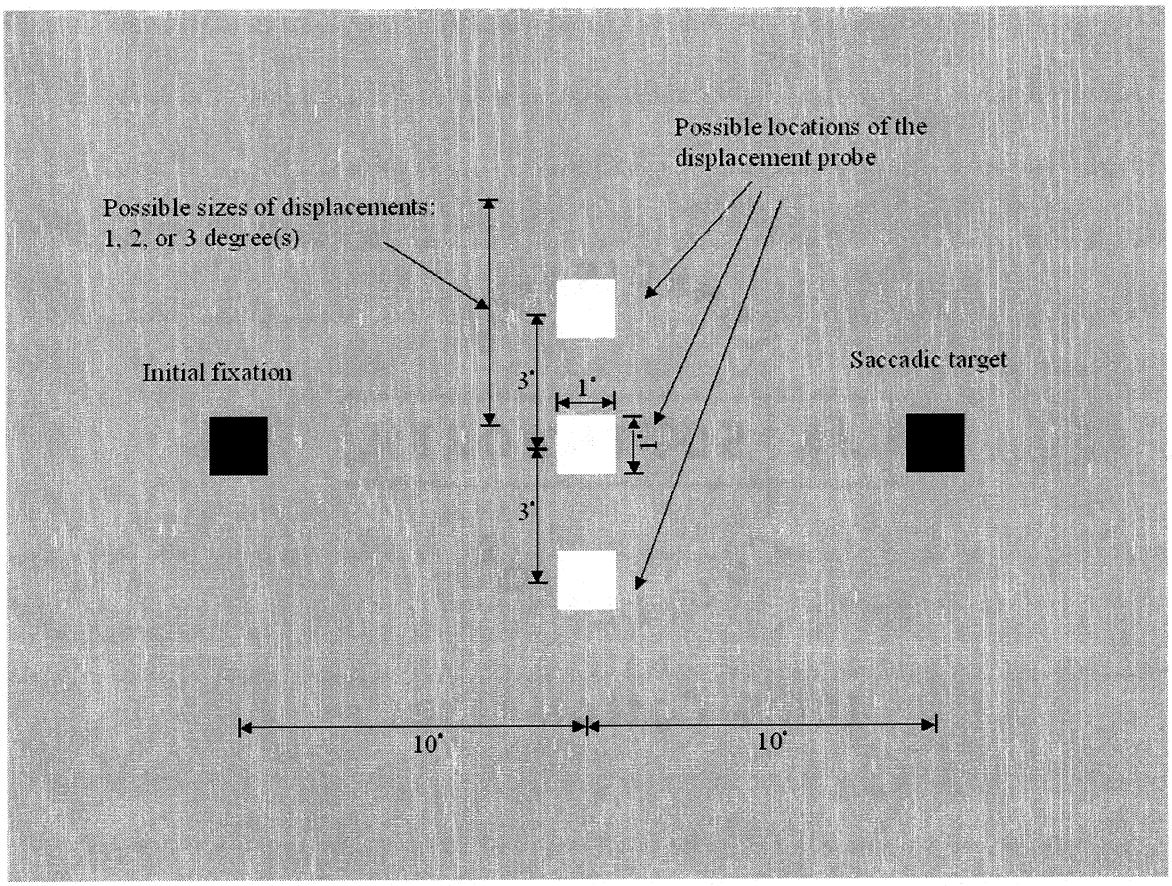


**Figure 3**. The configuration of stimuli in Experiment 3. The three white squares represent the potential probe positions at the beginning of a trial. Only one probe was shown in a given trial.

### *3.3.3. Procedures*

The procedures described here are based on horizontal saccade/vertical displacement. At the beginning of a trial, the initial fixation target appeared at 10 deg of eccentricity in the left or right visual field simultaneously with the displacement probe at one of its initial positions. Participants kept their gaze on the fixation target. After a duration randomly selected between 1500 and 2000 ms, the saccadic target appeared in the visual field opposite to the initial fixation. Participants made a saccade toward the saccadic target as soon as they saw the saccadic target, and were instructed to keep their fixation at the position of the saccadic target at the end of their eye movements. At 22 ms after the saccadic onset (speed exceeding 30°/s), the initial fixation, the saccadic target, and the displacement probe were erased. The probe reappeared at 8.3 ms later either at the same position (*no-displacement trials*) or at a new position 0.5, 1 or 2 degree(s) below or above the original position (*displacement trials*). The displaced probe was not erased until 1000 ms after the onset of the saccadic target. A tone reminded the participant to respond by pressing the button of the mouse after the disappearance of the probe. A trial was discarded if its saccadic magnitude fell out of the range between 15 and 25 degrees, and the same condition was thrown in the pool of trials for later selection.

For the displacement trials, there were three factors: the direction of displacement (upward/downward), the initial position of the probe (0/+2/-2), and the size of displacement (0.5, 1, or 2 degree[s]). There were 10 trials for each combination of factors, which totaled 180 trials. For the no-displacement trials, the only factor is the initial probe position. There were 20 no-displacement trials for each probe position, for a total of 60 trials. Thus, each participant performed 240 acceptable trials according to the saccade-magnitude criterion.

### *3.3.4. Results of Horizontal Saccade/Vertical Displacement*

Figure 4 shows the corrected hit rates in each condition (uncorrected hit rates and false alarms can be found in Table D3). The three-way interaction was significant, $F(4, 28) = 5.09$, $p < .01$. The three-way interaction can be best characterized as the differential interactions between displacement size and direction at the three different initial probe positions. For the "DOWN" position, the only significant difference was between upward (0.25) and downward (0.08) 0.5-degree displacement. For the "MID" position, upward displacement had higher corrected hit rates than downward displacement only when the displacement size was 1-degree (0.75 vs. 0.53; $p < .01$). Finally for the "UP" position, downward displacement had higher corrected hit rates than upward displacement when the size was 0.5-degree (0.19 vs. 0.02; $p < .05$) and 1-degree (0.44 vs. 0.24; $p < .01$).

The interaction between initial position and displacement direction was significant, $F(2, 14) = 4.13$, $MSE = 0.07$, $p < .05$. The effect of displacement size was highly significant, $F(2, 14) = 118.17$, $MSE = 0.12$, $p < .001$. The effect of probe initial position was significant, $F(2, 14) = 7.27$, $MSE = 0.15$, $p < .01$. These effects are not explored further because of the significant 3-way interaction.

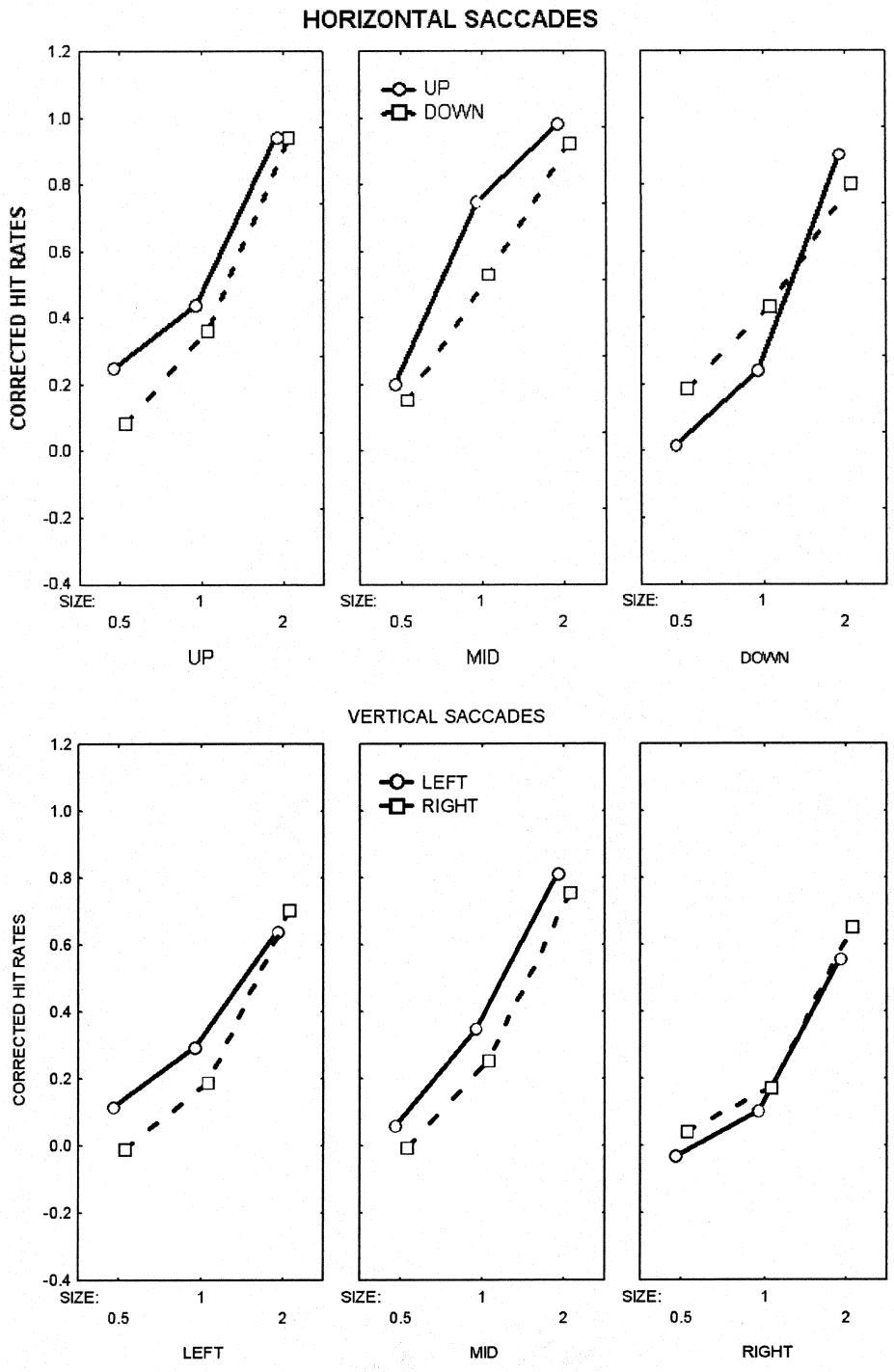


**Figure 4**. Corrected hit rates of orthogonal displacement detection during horizontal saccades (upper panel) and vertical saccades (lower panel) in Experiment 3. The three different initial positions are depicted in separate panels. The circle and solid line represent upward displacement, and the square and dashed line represent upward displacement.

### 3.3.5. Results of Vertical Saccade/Horizontal Displacement

The interaction between initial position and displacement size was significant, $F$ (4, 44) = 3.26, $MSE$ = 0.04, $p < .05$. For the 0.5-degree displacement, there was no significant difference between any pairing of initial positions. For the 1-degree displacement, the MID (.30) condition had higher corrected hit rates than the RIGHT condition (.14; $p < .05$). Finally, for the 2-degree displacement, the MID condition (.78) had higher corrected hit rate than either the LEFT or the RIGHT conditions (.67 and .60, respectively; both $p$s $< .05$).

The effect of displacement size was highly significant, $F$ (2, 22) = 67.67, $MSE$ = 0 .24, $p < .001$. The effect of initial position was marginally significant, $F$ (2, 22) = 3.06, $MSE$ = 0.16, $p = .06$. No other effect approached significance.

### *3.3.6 Discussion*

Contrasting the result of the current experiment with Experiment 1, the orthogonal displacement seems easier to detect than the collinear displacement. This can be confirmed by conducting a two-way mixed design ANOVA with the relationship of saccade/displacement dimension as the between-subject factor (Horizontal/Horizontal, Horizontal/Vertical, and Vertical/Horizontal) and size of displacement as the within subject factor[12]. The effect of saccade/displacement dimension was significant, $F$ (2, 24) = 32.36, $MSE$ = 0.10, $p < .001$. The vertical displacement during the horizontal saccade had the highest corrected hit rates (0.80), followed by horizontal displacement during

---

[12] For the data from Experiment 1, only the 22 ms displacement-onset condition was included, and the data were collapsed across congruent and incongruent conditions. For the data from Experiment 2, only trials from the center initial probe position and 1- and 2-degree displacements were included. The upward and downward (or leftward/rightward) displacement conditions were collapsed.

vertical saccades (0.59), and the collinear displacements had the lowest corrected hit rates (0.20) (See Figure 5). This rejects the claim that SSD is omnidirectional (Bridgeman & Stark, 1979; Bridgeman et al., 1975; Stark, 1976). The differential strength between SSD in various combinations of saccade and displacement directions suggests that the mechanism underlying SSD should not be a general inhibition or masking. The mechanism of SSD most likely involves information about saccades such as EEPI and spatial representations in the temporal vicinity of saccades.

One potential account for the directional SSD is that the end positions of saccades are more variable along the collinear than the orthogonal dimension. Because participants may perform the displacement detection by evaluating the relative distance from the endpoint of a saccade and the probe, greater variability may lead to greater difficulty in detection. The dimension with greater variability, namely the collinear directions, thus has lower hit rates than the dimension with less variability in saccade endpoint, which is the orthogonal dimension. As for the congruency effect, the variability in endpoints of congruent trials may be larger than those of incongruent trials. Similarly, orthogonal displacements are easier to detect in horizontal than in vertical saccades because of the greater variability in endpoints of vertical saccades than in horizontal saccades. The condition with smaller signal-to-noise ratio in detection should be more difficult to detect. To verify this hypothesis, the standard deviation of saccade magnitudes in each conditions of Experiment 1 were subject to a 3-way repeated ANOVA with the same design as the ANOVA on corrected hit rates. No effect was significant. If the endpoints-variability hypothesis was true, one should expect a significant interaction between displacement direction and displacement time matching the results of corrected hit rates (i.e., larger standard deviations for congruent than for incongruent displacements

at 22 and 56 ms, and the reverse at 106 ms). The endpoint-variability hypothesis is thus not supported.

Another explanation is that inhomogeneous spatial compression during saccades changes the perceived distance of displacements under different combinations of saccade direction and displacement direction. The change is such that one perceives congruent differently from incongruent displacements, and collinear differently from orthogonal displacements. This is a preferred explanation because it accommodates the data better than the first one, and it can be quantified with a mathematical model of perisaccadic mislocalization (see discussions in Section 3.4).

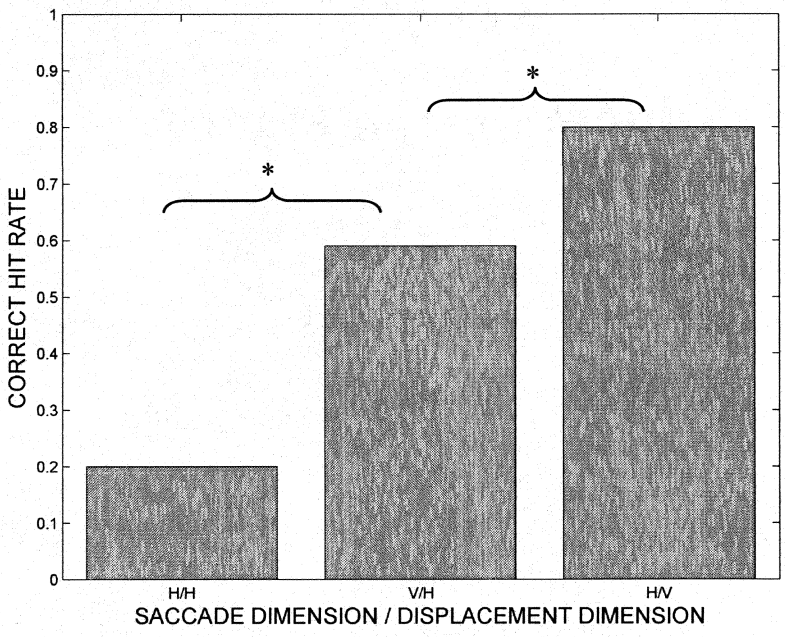


**Figure 5**. Corrected hit rates of different combinations of saccade and displacement dimensions from Experiment 1 and 3. Data for each bar were collapsed across different displacement sizes. Asterisks and brackets indicate significant differences.

### 3.4. The Relationship between SSD and Perisaccadic Spatial Representation

Because the displacement in the SSD experiment was in the form of apparent rather than continuous motion, correct detection of displacement should have relied to some extent on the perceived changes in probe positions. The perceived position of the probe before and after its shift in space determined the perceived size of that displacement. All else being equal, the perceived sizes of congruent and incongruent displacements may be different due to biases in the perceived location of the probe, and as revealed in Experiment 1, 3, and other studies (Bridgeman et al., 1975; Stark, 1976), displacements with the larger perceived size are detected more frequently. The perceived location of the probe could be biased in two different ways: mislocalization during saccades or during fixation.

In the case of intrasaccadic mislocalization, it has been demonstrated that localization of a spatial position was biased, or compressed, towards the saccadic target, and the extent of spatial compression was determined by the distance between the spatial position and the saccadic target (Lappe et al., 2000; Morrone et al., 1997). The extent of mislocalization is not homogenous across space, and may compress two physically identical distances to different extents, depending on where those locations are. It is possible that the perceived size of an incongruent displacement was larger than that of a congruent displacement due to perisaccadic mislocalization. Thus, congruent and incongruent displacements with the same size were not detected equally frequently.

As discussed in section 1.4.2, a few studies have shown that perisaccadic perception of spatial locations is not veridical (Matin, 1965; Matin et al., 1969; Matin et al., 1970; Honda, 1989, 1991a, b, 1993; Ross et al., 1997; Lappe et al., 2000; Kaiser &

Lappe, 2004). Among these studies, Morrone et al. (1997) was the only one offering a mathematical model quantifying the mislocalization. Therefore, their model will be adopted here to calculate the unequal perceived distance of congruent and incongruent displacements that have the same physical size. According to Morrone et al. (1997), the perceived position of a location in the spatiotopic coordinate at the temporal vicinity of saccades can be described as the following function:

$$P(x,t) = sign(E(x,t))|S|\left|\frac{E(x,t)}{S}\right|^{\varphi(t)} + O(t)\,. \qquad \text{Eq. 1}$$

The formal definitions of the components in Eq. 1 are described in Appendix A. Briefly, $O(t)$ represents the origin of the internal coordinate system that shifts from the initial fixation ($F_0$) to the saccadic target ($F_1$), $\varphi(t)$ is a gain function modulating the metric of internal space, and $E(x,t)$ is the retinal eccentricity function defined as the difference between the stimulus position and the position of the eye. Also, $x$ is the spatiotopic coordinate of a spatial location, and $t$ is the time relative to the saccade onset (in ms).

The perceived sizes of congruent and incongruent displacements are the distance between the perceived positions of the initial and end probe location. Let $P_0$, $P_i$, and $P_c$ denote the initial probe position, the probe position after an incongruent displacement, and the probe position after a congruent displacement, respectively. The perceived size of an incongruent displacement is thus $|P_0 - P_i|$; the perceived size of a congruent displacement is $|P_0 - P_c|$. To compare the perceived sizes, let $R_{CI}$ be the size ratio of the congruent to the incongruent displacement:

$$R_{CI} = |P_0 - P_c| / |P_0 - P_i| \qquad \text{Eq. 2}$$

Note that a $R_{CI}$ less than unity indicates that the perceived size of a congruent displacement is smaller than that of an incongruent displacement, where as a $R_{CI}$ larger than unity means the contrary.

In Eq. 1, the perceived position is a function of both real position ($x$) and temporal duration from saccade onset ($t$). The value of $x$ is fairly straight forward, but the value of $t$ requires some assumptions. Because the probe was constantly present before and after the saccade, it is reasonable to assume the time of $P_0$ to be the last moment when the probe was at the initial position, and the time of $P_i$ and $P_c$ to be the last moment when the probe was at the end position. This way the percepts were the most updated representation of the probe locations. Assuming that the saccade is *rightward,* let $x_0$ be the initial probe position, $t_d$ be the onset of the displacement, $x_\Delta$ be the size of displacement, and $t_\Delta$ be the duration between the onset of displacement and the final sample of the probe position. We can rewrite Eq. 2 into the following form,

$$R_{CI} = \frac{|P(x_0, t_d) - P(x_0 + x_\Delta, t_d + t_\Delta)|}{|P(x_0, t_d) - P(x_0 - x_\Delta, t_d + t_\Delta)|} \qquad \text{Eq. 3}$$

Because in our SSD experiment the displacement occurred after the first duty cycle of the CRT after saccade onset, we can assume the displacement onset ($t_d$) to be between 22 and 40 ms. The probe remains on the display until 1000 ms after the presence

of the saccadic target. Assuming that the average saccade onset is 250 ms, a $t_{\Delta}$ of 750 ms passes before the final sample of the probe is perceived[13]. This is also assuming that the duration of the saccade is 80 ms, and the average velocity is 250 °/sec (these two parameters are determined according to experiments in the current dissertation). Figure 6 plots the relationship between $t$ and $R_{CI}$ using the previous assumptions and the free parameters reported in Morrone et al. (1997). For all sets of parameters provided in their study, when $t_d$ was between 22 and 40 ms, $R_{CI}$ was smaller than unity. This indicates that congruent displacements with the same real sizes as incongruent displacements were perceived to be smaller, and should thus be more difficult to detect, which is consistent with our findings. Moreover, as the $t_d$ approaches the end of saccade duration, the $R_{CI}$ first touches the trough between 60 and 70 ms, and then bounces back toward unity quickly. After the end of the saccade, $R_{CI}$ is greater than unity. This indicates that the congruent displacement became more visible after the end of saccades, which is also consistent with the findings in Experiment 1.

One piece of result cannot be explained easily with this model is the higher corrected hit rates in the "horizontal saccade/vertical displacement" condition than the "vertical saccade/horizontal displacement" condition. To accommodate this, an additional assumption that localization is less accurate during vertical than horizontal saccades is necessary. This is not unreasonable because a) humans execute more horizontal than vertical saccades and could thus be better at representing locations during horizontal saccades, and b) vertical saccades may require bilateral activation of the brain region programming eye saccades in each hemisphere (INSERT GOLDBERG REF). The precise

---

[13] $R_{CI}$ remains smaller than unity for $t_{\Delta}$ varying from 0 to 750 ms (see Figure A1). Therefore, it doe not matter when during that period the participant sampled the new probe location.

localization during vertical saccades may rely on the communication of both hemispheres, which can be noisier when this process is carried out within a single hemisphere, as is in horizontal saccades. Whether orthogonal mislocalization is stronger during vertical than horizontal saccades require further study to verify this additional assumption.

Thus perisaccadic compression of space toward the saccade target may alter the perceived distance of displacement, and in turn induces the directional effect in Experiment 1 and 2. Moreover, Morrone et al. (1997) also demonstrate that spatial compression does not occur for the dimension orthogonal to the saccade direction. This also explains why the sensitivity to orthogonal displacements in Experiment 3 is much higher than that to collinear displacements. This account, however, does not explain why vertical displacements during horizontal saccades were easier to detect than horizontal displacements during vertical saccades (Figure 5).

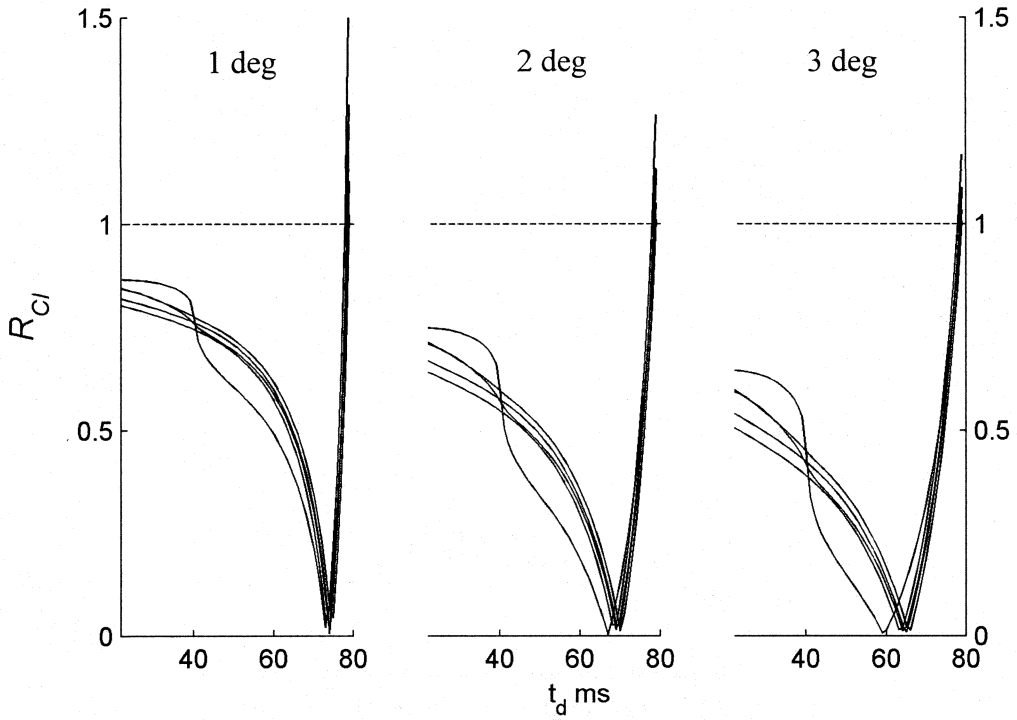


**Figure 6.** Ratio of congruent to incongruent displacement ($R_{CI}$) predicted by Morrone et al. (1997)'s model of perisaccadic mislocalization. The curves in this figure are plotted according to Eq. 3, using the free parameters estimated by Morrone et al. (1997). Each curve represents the estimation of $R_{CI}$ with the parameters of an individual in Morrone et al. (1997). The values of displacement onset ($t_d$) vary between 22 and 80 ms, and the duration of the displacement probe at the new location ($t_\Delta$) is assumed to be 750 ms. Each panel shows the time course of $R_{CI}$ under the displacement size of 1, 2, or 3 degrees. The dotted line represents unity and a $R_{CI}$ below unity indicates the perceived size of the congruent displacement is smaller than that of the incongruent displacement.

# 4. LOCATING THE CORTICAL AREAS NECESSARY FOR PERISACCADIC PERCEPTUAL CHANGES WITH TMS

The purpose of this series of experiment is to locate the cortical site(s) necessary for saccadic suppression of displacement. The interference induced by TMS to the right PPC has been shown to compromise the updating of the craniotopical representation (Donkelaar & Muri, 2001) in the left visual field. Studies on patients have also demonstrated that EEPI for horizontal saccades are contralaterally represented (Heide et al., 1995; Heide & Kompf, 1998; Duhamel, Goldberg et al., 1992). If the EEPI, or the cortical sites processing EEPI, involved with the double-step saccade task are also crucial for the perisaccadic perceptual changes, it can be predicted that TMS to the right PPC should modulate the saccadic suppression of displacement and the perisaccadic mislocalization during leftward saccades.

Two important factors influencing the TMS effects are the timing and the location of TMS administration. The interference induced by single-pulse TMS can last for 300 ms (Inghilleri, Berardelli, Cruccu, & Manfredi, 1993). The perisaccadic perceptual changes typically start 100 ms before the saccade onset, and the average onset of an endogenous saccade is about 200 ~ 250 ms after the "go" signal (Ro, Farne, & Chang, 2002). Therefore, administering TMS between 50 ~ 150 ms after the visual "go" signal should allow the influence of TMS to overlap with the cortical processing of perisaccadic perceptual changes. The location of TMS administration, when targeting on the PPC, has been diverse in previous studies. The vertex (Muri et al., 2002; Donkelaar & Muri, 2001) and the motor hand area (Terao et al., 1998) are two frequently used landmarks in defining the PPC. In this experiment, a circular coil stimulating a large area was used to

increase the probability that the critical cortical region is stimulated. When the most efficient timing of TMS stimulation is determined, a figure-eight coil with a focal area of stimulation was used in another experiment to enhance the spatial resolution of the localization.

It is not clear whether TMS administration would make the threshold distance of displacement detection higher or lower than the no-TMS condition. The threshold could increase because TMS disrupts spatial perception, or it could decrease because TMS eliminates mechanisms inhibiting displacement detection.

## 4.1. Experiment 4: Influence of TMS on Saccadic Suppression of Displacement: the Round Coil

This experiment examined how TMS over the PPC and the frontal cortex modulates SSD. TMS was administered with a large circular coil to disrupt cortical processing. Although the circular coil influences a relatively large region, it is still meaningful to separate the effect of frontal and parietal stimulation on SSD. If the modulation on SSD only occurs under parietal TMS, the spatial resolution can be enhanced using a figure-eight coil that directly stimulates a more confined region of parietal cortex than the circular coil.

### *4.1.1. Participants*

After informed consent, following the guidelines approved by the institutional review board of Rice University, ten participants were recruited in this experiment. All

participants reported having normal or corrected vision, and no history of any neurological or psychiatric disorders at the time of testing (mean age: 20.9 yrs; 5 males and 5 females; one left-handed and nine right-handed). Most of them were from the Rice University campus and paid $10 per hour for their participation.

### *4.1.2. Apparatus*

Transcranial magnetic stimulation was conducted using a Cadwell Laboratories MES-10 stimulator (Kennewick, Washington). The stimulator at maximum intensity creates a 2.2-Tesla field. A circular coil measuring 9 cm in diameter was used in this experiment. All of the other instrumentation, such as the CRT and the eye tracker, were the same as those in Experiment 1.

### *4.1.3. Stimulus*

The configurations of stimuli were similar to those in Experiment 1 (see Figure 1). However, only a 2-degree displacement was used, and the displacement only occurred 22 ms after the saccadic onset.

### *4.1.4. Procedures*

At the beginning of a trial, the initial fixation target appeared at 10 deg of eccentricity in the left or right visual field simultaneously with the displacement probe. Participants were required to keep their gaze at the fixation target. After a duration randomly selected between 1500 and 2000 ms, the saccadic target appeared in the visual field opposite to the initial fixation. The participant was required to make a saccade toward the saccadic target as soon as they saw the saccadic target, and to keep their

fixation at the position of the saccadic target at the end of their eye movements. The TMS pulse, if delivered, occurred at 50, 100, or 150 ms for duration of 70 μs after the onset of the saccade target. Twenty-two ms after the speed of the eye movement exceeded 30°/s, the initial fixation, the saccadic target, and the displacement probe were erased. The probe reappeared on average 22 ms later either at the same position (*no-displacement condition*) or at a new position 2 degrees leftward or rightward (*displacement condition*). The displaced probe was not erased until 1000 ms after the onset of the saccadic target. A tone reminded the participant to verbally respond "YES" or "NO" regarding whether a displacement was perceived or not[14]. A trial was discarded if its saccadic magnitude fell out of the range between 15 and 25 degrees, and the same condition was replaced in the pool of trials for later selection.

The experiment was divided into two sessions, one for frontal and the other for parietal TMS stimulation. The order of TMS site in the two sessions was counterbalanced across participants.

### *4.1.5. TMS administration*

The TMS site on the scalp was determined in the following way: each participant's right motor hand area was localized at the beginning of the experiment. The hand area was localized by moving the focus of the figure-eight coil around the region a few centimeters to the right of the vertex. The most anterior position where the TMS induced the most robust contraction of the contralateral hand was defined as the motor hand area. The output intensity of the TMS device was then decreased until a contraction

---

[14] The last three participants in this experiment made responses by pressing the mouse buttons, as those in Experiment 1, because the experimenter had to administer the experiment alone and could not hold the coil and press the mouse button simultaneously.

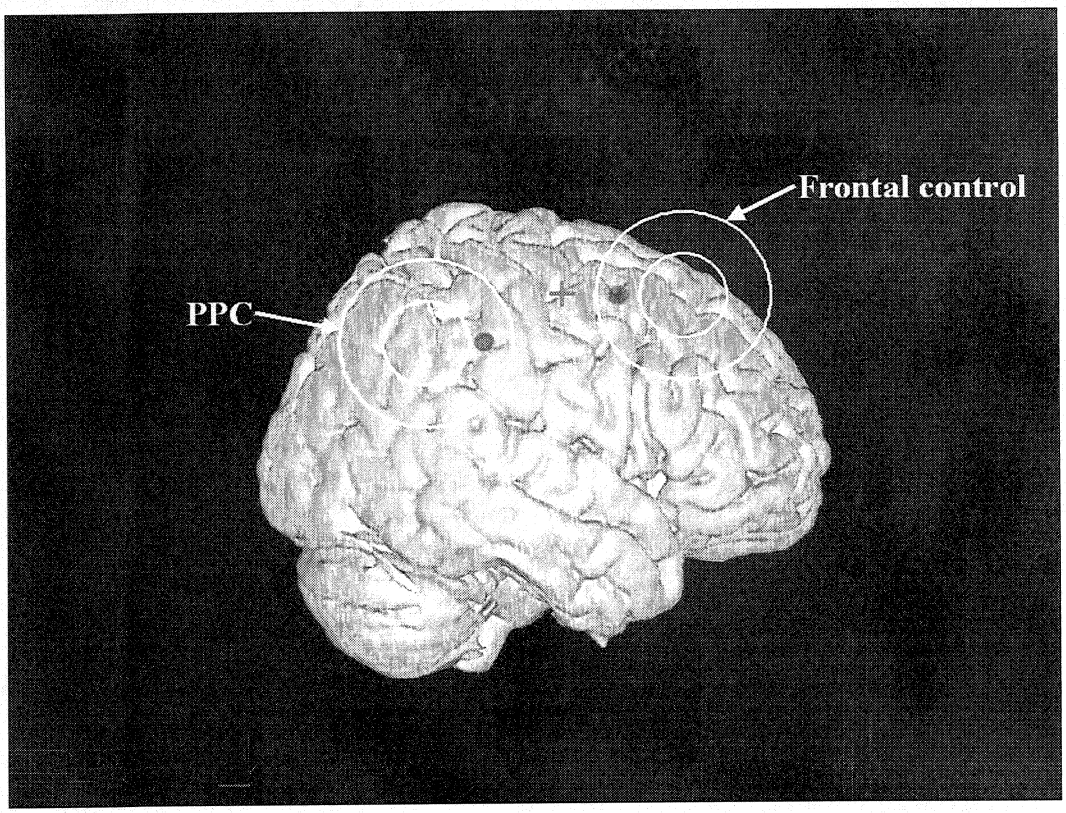


**Figure 7.** Illustration of the TMS round coil positions on the 3D cortical surface of a standard brain.

of the contralateral hand was no longer visible and then increased until a contraction is again visible. The latter intensity setting was defined as the motor threshold for the figure-eight coil. The circular coil was then applied over the located motor hand area, and the motor threshold for this larger coil was determined in the same fashion as did with the figure-eight coil. The handle of the circular coil was perpendicular to the anterior-posterior axis of the participant's head. The midpoint of the coil's anterior rim covered the motor hand area[15]. The mean intensity used for the experiment was 10% above the threshold value of the circular coil. With the TMS intensity 10% above motor threshold, the contralateral hand contraction should be triggered when the hand is at a relaxed state. The average motor threshold of the ten participants was 33% of the maximum output (equivalent to 0.73 Tesla).

The PPC site was marked on the scalp at the position 3 cm posterior and 2 cm lateral to the motor hand area; whereas the frontal site was defined as a position 2 cm anterior to the motor hand area. The exact position of the PPC site has been defined in various ways in TMS studies. Some researchers defined it as 3 cm posterior and 3 cm lateral to the vertex (Donkelaar & Muri, 2001), which was claimed to correspond to the P4 or P3 site in the international 10-20 system. Other researchers defined it with reference to the functional localization of the motor hand area, either 7 cm posterior (Terao et al., 1998) or 4.5 cm posterior and 0.5 cm medial to the motor hand "hot spot." The coordinates in this experiment were chosen based on measurements of the relative spatial relationship between the central sulcus and the medial portion of the intraparietal sulcus of a model brain. Because of the large spatial range of the circular coil, it should cover the desired region even if the coordinates were not exactly where the PPC was.

---

[15] With a circular coil, the peak intensity of stimulation occurs at the rim rather than the center of the coil.

Each experiment was divided into the frontal and the PPC stimulation sessions. Trials with TMS and without TMS were mixed in a random sequence within each session. The anterior rim of the coil covered the PPC site in the PPC block, and the posterior rim of the coil covered the frontal site in the frontal block (Figure 7). After the TMS landmarks were determined, the participant went through the eye tracker calibration in the same way as described in Experiment 1 prior to data collection.

### *4.1.6. Data Analysis*

There were four independent variables: TMS site (parietal/frontal), saccade direction (left/right), the displacement direction (congruent/incongruent), and the timing of TMS administration (No TMS or TMS at 50 ms/100 ms/150 ms after the presentation of the saccadic target). Each combination of the conditions had 10 trials, amounting to 240 trials for each TMS site. Hit rates for the displacement condition and false alarm rates for the no-displacement condition were arcsine-square-root transformed. The transformed hit rates were corrected by subtracting the transformed false alarmed rates and then subject to a 2 × 2 × 2 × 4 repeated-measure ANOVA. The untransformed, uncorrected hit rates and false alarms can be found in Table D4. Although the statistical results were based on the transformed values, the "Results" section reports the untransformed numerical values of corrected hit rates for the convenience of reading.

### *4.1.7. Results*

The most important finding from the four-way repeated-measure ANOVA was the significant interaction among TMS site, displacement direction, saccade direction, and TMS time, $F(3, 27) = 3.19$, $MSE = 0.10$, $p < .05$ (Figure 8). To explore this three-way

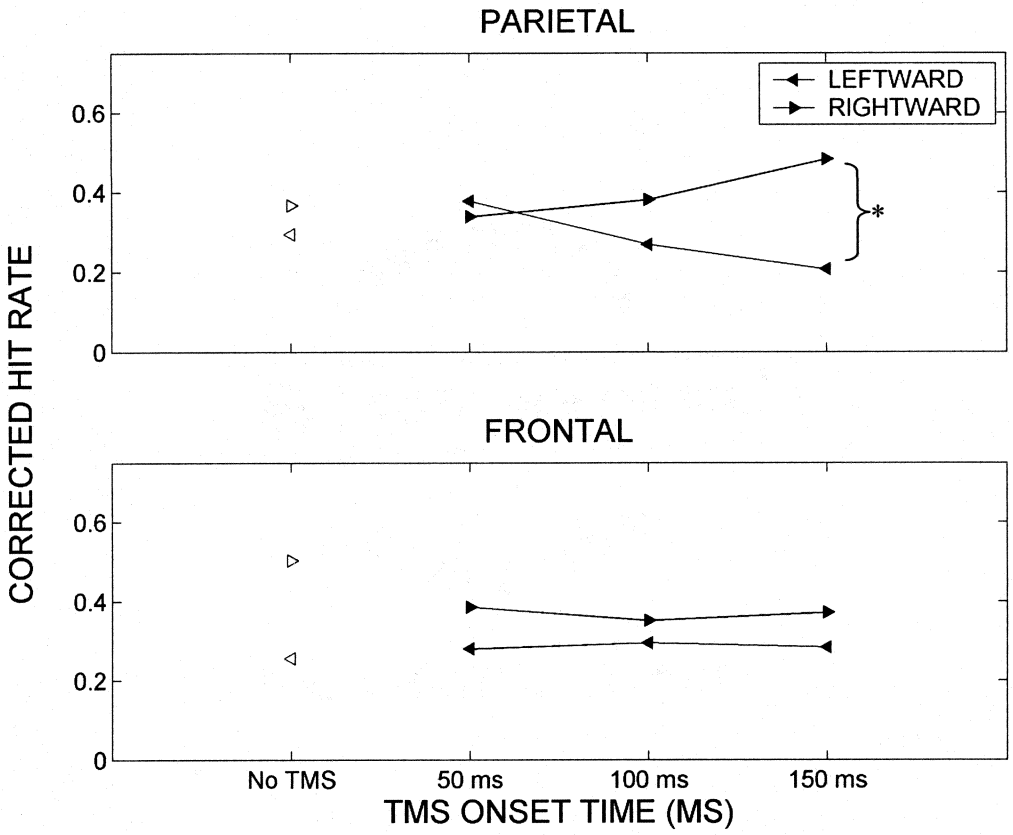


**Figure 8.** The corrected hit rates for leftward and rightward saccades at each TMS timing and stimulated site in Experiment 4. The left and right pointing triangles indicate leftward and rightward saccades, respectively. Empty symbols indicate No TMS conditions.

interaction, two additional two-way ANOVA's with TMS time and saccade direction as the factors were conducted on the data of each TMS site. No effect was significant for the frontal TMS site. Although the difference between leftward and rightward saccades in the No TMS condition of the frontal control site (Figure 8, bottom) seems to be huge, the great variability in the data make this difference statistically not significant (see Table D4). In contrast, the interaction between TMS time and saccade direction was significant for the parietal TMS site, $F(3, 27) = 3.72$, $MSE = 0.10$, $p < .05$. Linear contrast revealed that when TMS was applied over the parietal cortex at 150 ms TMS-saccade-target SOA, there was a significant difference between leftward and rightward saccades (.21 vs. .48; $p < .001$). At no other timing did TMS induce a significant difference between two saccade directions.

Returning to the four-way ANOVA, there was a significant effect of saccade direction, $F(1, 9) = 8.70$, $MSE = 0.23$, $p < .05$. Rightward saccade generally had higher corrected hit rates (0.40) than leftward saccades (0.28). The effect of displacement direction was significant[16], $F(1, 9) = 3.87$, $MSE = 2.27$, $p < .04$. Incongruent displacements (.59) were detected more frequently than congruent displacements (.26). No other effects reached significance.

*Saccade latency, duration, and magnitude.* To ensure that the site, direction, and time-specific TMS effects on SSD did not result from disruptions of saccades, a four-way repeated measures ANOVA was also conducted on saccade latency, duration, and magnitude, respectively. For saccade latency, there was a significant effect of TMS time,

[16] It was one-tailed because the corrected hit rates of the incongruent condition was expected to be higher than the congruent condition.

$F$ (3, 27) = 7.836, $MSE$ = 1227.12, $p$ < .001. This is an effect consistent across both TMS sites. Linear contrasts found that when TMS was applied at 50 ms, the saccade latency (249 ms) was shorter than the No TMS, the 100 ms, and the 150 ms condition (270, 267, and 274 ms, respectively; all $p$s < .01). For the saccade duration, there was a significant interaction between TMS time and saccade direction, $F$ (3, 27) = 3.89, $MSE$ = 58, $p$ < .05. Linear contrasts found that when TMS was applied at 100 ms, the leftward saccades had a shorter mean duration (77 ms) than rightward saccades (82 ms). The difference in leftward and rightward durations did not reach significance in all the other TMS timings. For the saccade magnitude, there was a significant main effect of TMS timing, $F$ (3, 27) = 4.61, $p$ < .01, and a significant effect of saccade direction, $F$ (1, 9) = 8.14, $MSE$ = 6.1, $p$ < .05. When TMS was applied at the 150 ms SOA, the saccade magnitude (19.21°) was shorter than that at all the other TMS timing (19.44, 19.57, and 19.40° for the No TMS, 50 ms, and 100 ms SOA, respectively; all $p$s < .05). Leftward saccades had a larger mean magnitude (19.8°) than rightward saccades (19°). No other effects were significant for all of the three measures. Although some of the effects were associated with TMS timing, none of the interactions associated with TMS site was significant. Thus the significant interaction between TMS site, saccade direction, and TMS time in corrected hit rates cannot be attributed to peculiarities in saccades.

### *4.1.8. Discussion*

The main finding of this experiment is that, when TMS was applied to the right PPC just prior to the saccade onset, the sensitivity to displacement during leftward saccades became significantly worse than during rightward saccades. In contrast, TMS over the frontal control site did not induce any significant effect. The specific timing,

saccade direction, and cortical site of the TMS effect support the hypothesis that the PPC contributes to SSD. Before the experiment was conducted, it was not certain whether TMS over the PPC would enhance or compromise displacement detection. If SSD is the manifestation of inhibitory processes in the PPC, disrupting the inhibition should reduce SSD, and thus provide a higher sensitivity to displacements. On the contrary, if SSD is the consequence of a spatial representation that is in the process of updating during saccades, introducing disruption into the PPC would further disturb the spatial representation and result in an even worse performance on displacement detection. The current result is more consistent with the latter explanation.

The timing of the effect also coincides with the finding of Donkelaar et al. (2001) that TMS administered immediately before the second saccade in the double-step saccade task disrupts the compensation for errors in amplitudes of the first saccade. In the current experiment the TMS effect on the contralateral saccade occurred at 150 ms after the onset of saccade target, which is approximately within 100 ms from the saccade onset. The spatial updating process pertaining to the saccade was probably within the time window of TMS effect.

The TMS-induced modulation of SSD can be related to the disruption of perisaccadic spatial compression. The visual space is represented contralaterally in the PPC. Thus, TMS over the right PPC might have disrupted the spatial compression in the left visual field. In Section 3.4 I proposed that SSD could be a consequence of spatial compression. The disruption of spatial compression in the LVF *reduced* the strength of SSD. At the end of a leftward saccade, the probe location was in the RVF and represented by the left PPC; in contrast, at the end of a rightward saccade, the probe location was in the LVF and represented by the right PPC. Therefore, the spatial compression was

stronger in the RVF than in the LVF, and the SSD should be stronger in the RVF than in the LVF. This explains why TMS strengthen the SSD during leftward saccades, as opposed to the strength of SSD during rightward saccades with the same TMS timing.

One may question that the strengthened SSD may not necessarily be the consequence of a disrupted spatial representation. The circular coil stimulated quite large a cortical area, probably covering the entire parietal cortex. Though the fact that frontal stimulation had no effect on SSD narrowed down the relevant region to the parietal cortex, the parietal cortex is still involved with a wide range of perceptual (Thier & Karnath, 1997), oculomotor (Pierrot-Deseilligny, Ploner, Muri, Gaymard, & Rivaud-Pechoux, 2002), and especially attentional processes (Driver, Vuilleumier, & Husain, 2004). The decreased sensitivity to intrasaccadic displacement could, for example, be a consequence of TMS-induced visuospatial neglect (Muri et al., 2002; Pourtois, Vandermeeren, Olivier, & de Gelder, 2001; Fierro, Brighina, Piazza, Oliveri, & Bisiach, 2001). One way to clarify this is to examine whether the sensitivity to vertical displacements are also prone to the TMS over the PPC. If the decreased sensitivity to horizontal displacement was because of impairment in attention, the sensitivity to vertical displacement should also be influenced by TMS because it also occurs in the contralateral visual field. The dissociation in the performance on collinear and orthogonal displacements under TMS would suggest the mechanisms disturbed in the PPC when performing SSD task should be more related to perisaccadic spatial representation. This possibility will be considered further after Experiment 5, where a figure-eight coil will be used in the SSD task to confine the stimulation within a much smaller region than the current experiment.

It is worth mentioning that the congruency effect was replicated again in the current experiment. The difference between incongruent and congruent conditions,

however, were not modulated by TMS. If the congruency effect results from the differences between perceived distance of congruent and incongruent displacements, TMS did not change the relative size of the perceived distance.

## 4.2. Experiment 5: Influence of TMS on Saccadic Suppression of Displacement: the Figure-Eight Coil and MRI Guided Localization

The purpose of this experiment is to locate the PPC with a greater spatial resolution, using a figure-of-eight TMS coil. The TMS site was localized by coregistering individual participant's structural MRI image and scalp landmarks to ensure the stimulation was delivered precisely over the desired brain region on each individual[17].

### *4.2.1. Participants*

After informed consent, following the guidelines approved by the institutional review board of Rice University, three subjects completed this experiment (2 females and 1 male; mean age: 22.3 yrs, ranging from 18~23 yrs)[18]. One of the female participants is left-handed but uses the computer mouse with her right hand in daily life. The other participants were right-handed. All participants reported having normal or corrected vision, and no history of any neurological or psychiatric disorders at the time of testing. They were recruited from the Rice University campus and paid $10/hour for their

---

[17] A pilot study used the location 3 cm posterior and 2 cm lateral to the motor hand area as the PPC site, and another two sites as controls. However, no systematic modulation of TMS on SSD was observed using the focal coil. Since the spatial range of effect is much smaller with a figure-eight coil, stimulating fixed surface coordinates on every participant could have missed the optimal position.

[18] Actually six volunteers were tested for the experiment. The co-registration procedures did not locate the motor cortex accurately in two of the participants, and another participant could not perform the SSD task because of the inability to make 20-degree saccades without stopping at the displacement probe.

participation.

### *4.2.2. Apparatus*

The apparatus was the same as those in Experiment 4 except that the TMS was administered with a figure-eight coil instead of a round coil. The figure-eight coil has a diameter of 4.5 cm in each round component with a maximum focus at the intersection of the two components. Based on the topography of activation of individual finger movements induced by this coil, it is estimated that this coil consistently interrupts less than 1 $cm^3$ of cortex. The actual spatial extent of the TMS disruption, however, could be variable across brain areas and participants due to differences in neuronal architecture and the distribution of electric current flow.

### *4.2.3. TMS administration*

Two different TMS sites, the lateral intraparietal sulcus (LIP) and the anterior intraparietal sulcus (AIP), were localized by the coregistration of individual participant's structural MRI scan and the head. The MRI images were high-resolution MP-RAGE anatomical scans with a 240 mm FOV (192 1 mm-thick axial slices, TR=1200 ms, TE=2.93 ms), acquired with one of the two 3-Tesla Siemens Allegra head-only scanners in the Human Neuroimaging Laboratory of Baylor College of Medicine. The image was preprocessed in MRICro (Rorden, 2004a) for orientation adjustment and region-of-interests (ROI) marking. Marking the ROI on the right motor hand area, lateral intraparietal sulcus, anterior intraparietal sulcus, and five landmarks with punctate color spots visualizes the target coordinates on the image and facilitates the coregistration process.

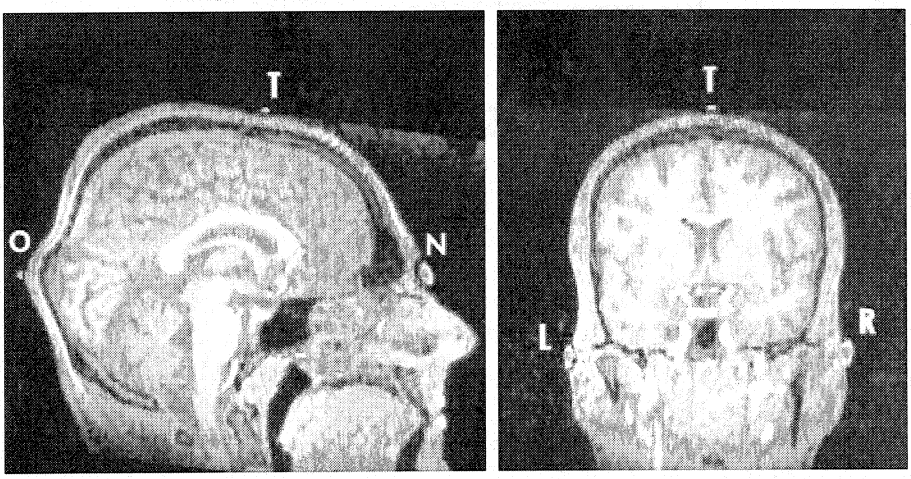


**Figure 9.** The five landmarks used in 3D co-registration in Experiment 5. The green spots were where the landmarks located. See the text for definition of each location.

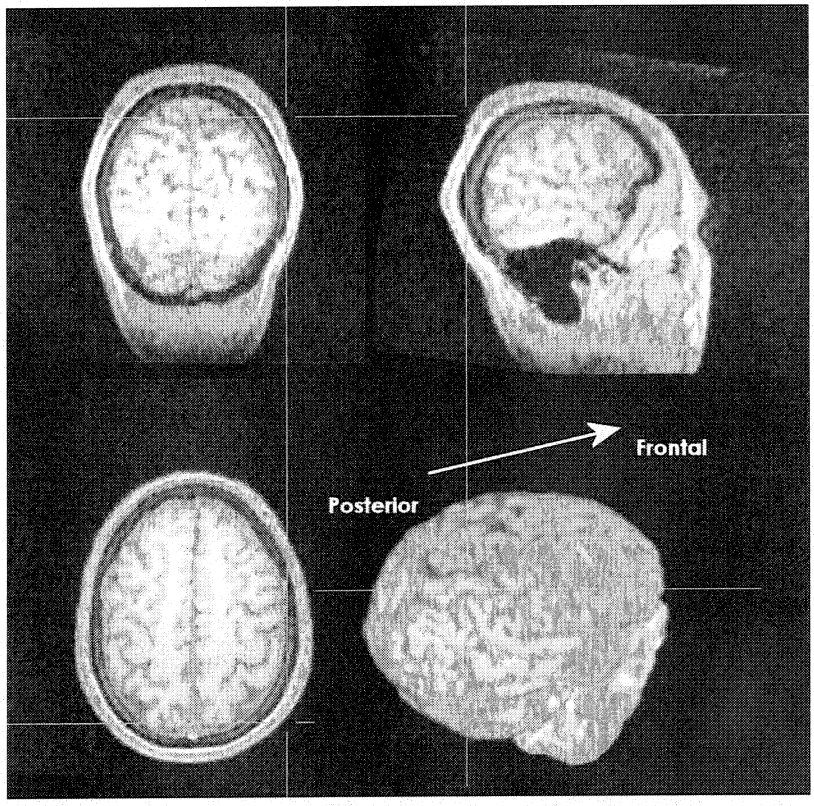


**Figure 10.** Illustration of the TMS coil position and the lateral intraparietal sulcus in Experiment 5. The green dot indicates the target location on the cortex from which the coregistration algorithm searches for a scalp position with a minimal distance (the cross hair).

At least five arbitrary landmarks on the head were necessary for the coregistration algorithm (Rorden & Brett, 2000). The five locations selected here were nasion (N), left tragus (L), right tragus (R), the midpoint of the left and right tragus along the coronal plane (T), and the projection of the nasion at the occipital portion of the scalp (O). The first three landmarks stand out quite well in the MRI image. T and O were created manually in the MRI image by marking appropriate locations after careful visual inspection. The path distance between the N and O or T along the scalp in the MRI image was measured using the ImageJ software (developed at the U.S. National Institutes of Health and available on the internet at http://rsb.info.nih.gov/nih-image/).

The 3D coregistration was achieved by using MRIreg and MRICro (Rorden & Brett, 2000; Rorden, 2004a, b) and a Polhemus FASTRACK® 3SPACE® tracking system (Polhemus, Inc.). After the participant's real head space was co-registered with the MRI image, the scalp location with shortest distance from the motor hand area as defined morphologically (c.f.Yosury et al., 1997) was marked, and TMS was applied over this spot to validate the co-registration. The process was repeated until the TMS over the right motor hand area triggered the contraction of the left hand.

For participants whose motor hand area were localized accurately with the coregistration, the scalp locations with shortest distance to LIP and AIP in the MRI image were also marked for TMS stimulation. Figure 10 shows the LIP in one male participant's structural scan on the saggital, coronal, and horizontal plane, as well as the 3D cortical surface.

### *4.2.4. Procedures*

Instead of measuring the hit rates and false alarms of the 2-degree displacement

under various conditions, the threshold distance of 50% left and right discrimination responses was estimated with the QUEST procedure (King Smith, Grigsby, Vingrys, & Benes, 1994; Watson & Pelli, 1983)[19]. For each saccade direction, there were a leftward and a rightward displacement sequence starting at the displacement size of 2 degree. The participant's task was to judge the direction of displacement (left or right) in every trial. For a given sequence, the size and direction of displacement in an upcoming trial was contingent on the presumed psychometric function (a Weibull function was adopted) and all responses of previous trials belonging to that sequence. A sequence was terminated either when it proceeded to 40 trials or its standard deviation of the threshold estimate became smaller than .05 degree. On each TMS site, the 50% threshold distance of leftward or rightward judgments were estimated for twelve different conditions combined by three different TMS timing (No TMS /100 ms/ 150 ms), two saccade directions (left/right), and two displacement directions (congruent/incongruent).

[19] One can download the c codes of the QUEST procedure from http://vision.nyu.edu/VideoToolbox/Download.html.

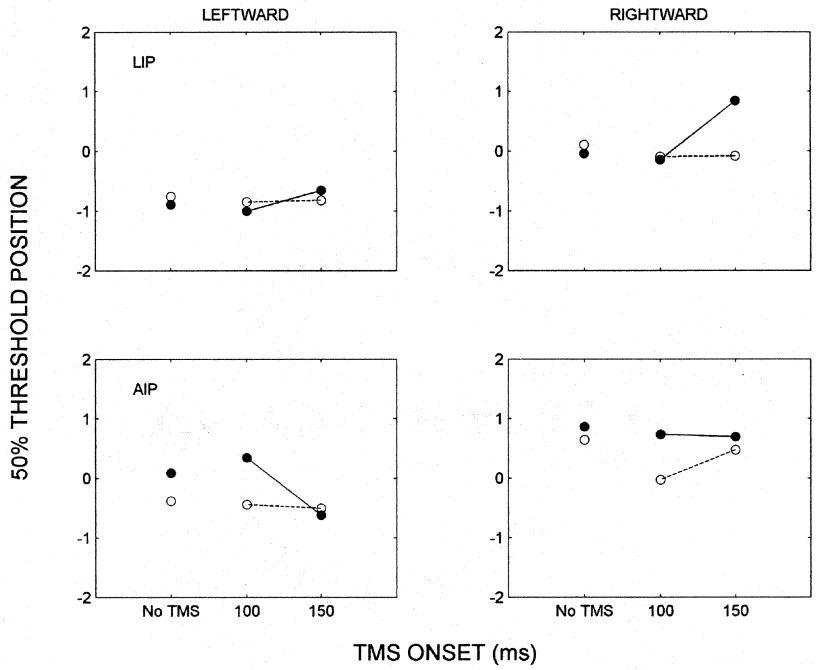


**Figure 11**. The 50% threshold position of left/right discrimination in each condition of Experiment 5. The filled circle and solid line represent incongruent displacements, the empty circle and dashed line represent congruent displacements. The ordinate represents the extent of directional bias in perceiving the probe displacement, with positive values indicating biases in the congruent direction and negative values indicating biases in the incongruent direction. Note that a displacement is congruent or incongruent depending on the saccade direction.

### *4.2.5. Results*

The thresholds for 3 participants at each TMS timing, saccade and displacement direction are illustrated in Figure 11. The data of threshold position in each condition was subject to a 2 × 2 × 2 × 3 repeated-measures ANOVA with TMS site (LIP/AIP), saccade direction (left/right), initial displacement direction of the sequence (congruent/incongruent) and TMS time (No TMS/100 ms/150 ms) as the four factors. Probably because of the lack of power, none of the effects was significant.

### *4.2.6. Discussion*

Apart from the lack of power, the control site, AIP, was probably not ideal because it is too close to the targeted LIP site. Although applying TMS on AIP produces tactile and auditory sensation matching that of TMS over LIP, the TMS effect might have spread to LIP and may obscure the purpose of the control site. In the future studies, it is probably wise to use a control site farther away from the target site (like the vertex).

Another potential problem with this experiment is the way LIP was identified. The author identified the LIP according to the anatomical features. Usually the intraparietal sulcus sits right above the supramarginal and angular gyri, with its anterior end contacting the postcentral sulcus, and the posterior end terminates at the parieto-occipital sulcus. In reality, however, the anatomical features in the participants' images are more variable than in a standardized brain, and the identification may have been prone to error. Unlike the motor hand area, there is no quick and simple response measure to validate the LIP before entering the long experimental session. This may be a line of research worth pursuing: a task capable of localizing the LIP efficiently like the one developed for locating the frontal eye fields (Ro et al., 2002). In a pilot study, a double-step saccade

task was tested for this purpose, but the TMS did not produce significant differences in spatial compensation of the second saccades in the ipsilateral and the contralateral direction. Another solution worth pursuing in locating the relevant cortical site for SSD is to conduct an fMRI study. TMS can then be applied to the region correlated with the task performance. A PET study has shown diminution of cerebral blood flow activity in V1, V2, and parietal cortex when participants make saccades in the darkness (Tomas, 1995).

# 5. PERISACCADIC MISLOCALIZATION

Experiment 4 demonstrated that the posterior parietal cortex contributes to SSD. As was hypothesized in the introduction, SSD could be a consequence of compressed perceived distance of displacement during saccades. This predicts that TMS over the PPC should also strengthen the perisaccadic mislocalization during contralateral saccades. The current series of experiments examine this prediction.

## 5.1 Experiment 6. Perisaccadic Mislocalization along the Saccade Direction

This experiment will map the perceived position of spatial locations during saccades. In the Morrone et al. (1997) study, the probe to be localized during saccades was a bar extending 50 degrees vertically, which is considerably different from our SSD displacement probe. In this experiment, the localization probe will be a 1×1 degree white square as used in the SSD experiments. In addition, instead of reporting numbers on the ruler indicating where the probe was, as in the Morrone et al. (1997) study, the

participants marked where they perceived the probe with a computer mouse pointer (c.f. Lappe et al., 2000; Michels & Lappe, 2004). This is a better method because a continuously presented ruler may interfere with the perception of the probe during saccades. Finally, the compression indices at different probe positions were computed separately rather than collapsed, as was done in Lappe's studies. Lappe et al. (2000) defined the spatial compression index as the standard deviation of the normalized mean localization coordinate *across* all of the different probe locations. Complete compression will result in a value of zero for this measure because every response clusters at the same location and thus there will be no variation in their coordinates. This measure does reflect compression, but does not tell where compression is centered. One can perceive all probe location at somewhere different from the saccade target but still get a zero on Lappe's compression index.

### *5.1.1. Participants*

After informed consent, following the guidelines approved by the institutional review board of Rice University, eight subjects completed this experiment (4 Males and 4 females; mean age: 19.6 yrs, ranging from 18 ~23 yrs). All subjects were right-handed, reported having normal or corrected vision. They were recruited from the Rice University campus for fulfillment of course requirements.

### *5.1.2. Apparatus and Stimulus*

The vertical retrace rate of the CRT was adjusted to 120Hz, which is the highest possible rate of the Sony Trinitron CRT, so that the localization probe could be presented as soon as possible after saccade onset. The viewing distance was shortened to 28.5 cm to

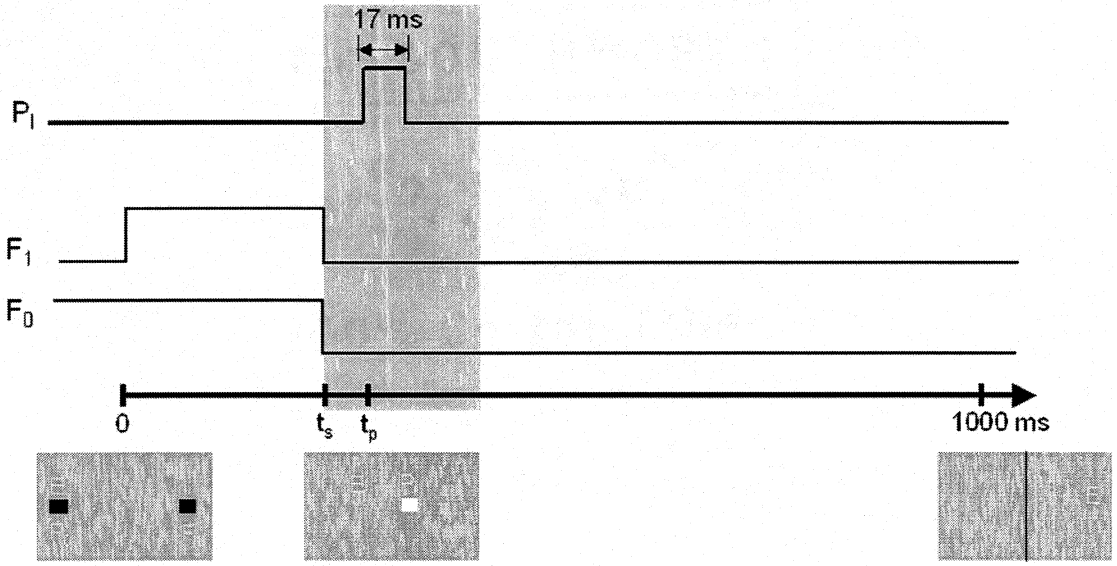


**Figure 12**. The sequence of events in a trial with rightward saccade in Experiment 6. The shaded area represents the duration of saccades. The raised portion of the line graph indicates the onset of that stimulus. The two small windows at the bottom show what the participant saw when saccade target appeared and when the probe was presented. $P_1$: localization probe; $F_0$: initial fixation; $F_1$: saccade target; $t_s$: saccade onset; $t_l$: probe onset; $P_0$: initial probe position; E: eye position. Note that the duration of events was not drawn to scale.

increase the size of visual field where stimuli can be presented (60 × 46 degrees). The background was uniform and gray (16.92 cd/$m^2$). The initial fixation and the saccadic target were black squares (luminance: 6.39 cd/$m^2$; contrast ratio: 0.45). The localization probe was a white square (70.87 cd/$m^2$; contrast: 0.61). All squares extended 1×1 degree of visual angle.

### *5.1.3. Procedures*

The experiment consisted of one session with horizontal saccades and another with vertical saccades. Here the horizontal condition is described in more detail. The stimulus configuration of the vertical condition was merely a 90-degree rotation of the horizontal condition. For the horizontal coordinate, positive values indicate rightward direction; for the vertical coordinate, positive values indicate upward direction.

Figure 12 shows the sequence of events in a trial. At the beginning, the initial fixation target appeared at 10-degrees eccentricity in the left or right visual field where the participant was required to fixate. After a random duration between 1500 and 2000 ms, the saccadic target appeared in the opposite visual field, mirroring the initial fixation. Participants made a saccade toward the saccadic target as soon as they saw it and kept their fixation at the position of the saccadic target until the localization response was made. At 18 ms after the speed of the eye movement exceeded 30°/s (the saccadic onset) the initial fixation and the saccadic target were erased, and the localization probe was presented for 17 ms. The probe position was randomly selected from one of 5 predetermined locations on the head-centered horizontal coordinate: ±15, ±5, and 0 degree. At 1000 ms after the presentation of the saccadic target, a thin vertical black line extending from the top to the bottom of the CRT display appeared at 5 degrees either to

the left or to the right of the probe location. The participant moved the black line with a computer mouse to where they perceived the localization probe, and then clicked on the left button of the mouse to indicate that they had reached the perceived position. The computer registered the horizontal position of the vertical line for off-line analysis. The participant held their viewing direction at the saccadic target while making the localization response[20]. A trial was discarded if its saccadic magnitude fell out of the range between 15 and 25 degrees, and the same condition was replaced in the pool of trials for later selection.

### *5.1.4. Data Analysis*

A compression index ($I_c$) was calculated in the following way: the ratio of the perceived-position-to-saccade-target distance to the physical-distance-to-saccade-target distance was first computed, and the $I_c$ is defined as 1 minus the distance ratio. An $I_c$ of 0 indicates perfect perception, whereas an $I_c$ of 1 indicates complete compression. Negative $I_c$ is rare but possible, indicating the perceived location is farther away from the saccade target than the physical probe location. The $I_c$ data were subjected to a two-way repeated measure ANOVA (saccade direction [2] x probe position [5]).

### *5.1.5. Results of Horizontal saccades*

*Apparent Location.* Figure 13 (upper panels) shows the perceived location as the function of the physical location of the probes during leftward and rightward saccades. Although

[20] Holding their gaze at the saccade target avoid potential confounding from introducing a new saccade to the probe position or other locations, which may alter the representation of the probe position. This concern, however, was suggested to be unnecessary according to Dr. Markus Lappe's unpublished data on perisaccadic mislocalization.

the most eccentric probes (±15 degree) seem to bias from veridical perception (diagonal lines) toward the saccade target (arrowhead), the other probe positions did not seem to bias in either direction. The compression index will quantify this tendency.

*Compression Index* ($I_c$). The mean and standard deviation of each condition for every individual participant can be found in Table E1 and E2. The only significant effect was probe position, $F(4, 28) = 26.85$, $MSE = 0.036$, $p < .0001$. Post hoc comparisons found that $I_c$ for the 15-degree probe was significantly larger (0.57) than all the other conditions ($I_c$ ranging between -0.04 ~0.16; all $p$s $< .001$), indicating a stronger compression at that probe location (Figure 14, upper panel). One may concern about the fact that the computation of $I_c$ may exaggerate the size of compression for probes closer to the saccade target. This caveat may be reconciled by noting the fact that probes at the 5 and 15 degrees have the same distance from the saccade target, yet the $I_c$ for the 15-degree probe was still larger than the 5-degree probe.

### *5.1.6. Results of Vertical Saccades*

*Apparent Location.* Figure 13 (lower panels) shows the perceived location as the function of the physical location of the probes during upward and downward saccades. Similar to horizontal saccades, the most eccentric probes showed more biased toward the saccade target than the less eccentric probes.

*Compression Index ($I_c$).* The mean and standard deviation of each condition for every individual participant can be found in Table E1 and E2. The only significant effect was probe position, $F(4, 28) = 10.35$, $MSE = 0.05$, $p < .0001$. Post hoc comparisons found

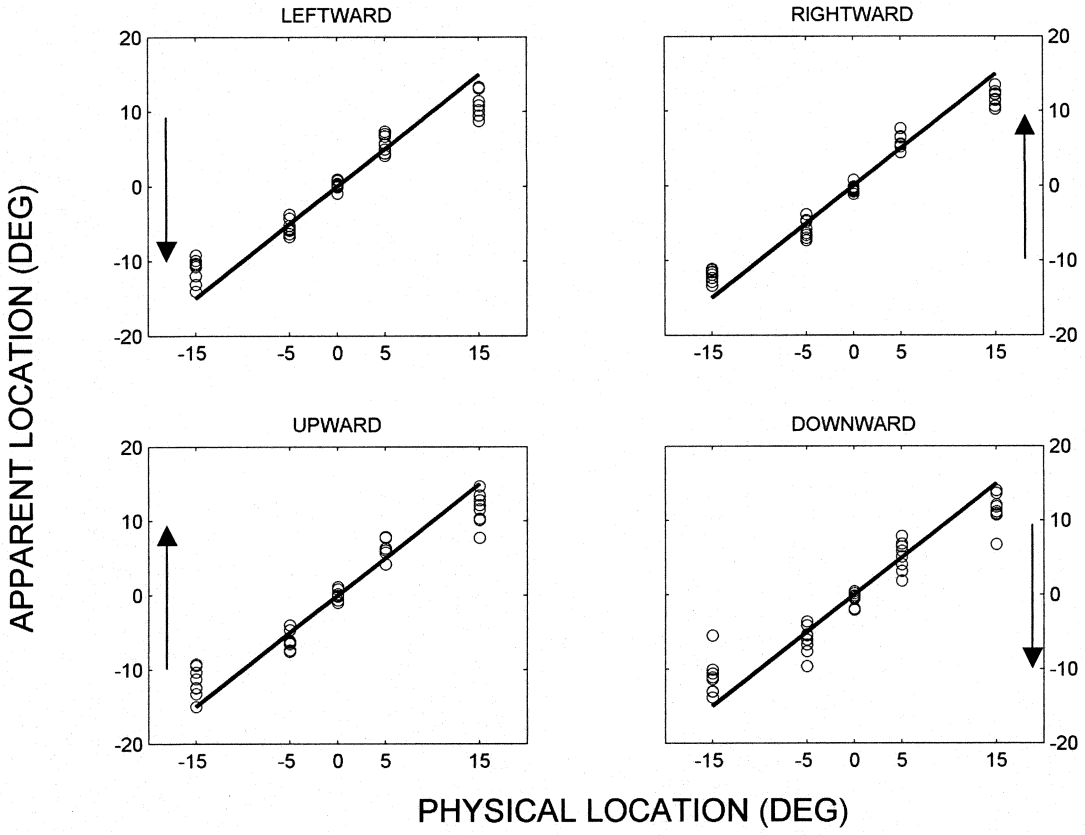


**Figure 13.** The mean normalized coordinates of localization responses in Experiment 6. Each circle represents the mean localization responses (ordinate) at each probe's physical location (abscissa) from an individual participant. The solid, diagonal line in each panel represents veridical perception. The arrow in each panel represents the saccade direction. Compression occurred when a circle deviated from the diagonal line and approached the eccentricity indicated by the arrowhead.

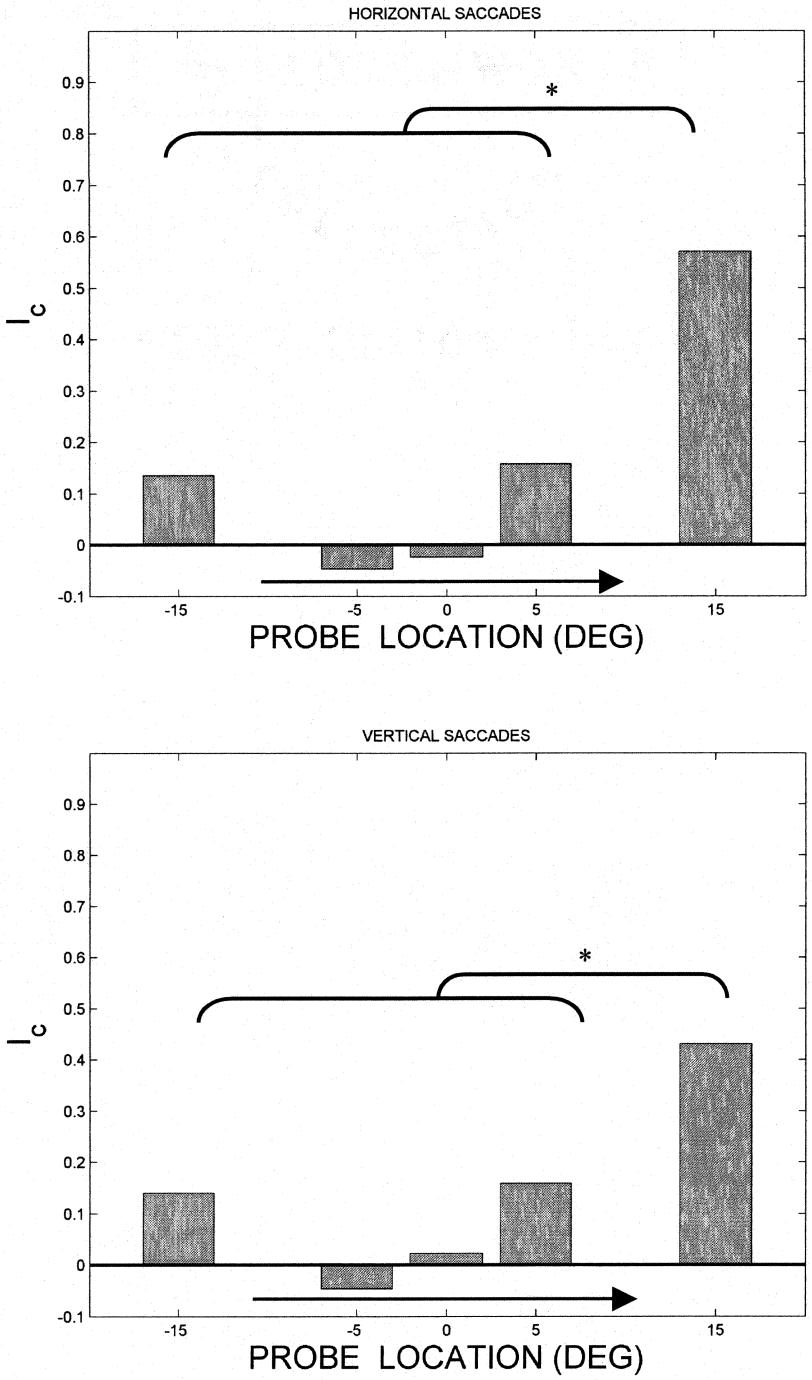


**Figure 14.** The compression index ($I_c$) at each probe position in Experiment 6. Data were collapsed across both saccade directions for the horizontal and the vertical dimensions, respectively. An $I_c$ of zero indicates no compression, and an $I_c$ of one indicates complete compression toward the saccade target. The bracket and asterisk indicate that the $I_c$ at the 15-degree probe position differs from the $I_c$'s at all the other probe locations.

that $I_c$ for the 15-degree probe was significantly larger (0.43) than all the other conditions (ranging between -0.04 ~ 0.15; all *p*s < .05), indicating a stronger compression at that probe location (Figure 14, lower panel).

### *5.1.7. Discussion*

The patterns of mislocalization were similar in horizontal and vertical saccades. Also, the spatial compression did not differ between leftward and rightward saccades, as well as between upward and downward saccades. The results of the compression index suggest that mislocalization was not homogeneous in space: the perception of the location more eccentric than the saccade target shifted opposite the saccade direction, but the perception of the location between initial fixation and the saccade target did not shift significantly toward any other location.

The lack of compression for probe positions between initial and end fixation has been reported for probe positions along the dimension orthogonal to the saccade direction (Kaiser & Lappe, 2004), but not for positions along the parallel dimensions. The current results contrast with the strong perisaccadic compression toward the saccade target in other studies (Lappe et al., 2000; Michels & Lappe, 2004; Morrone et al., 1997; Ross et al., 1997). There are at least two reasons for the lack of compression: First, the contrast between the probe and the background was high. Michels and Lappe (2004) demonstrated that the strength of perisaccadic mislocalization increases as the contrast ratio of the probe to the background decreases, which was consistent with other studies (Awater, Krekelberg, & Lappe, 2000; Lappe et al., 2000; Honda, 1999). In Morrone et al. (1997), the compression in the luminance and equiluminance condition was similar, but the peak amplitude of mislocalization was somewhat stronger in the equiluminant than in the

luminant condition. Michels and Lappe (2004) suggested the dependence of spatial compression on contrast is because stimuli of lower contrast induces lower neural activity in MT and MST (Martinez-Trujillo & Treue, 2002), the cortical regions encoding spatial coordinates and whose activity is influenced by saccades in a way to induce spatial compression (Krekelberg et al., 2003).

The second reason the compression was weaker could be that there were minimal visual references in the current stimulus configuration. Lappe et al, (2000) observed a compression magnitude of approximately -2.5% in the "without-visual-reference" condition of their perisaccadic localization task, as opposed to the 25% compression in the "postsaccadic visual reference" condition (see their Fig. 3). The presence of visual references may change the population activity of neurons representing spatial locations. Think of the spatial representation of a location as the sum of "vectors" contributed by each neuron. The presence of a ruler might have somehow kept the neural vectors of the saccadic target active for a longer time than its absence, and thus the representation of the saccade target may influence the representation of the briefly flashed probe when the neuronal vectors are summed.

Another possibility is that there were no baseline conditions examining mislocalization outside the time window of saccades. The perisaccadic mislocalization could have been inflated or underestimated here because using the physical coordinate as the baseline may not be appropriate. In fact, other studies have demonstrated that spatial perception during fixation is biased toward fovea (van der Heijden, van der Geest, de Leeuw, Krikke, & Musseler, 1999; O'Regan, 1984; Mateeff & Gourevich, 1983; Sheth & Shimojo, 2001; Muesseler et al., 1999). That being the case, using the actual distance as the baseline would deflate the estimate of the perisaccadic mislocalization. The next

experiment amends the problems of contrast and baseline by adopting stimulus with both low and high contrast and presenting probes both pre- and perisaccadically.

## 5.2 Experiment 7. Perisaccadic Mislocalization of Low-contrast and High-Contrast Stimuli

### *5.2.1. Participants*

After informed consent, following the guidelines approved by the institutional review board of Rice University, eight subjects completed this experiment (2 males and 6 females; mean age: 18.5 yrs, ranging from 18 to 19 yrs). All subjects were right-handed, reported having normal or corrected vision. They were recruited from the Rice University campus for fulfillment of course requirements.

### *5.2.2. Apparatus and Stimulus*

The apparatus was identical to that in Experiment 6. There were two different stimulus configurations: In the low-contrast condition, the background was red (10.72 $cd/m^2$) and the probe was green (13.54 $cd/m^2$; contrast ratio: 0.11); whereas in the high-contrast condition, the background was gray (16.92 $cd/m^2$) and the probe was white (70.87 $cd/m^2$; contrast ratio: 0.61). The initial fixation and the saccade target were both black (6.39 $cd/m^2$). Because horizontal and vertical saccades led to similar patterns of spatial bias in the last experiment, only horizontal saccades were examined in this experiment. The number of probe locations was reduced to two for each saccade direction: one at 0 degree, and the other at 15 degree in the left or right visual field for left and right

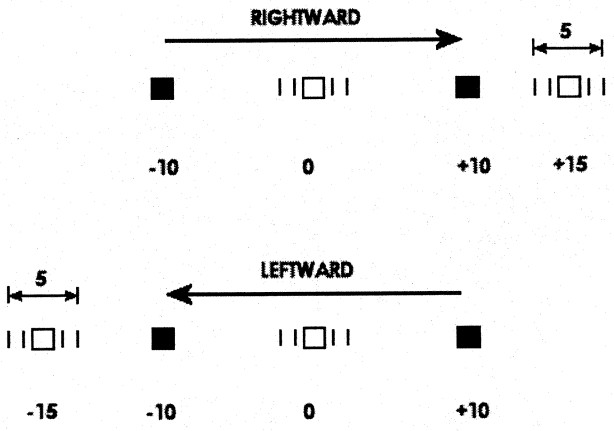


**Figure 15**. Spatial arrangement of stimuli in Experiment 7. The upper half represents stimuli in rightward saccades, and the bottom half leftward saccades. The black squares are initial fixation or saccade target, depending on the saccade direction. The white squares represent the localization probes. The numbers below each stimulus indicate the spatiotopic coordinates in degrees. The vertical short lines flanking the probes indicate the center positions of the probe when it is jittered. The jittering of probe position is within a range of 5 degrees.

saccades, respectively. For each probe location, the actual probe position was randomly jittered within a spatial range of 5 degree, with the center at the specified eccentricity (0 or 15 degree) and a 1-degree separation between adjacent jittering positions. The response, however, was normalized to the real distance between the probe and the saccade target and averaged across all jittered positions belonging to that center eccentricity. The purpose of jittering was to avoid anticipation of probes being in the same location repeatedly.

### *5.2.3. Procedures*

At the beginning of a trial, the initial fixation target appeared at 10-degrees eccentricity in the left or right visual field where the participant was required to fixate. After a random duration between 1500 and 2000 ms, the saccadic target appeared in the opposite visual field, mirroring the initial fixation. The participant made a saccade toward the saccadic target as soon as he or she saw it and kept fixation at the position of the saccadic target until the mouse cursor appeared. In the presaccadic probe condition, the localization probe appeared 50 ms after the onset of saccade target; whereas in the perisaccadic condition, the probe appeared on average 18 ms after the speed of the eye movement exceeded 30°/s, after the initial fixation and the saccadic target were erased. In both conditions, the localization probe was presented for 34 ms. The probe position was randomly selected from either set of jittered locations. At 1000 ms after the presentation of the saccadic target, a white cross, serving as the mouse cursor, appeared at the location of the click at the end of the previous trial. Participants moved the cross to where they perceived the probe and clicked on the left button of the mouse to indicate that they had completed the judgment. In the trials when the probe was not detected, they were

required to click the right mouse button. The computer registered the horizontal position of the cursor for off-line analysis. Participants were free to shift their gaze after the cursor appeared[21]. A trial was discarded if its saccadic magnitude fell out of the range between 15 and 25 degrees or if the probe was not perceived, and the same condition was replaced in the pool of trials for later selection.

There were four independent variables: color type (red-background-green-probe vs. gray-background-white-probe), saccade direction (left vs. right), probe location (0 and 15 degree for rightward saccades, and 0 and –15 degree for leftward saccade), and probe timing (presaccadic or perisaccadic). For each combination of the conditions, there were 15 trials. The main dependent variable was the x-y coordinate of the mouse cursor where the participant marked on the display. Saccade latency, duration, and amplitude were also analyzed to examine if the kinematics of saccades were different across conditions.

### *5.2.4. Data Analysis*

A compression index was calculated to quantify the spatial compression. Note that the compression index defined in this experiment differed from that in Experiment 6 (see section 5.1.4) in that here the presaccadic biases were taken into consideration. The compression was expressed as ratio of perisaccadic to presaccadic components.

The spatial coordinates of localization responses along the saccade dimension were normalized to the coordinate of the saccade target (see Appendix B for details). To simplify the analysis, the horizontal coordinates of probes and localization responses for leftward saccades were reversed in sign and collapsed with the data of rightward saccades.

---

[21] According to Lappe (2004, personal communication), neither the gaze direction nor the initial location of the cursor mattered in his pilot studies of perisaccadic localization.

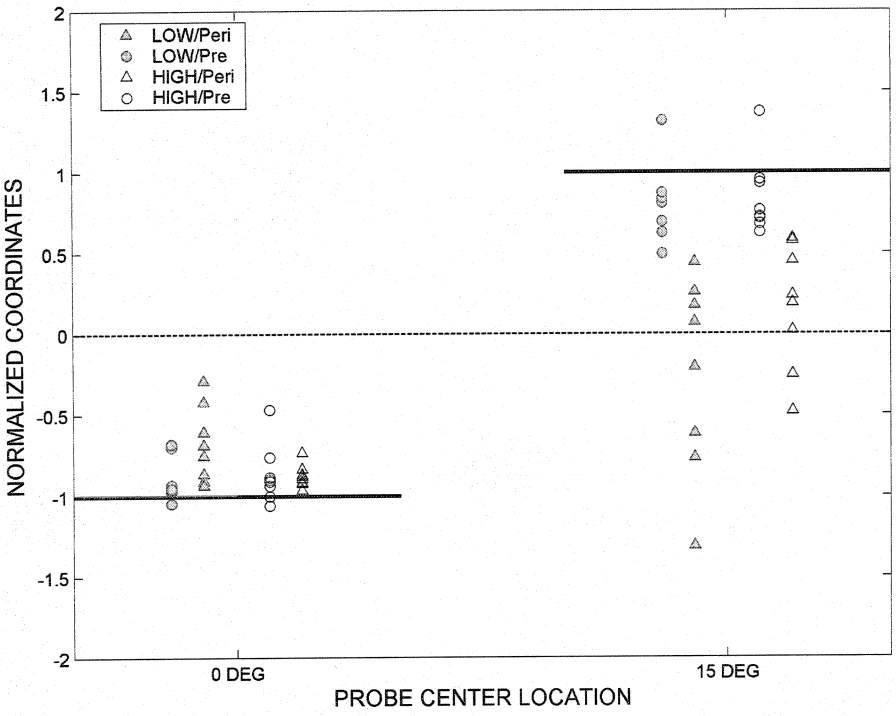


**Figure 16.** The mean normalized coordinates of the localization responses in Experiment 7. Data are from eight participants. Solid symbols represent the low-contrast condition (LOW), and empty symbols the high-contrast condition (HIGH). Triangles represent the perisaccadic condition, and circles represent the presaccadic condition. The probe center location is the geometric center of the jittering positions (see Figure 15 for the definition of jittering). The horizontal solid line segments at each probe location indicate perfect perception when no compression occurred, whereas the dashed line crossing 0 on the ordinate represents complete compression on the saccade target.

In brief, the horizontal coordinate of the perceived probe position relative to the saccadic target was normalized by dividing the physical distance between the probe and the saccade target in that trial. The normalization makes responses at probe positions jittered within the 5-degree range centered at the same spatial location (0 or 15 degree) comparable, and reduces the number of probe positions from ten to two.

The compression index ($I_c$) quantifies the strength of spatial compression. It is defined as 1 minus the ratio of the perisaccadic to presaccadic normalized distance from the saccade target in each condition. A *larger* $I_c$ indicates *stronger* compression toward the saccade target. All dependent measures were subject to a 2 × 2 repeated-measures ANOVA, respectively, with probe position and luminance as the two factors.

### *5.2.5. Results*

*Normalized coordinates.* Figure 16 shows the normalized perceived coordinates of each probe location under both luminance conditions. The non-normalized coordinates can be found in Table E4 and E5 in Appendix E. Responses to perisaccadic probes appear to be farther away from veridical perception (±1) than responses to the presaccadic probes. One can also observe that the presaccadic probes also tended to bias toward the saccade target. This could be a consequence of foveal bias during fixation (Muesseler et al., 1999; Sheth & Shimojo, 2001). This tendency is more obvious for low-contrast probes than for high-contrast probes, meaning more precise perisaccadic localization under the high-contrast condition. The bias is also stronger at the 15-degree probe than at the 0-degree probe. The spatial compression is quantified in the analysis of the compression index.

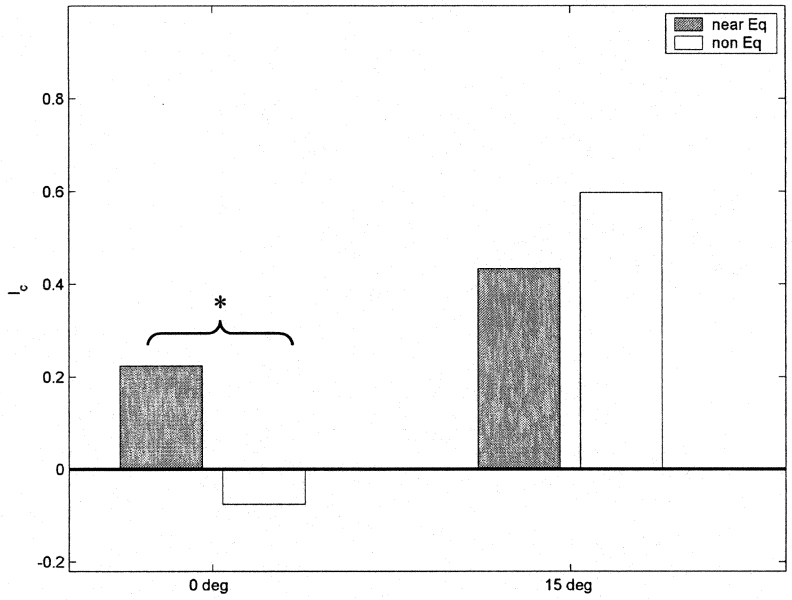


**Figure 17.** The mean compression index ($I_c$) at each probe position under different luminance conditions in Experiment 7. The gray bars indicate $I_c$ in the near equiluminant condition (near Eq), and the white bars indicate mean $I_c$'s in the high-contrast condition (non Eq). An $I_c$ of zero indicates no compression, and an $I_c$ of unity indicates total compression toward the saccade target. A negative $I_c$ means the probe was perceived as farther away from the saccadic target during saccades than before saccades.

*Compression Index* ($I_c$). The mean $I_c$ in each condition for every participant can be found in Table E6. The interaction between type and probe position was significant, $F(1, 7) = 5.96$, $MSE = 0.07$, $p < .05$ (Figure 17). At the 0-degree probe position, compression for the color-defined probe (0.22) was stronger than the luminance-defined probe (-0.07; $p = .06$); whereas at the 15-degree probe position, there was a reversed but insignificant trend showing stronger compression for the high-contrast condition (0.59 vs. 0.43; $p = .22$). The main effect of probe position was significant, $F(1, 7) = 14.57$, $MSE = 0.11$, $p < .01$. The main effect of luminance did not reach significance.

### *5.2.6. Discussion*

Consistent with the last experiment, the spatial compression was in general stronger at the 15-degree probe location. The inhomogeneous mislocalization across the visual fields has not been systematically examined in the literature, but it has been shown in Matsumiya and Uchikawa (2003) and in Morrone et al. (1997, Figure 3). One participant in Morrone et al. (1997)'s localization task showed the same results as the participants in this experiment, whereas the other two showed greater compression at the position between the initial fixation and the saccade target. It is difficult to find a plausible account for inhomogeneity if the pattern is different across individuals. The current results, however, showed clearly stronger perisaccadic compression at locations more eccentric than the saccade target, as opposed to probes between initial fixation and the saccade target. This tendency is more obvious for the high-contrast condition.

The seemingly smaller compression in the low-contrast condition at the 15-degree probe position is not because of the absence of mislocalization. On the contrary, as can be seen in Figure 16, some participants mislocalized the probe opposite the saccade direction

so much that the mean responses approached the straight-ahead (-1.5 on the normalized coordinate for the 15-degree probe). It has been demonstrated that the intrasaccadic sensitivity to equiluminant gratings, one type of stimuli the parvocellular pathway of the visual system is sensitive to, is not suppressed during saccades, whereas the sensitivity to luminant gratings is (Burr, Morrone, & Ross, 1994). Nevertheless, the ability to resolve fine details is not necessarily the same ability as localizing a spatial position. The erratic localization for the low-contrast stimuli can either characterize the spatial representation in the parvocellular visual system, or the spatial representation in the magnocellular system under low contrast. Because the low-contrast stimulus resulted in obvious mislocalization in both probe positions, in Experiment 8 it will be used as the sole stimulus for the localization task.

## 6. EXPERIMENT 8. INFLUENCE OF TMS ON PERISACCADIC MISLOCALIZATION

This experiment examined how TMS modulates the perisaccadic mislocalization. The circular coil was used again in the current experiment to maximize the chance of observing TMS effects. In addition, to enhance the effect of spatial compression, equiluminant stimuli were used for localization.

### *6.1. Participants*

After informed consent, following the guidelines approved by the institutional review board of Rice University, five subjects completed this experiment (one male and four females; mean age: 23.2 yrs, range: 18~23 yrs; two left-handed and three

right-handed)[22]. All subjects reported having normal or corrected vision and no history of any neurological or psychiatric disorders at the time of testing. They were recruited from the Rice University campus and paid for their participation.

### *6.2. Apparatus, Stimulus, and Procedures*

The apparatus was the same as those in previous experiments. The stimulus configuration was the same as that in the equiluminant condition of Experiment 7 (see 5.1.2), except that the intensity of the green probe was matched with the red background (luminance fixed at 13.7 cd/m$^2$) with minimal flicker photometry for each subject. The average luminance of the matched green color was 14.67 cd/m$^2$, with a range between 13.28 ~ 16.23 cd/m$^2$. The probe positions were jittered around 0, 15, or –15 degree in the same way as those in Experiment 7.

*TMS administration.* The procedures were also similar to those in Experiment 7, except that TMS was administrated in 3/4 of the trials. The average motor threshold of the circular coil was 36% (0.79 Tesla), and the average TMS intensity in the experiment was thus 40% (0.88 Tesla). The experiment was divided into two sessions, each with a different TMS site: the right posterior parietal cortex and a right frontal control site (positions of the coil is the same as those in Section 4.1.5). For each TMS site, there were three factors: saccade direction (left/right), the probe position (+15 and 0 degrees or –15 and 0 degree), probe onset (presaccadic or perisaccadic) and the TMS administration (50/100/150/No TMS). There were 10 trials for each combination of the above factors, totaling 200.

---

[22] Eight participants were actually recruited for this experiment, but three of them cannot do the task because of blinking triggered by TMS. The computer algorithm detecting saccades online cannot tell blinking from saccades, and will present the displacement at the wrong time if a participant blinks in a trial.

### *6.3. Data Analysis*

The coordinates localization responses were normalized in the same fashion as in Experiment 7, as was the compression index. To recap the definition: a normalized coordinate of 0 indicates the localization response was exactly at the saccade target, and a normalized coordinate of ±1 indicates the localization response was exactly at the 0 or ± 15 degree probe location (the sign determined by the saccade direction and probe position); a compression index ($I_c$) of unity indicates complete compression toward the saccade target, whereas a compression index of zero indicates no compression at all.

For the analysis of the compression index, the mean $I_c$ of the No TMS condition was subtracted from the other TMS conditions to obtain the measure of TMS modulation on spatial compression. The TMS modulation on spatial compression of each condition was were subject to a 2 × 2 × 3 repeated-measure ANOVA, with probe positions (0/15 degree), saccade direction (leftward/rightward), and TMS (100/150/200 ms) onsets as the three factors.

### *6.4. Results*

*Normalized coordinates*. The mean normalized coordinates of responses for each participant are depicted in Figure 18 (also see Table E7 and E8 in Appendix E for the mean and standard deviation of non-normalized coordinates in each condition). The red symbols represent perisaccadic localization responses, whereas the black symbols represent presaccadic responses. From visual inspection, the red symbols are generally closer to the zero on the ordinate than the black symbols are, meaning that the perisaccadic perceived locations were closer to the saccadic target than the presaccadic

perceived locations were. In other words, there was a tendency of perisaccadic compression toward the saccade target. The compression index quantified this tendency in each condition.

*Compression Index.* Figure 19 shows the difference between leftward and rightward saccades in TMS modulation. A positive value on the ordinate indicates a stronger modulation during leftward than rightward saccades, and a negative value indicates the opposite. For the posterior parietal TMS, there was a significant 3-way interaction, $F$ (2, 8) = 45.54, $MSE$ = 0.001, $p < .00001$. The 3-way interaction was because the relative strength of compression between leftward and rightward saccades varied in each probe position and TMS onset. Linear contrast found that the difference between leftward and rightward saccades only reached significance at the 200-ms TMS onset: For the 0-degree probe position, leftward saccades resulted in *stronger* spatial compression than rightward saccades (leftward vs. rightward difference = 0.09; $p < .01$), whereas for the 15-degree probe position, leftward saccades resulted in *weaker* spatial compression than rightward saccades ($p = .06$).

Besides the 3-way interaction, the TMS onset × probe position interaction was significant, $F$ (2, 8) = 40.45, $MSE$ = 0.0007, $p < .00001$, and the main effect of TMS onsets was also significant, $F$ (2, 8) = 26.52, $MSE$ = 0.001, $p < .001$. These effects are not explored further because of the significant 3-way interaction. No effect in the frontal control site approached significance because of greater variance[23](see Table E9 for the mean $I_c$ in each condition for every participant).

---

[23] The L-R TMS modulation on spatial compression of the 0-degree probe at the 100-ms TMS onset would be significantly greater than 0 for the frontal control site, if subject to the linear contrast regardless of the absence of a three-way interaction.

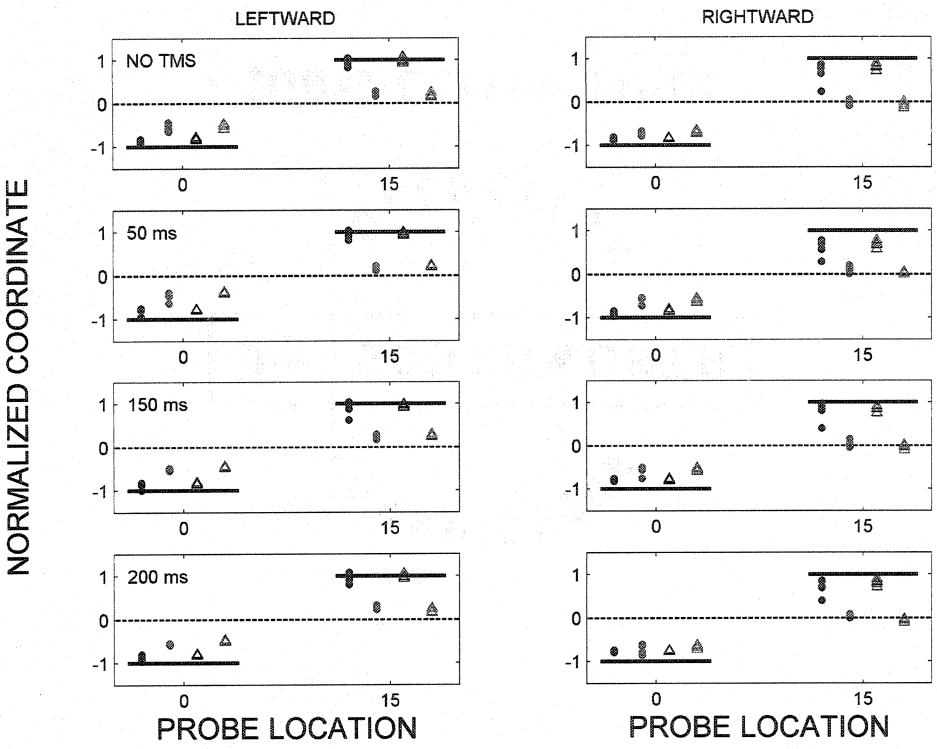


**Figure 18.** The mean normalized coordinates of localization responses in Experiment 8. Data were from five participants. Each individual symbol represents the mean response of a participant in that condition. Circles represent responses from the parietal TMS site, and triangles represent responses from the frontal TMS site. Black symbols represent the presaccadic conditions, and red symbols represent the perisaccadic conditions. The horizontal solid line segments at each probe location indicate perfect perception when no compression occurred, whereas the dashed line crossing 0 on the ordinate represents complete compression on the saccade target.

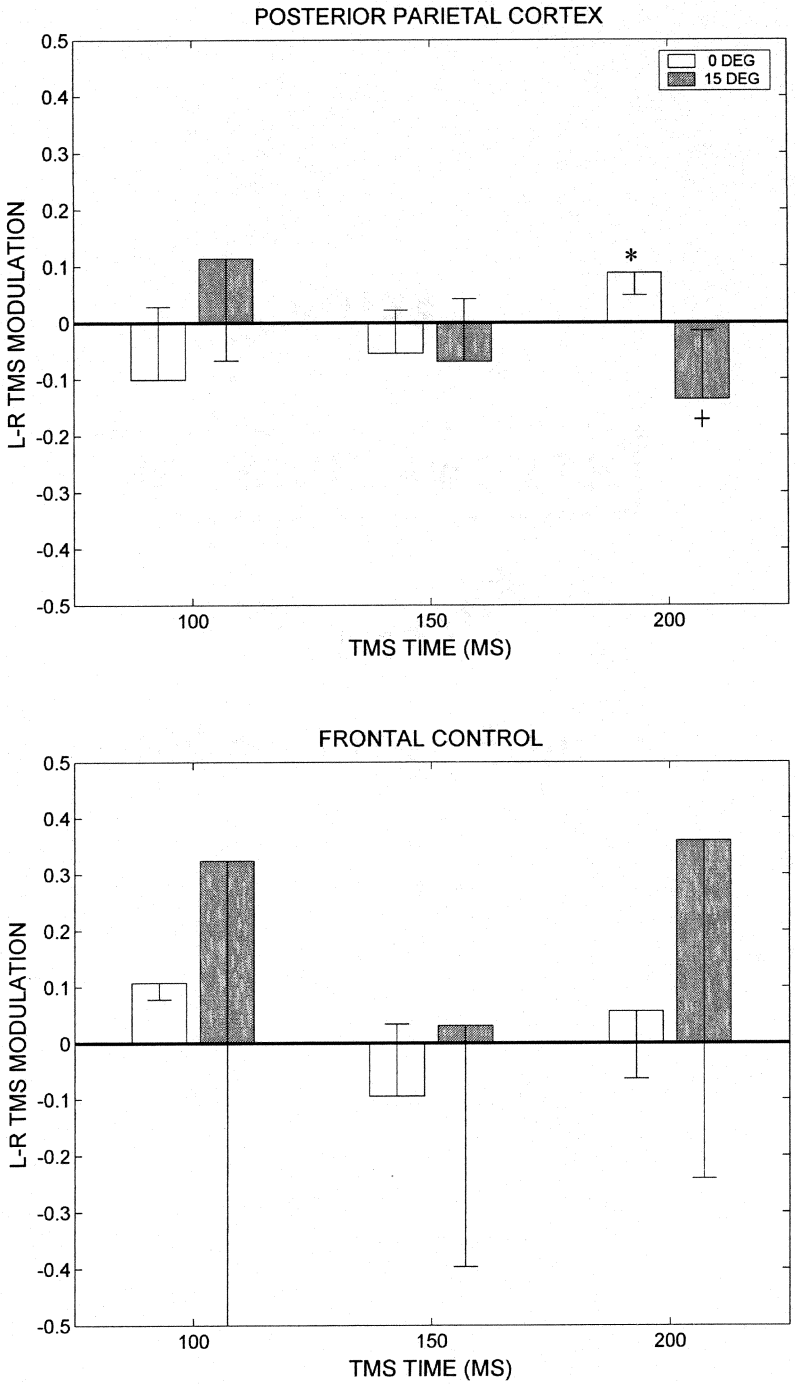


**Figure 19.** TMS modulation of spatial compression in Experiment 8. Each bar represents the difference between leftward and rightward saccades in that condition. The asterisk above a bar indicates significant difference between leftward and rightward saccades in that condition (i.e., the bar's height is significantly different from zero), and the cross indicates marginal significance ($p = .066$). The error bars represent one standard deviation from the mean.

*6.5. Discussion*

The results of compression index indicate that TMS only influenced spatial compression when applied over the PPC. Generally speaking, TMS resulted in greater difference between leftward and rightward saccades when applied at the 200 ms. The way TMS modulated the relative strength of compression during the two saccade directions, however, was opposite at different probe positions: At the 0-degree probe, the compression toward the saccade target was stronger during leftward than during rightward saccades, whereas at the ±15-degree probe, the compression toward the saccade target was weaker during leftward than during rightward saccades. Figure 20 depicted the differential TMS modulation at the 200-ms onset graphically.

This result can be interpreted as indicating that TMS over the right PPC reduces the spatial compression in the left visual field by disrupting the remapping of spatial representation. When a probe is flashed at -15-degree during a leftward saccade, it falls in the left visual field. One hypothesis to account for spatial compression is that different groups of parietal neurons representing old and new receptive fields respond simultaneously and thus a position is perceived to be in a wider range of physical space when activity of both types of neurons are accessed by a higher level mechanism (Burr & Morrone, 2003; Ross et al., 2001a; Morrone et al., 1997; Ross et al., 1997). TMS over the right PPC may have disrupted the processing of EEPI and the remapping of receptive fields in the left visual field. Spatial compression is reduced because fewer neurons are responding to new receptive fields, and the collective neuronal activity more consistently represents the old position. In contrast, a probe flashed at the 15-degree position during a rightward saccade falls in the right visual field, where the remapping process is not disturbed by the TMS. Factors causing spatial compression remain the same, and thus

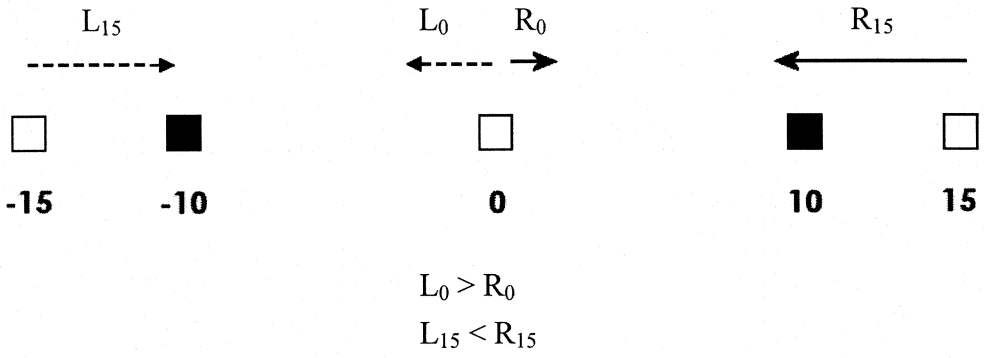


**Figure 20**. Illustration of the TMS-modulated strength of spatial compression in Experiment 8. This effect occurred at the 200-ms TMS onset for the PPC site. The black squares are the initial fixation or the saccade target, depending on the saccade direction. The arrows $L_0$ and $R_0$ represent the strength of spatial compression during leftward and rightward saccades, respectively, at the 0-degree probe position; the arrows $L_{15}$ and $R_{15}$ represent the strength of spatial compression during leftward and rightward saccades, respectively, at the 0-degree probe position. The strength of compression at the 15-dgeree probe positions is larger than that at the 0-degree. At different probe positions, the way TMS modulated the compression strength was different: at the 0-degree probe position, TMS made the compression toward the saccade target stronger for leftward than for rightward saccades; whereas at the 15-degree probe position, the pattern reversed.

spatial compression in this condition is relatively stronger than that during leftward saccades.

The same logic applies to the 0-degree probe position. For a leftward saccade, before the participant started the localization response, the probe position was in the right visual field, which should be represented in the left hemisphere and not subject to the influence of TMS over the right PPC. In contrast, for a rightward saccade, the 0-degree probe fell in the left visual field before the localization response started and is subject to the TMS influence. Because of the same reason that spatial compression is reduced in the LVF but not in the RVF, the compression strength at 0-degree is thus stronger during a leftward than during a rightward saccade.

# 7. GENERAL DISCUSSION

This dissertation is motivated by two main questions: First, does the cortical site that contributes to visuomotor integration across saccades also play a role in perisaccadic perceptual stability? Second, is there a functional relationship between two types of perisaccadic perceptual changes, namely saccadic suppression of displacement and mislocalization? The four series of experiments conducted in this study have provided answers to these questions.

## *7.1. Contribution of the Current Dissertation*

In regard to the first question, two novel findings from TMS experiments are consistent with the idea that the PPC is the site, or at least one of the sites, contributing to visual stability: Experiment 4 showed that TMS over the PPC increased the strength of SSD along the saccade direction contralateral to the TMS site; moreover, Experiment 8

showed that TMS over the PPC reduces the spatial compression at the visual field contralateral to the stimulation. These two results indicate, for the first time in the literature studying healthy human population, that the PPC is not only responsible for perisaccadic visuomotor integration, but also contributes to perisaccadic visuospatial perception.

With respect to the second question, the successful application of a mathematical model (section 3.4) in explaining the directional effect of SSD (Experiment 1 and 2) suggests that SSD can be viewed as the consequence of compressed perceived distance during saccades. The stronger SSD in the saccade direction is because the displacements *in* the saccade direction "shrink" more than those opposite saccade direction. The connection between perisaccadic mislocalization and SSD has been speculated elsewhere (Matsumiya & Uchikawa, 2003; also see Michels & Lappe, 2004 for the potential link between perisaccadic mislocalization and other types of saccadic suppression), but the current dissertation is the first study demonstrating this connection quantitatively.

Another contribution of this dissertation is that it shows that saccadic suppression is not omnidirectional. Experiment 3 clearly demonstrated that SSD is stronger along the dimension collinear with the saccade direction than along the dimension orthogonal to saccades. This result provides additional support that extraretinal factors in addition to visual masking are involved with SSD: the EEPI may compensate for image displacements or trigger mechanisms suppressing the perception of displacement. This operation is direction specific, as suggested by the modeling results in section 3.4.

Finally, this dissertation also demonstrated systematically that the strength of perisaccadic mislocalization is inhomogeneous in the visual field, and is modulated by the luminance condition of the stimulus. In general the mislocalization is stronger for

targets more eccentric than the saccade target. For positions in between the initial fixation and saccade target, the mislocalization is only observed for equiluminant stimulus. This result suggests that the parvocellular pathway, which is not suppressed during saccades, may indirectly contribute to the perisaccadic mislocalization.

### *7.2. Potential Neural Mechanisms Underlying Visual Stability in the PPC*

The cortical mechanisms underlying SSD and perisaccadic mislocalization will now be elaborated further. Prior to saccade onset, the receptive fields of some neurons representing the visual space start shifting toward their future location, while others remain responding only to the original receptive fields (Duhamel, Colby et al., 1992; Kusunoki, Colby, Duhamel, & Goldberg, 1997; Kusunoki & Goldberg, 2003). The same physical location induces the neural activities encoding different locations, and thus make the brain regions receiving inputs from both group of neurons interpret stimuli arising from a wide region of space as being from the same location (Burr & Morrone, 2003), which is phenomenally spatial compression. Following the same vein, SSD occurred because the initial and end point of the displacement are considered as the same location or locations much closer than they actually are. When the remapping of receptive field is disturbed, it is possible to reduce the extent of spatial compression, and consequently the strength of SSD. Applying TMS over the right PPC might have disrupted the remapping process and resulted in the reduced strength of spatial compression and SSD in the left visual field. The results of Experiment 4 and 8 support this hypothesis. This hypothesis also predicts more precise perisaccadic perception of locations in the visual field contralateral to the stimulated hemisphere because of the removal of spatial compression. Whether this prediction is true or not awaits further study.

One may wonder whether TMS over the PPC also reduces sensitivity to displacement during fixation. It has been demonstrated that TMS over V5/MT interferes the processing of continuous motion (Theoret, Kobayashi, Ganis, Di Capua, & Pascual-Leone, 2002; McGraw, Walsh, & Barrett, 2004) and apparent motion (Beckers & Zeki, 1995). Technically detecting apparent motion is different from detecting displacements. Even if V5/MT do contribute to SSD, the temporal parameters that TMS influences motion detection and SSD may be very different. In Beckers and Zeki (1995), TMS modulated the perception of apparent motion when applied at –20 ms to +10 ms from the onset of visual stimulation. In Experiment 4 of this dissertation, the displacement occurred between 22 to 40 ms after saccade onset. The TMS closest to saccade onset is applied 200 ms after the onset of saccade target. The average saccade onset is 250 ms after the target is presented. Thus, there is a 72-ms minimal gap in time between TMS and the displacement, which seems to be outside the time window of Beckers and Zeki's TMS effect on V5. The TMS effect on SSD in Experiment 4 is thus probably different form the TMS effect on apparent motion in Beckers and Zeki (1995).

The introduction made the distinction between SSD and other types of saccadic suppression. A recent study found that, while retinal phosphenes caused by electrical stimulation were suppressed during saccades, cortical phosphenes induced by TMS over V1 were not (Thilo, Santoro, Walsh, & Blakemore, 2004). This suggests that the site of saccadic suppression of vision (SSV) is at a level earlier than V1, probably somewhere between retina and V1, such as LGN (Reppas et al., 2002). Putting Thilo et al.'s results together with the result that the PPC is involved in SSD, the current study provides another piece of evidence that the suppression of displacement involves mechanisms different from the suppression of light sensitivity during saccades (Matin, 1974;

Volkmann, 1986; Li & Matin, 1997; MacAskill et al., 2003) .

*7.3. Future Directions*

Although the current study supports the role of extraretinal processes (in the PPC) in visual stability, it does not exclude the involvement of other processes or cortical regions. The clear postsaccadic scene may also mask intrasaccadic perception (Campbell & Wurtz, 1978; Deubel, Schneider, & Bridgeman, 2002; Deubel et al., 1996). The contribution of visual masking may occur earlier along the visual pathway such as V1 (Breitmeyer, 1984). Moreover, besides the PPC, the predicative remapping of receptive field has also been found in frontal eye field (FEF) (Umeno & Goldberg, 1997), a medial parietal region associated with reaching (Batista et al., 1999), superior colliculus (Walker et al., 1995), and in earlier stages in the extrastriate cortex such as V4, V3, and V4 (Nakamura & Colby, 2002). These neural substrates could potentially contribute to visual stability or instabilty. The lack of effect in frontal TMS condition in Experiment 4 seems to preclude FEF's role in perceptual stability. All of the rest regions but superior colliculus could be examined with TMS.

The potential relationship between SSD and perisaccadic mislocalization, as modeled in section 3.4, is based upon the validity of the model in Morrone et al. (1997). As criticized by Pola (2004), the majority of studies on perisaccadic localization fail to consider the fact that a flash elicits retinal responses lasting for up to a few hundred milliseconds. After considering the temporal impulse response on the retina, the estimated EEPI is very different from that reported by other studies. However, Burr and Morrone (1996) also reported that temporal impulse response becomes faster during saccades. It will be worthwhile to examine which result can be replicated, as it will determine

whether the observed spatial compression can be attributed to EEPI or not, as well as the validity of the model describing the relationship between SSD and mislocalization.

One may also wonder whether the perceptual changes induced by eye presses or paralysis, and the perceived location of afterimages during saccades are also subject to the influence of TMS on the PPC. For the eye press and the intrasaccadic afterimage perception, it should be easy enough to synchronize the single-pulse TMS with the eye movement and examine how subjective experience is altered. With the eye paralysis situation, however, there is no easy way to infer the timing of TMS relative to the generation of the covert intention to move the eye. It has been shown that the conscious awareness of intention to perform voluntary actions lags the sensory consequence of that action (Haggard, Clark, & Kalogeras, 2002; Blakemore, Frith, & Wolpert, 1999). That is, we are ready to perform an action before we are aware of it. If our awareness of our own will occurs later than the consequence of that will, it may not be possible to infer precisely when TMS modulates the generation of efference copy according to the subject's report.

The study of visual stability should be also considered in a wider context of perceptual stability. Not only that we do not "see" things change location as we move our eyes, we do not think there is an earthquake when we walk or feel a still object is moving as we slide our palms over its surface, either. What is asked in studying visual stability leads to questions on stability in other senses: Is our tactile representation of the space distorted by our own body movements? What are the neural substrates maintaining the perceptual stability during walking and active touching? Do perceptual stabilities from difference sensory modalities interact? Similar principles in visual stability may apply to the answers of these questions.

References

Anagnostou, E., Kleiser, R., & Skrandies, W. (2000). Electrophysiological correlates of human intrasaccadic processing. *Experimental Brain Research, 130*(2), 177-187.

Anand, S., & Bridgeman, B. (2002a). An unbiased measure of the contributions of chroma and luminance to saccadic suppression of displacement. *Experimental Brain Research, 142*, 335-341.

Anand, S., & Bridgeman, B. (2002b). An unbiased measure of the contributions of chroma and luminance to saccadic suppression of displacement. *Experimental Brain Research, 142*(3), 335-341.

Andersen, R. A., Essick, G. K., & Siegel, R. M. (1985). Encoding of spatial location by posterior parietal neurons. *Science, 230*, 456-458.

Andersen, R. A., & Gnadt, J. W. (1989). Posterior parietal cortex. In R. H. Wurtz & M. E. Goldberg (Eds.), *The neurobiology of saccadic eye movements. Review of oculomotor research* (Vol. 3, pp. 315-335). Amsterdam: Elsevier.

Andersen, R. A., & Mountcastle, V. B. (1983). The influence of the angle of gaze upon the excitability of the light-sensitive neurons of teh posterior parietal cortex. *Journal of Neuroscience, 3*, 532-548.

Awater, H., Krekelberg, B., & Lappe, M. (2000). Perisaccadic visual stimulation changes perceived target positions. *Perception, 29*, 8-8.

Batista, A. P., Buneo, C. A., Snyder, L. H., & Andersen, R. A. (1999). Reach plans in eye-centered coordinates. *Science, 285*(5425), 257-260.

Beckers, G., & Zeki, S. (1995). The Consequences of Inactivating Areas V1 and V5 on Visual-Motion Perception. *Brain, 118*, 49-60.

Beeler, G. (1967). Visual threshold changes resulting from spontaneous saccadic movements. *Vision Research, 7*, 769-775.

Blakemore, S. J., Frith, C. D., & Wolpert, D. M. (1999). Spatio-temporal prediction modulates the perception of self-produced stimuli. *Journal of Cognitive Neuroscience, 11*(5), 551-559.

Blatt, G. J., Anderson, R. A., & Stoner, G. R. (1990). Visual receptive-field organization and corticocortical connections of the lateral intraparietal area. II. changes of motor plan. *Journal of Neurophysiology, 76*, 1457-1464.

Bodis-Wollner, I., Bucher, S., Seelos, K., Paulus, W., Reiser, M., & Oertel, W. (1997). Functional MRI mapping of occipital and frontal cortical activity during voluntary and imagined saccades. *Neurology, 49*(2), 416-420.

Bowen, R. W., Pola, J., & Matin, L. (1974). Visual persistence: Effects of flash luminance,

duration and energy. *Vision Research, 14*(4), 295-303.

Breitmeyer, B. G. (1984). *Visual masking: An integrative approach.* Oxford: Clarendon Press.

Breitmeyer, B. G., & Ganz, L. (1976). Implications of sustained and transient channels for theories of visual pattern masking, saccadic suppression, and information processing. *Psychological Review, 83*(1), 1-36.

Bremmer, F., Kusunoki, M., Hoffmann, K. P., & Krekelberg, B. (2002). Neural dynamics of saccadic suppression. *Society of the Neurosciences Abstract, 28 (Program No. 57.2).*

Bridgeman, B. (1975). Correlates of metacontrast in single cells of the cat visual system. *Vision Research, 15*(1), 91-99.

Bridgeman, B. (1995). Extraretinal signals in visual orientation. In B. Bridgeman (Ed.), *Handbook of perception and action* (pp. 191-223). New York: Academic Press.

Bridgeman, B., & Fisher, B. (1990). Saccadic suppression of displacement is strongest in central vision. *Perception, 19*(1), 103-111.

Bridgeman, B., Hendry, D., & Stark, L. (1975). Failure to detect displacement of the visual world during saccadic eye movements. *Vision Research, 15*(6), 719-722.

Bridgeman, B., Lewis, S., Heit, G., & Nagle, M. (1979). Relation between cognitive and motor-oriented systems of visual position perception. *Journal of Experimental Psychology, 5*, 692-700.

Bridgeman, B., & Macknik, S. L. (1995). Saccadic suppression relies on luminance information. *Psychological Research, 58*(3), 163-168.

Bridgeman, B., & Stark, L. (1979). Omindirectional increase in threshold for image shifts during saccadic eye movements. *Perception and Psychophysics, 25*, 241-243.

Bridgeman, B., & Stark, L. (1991). Ocular proprioception and efference copy in registering visual direction. *Vision Research, 31*(11), 1903-1913.

Bridgeman, B., Van der Hejiden, A. H. C., & Velichkovsky, B. M. (1994). A theory of visual stability across saccadic eye movements. *Behavioral and Brain Sciences, 17*(2), 247-292.

Brindley, G. S., Goodwin, G. M., Kulikowski, J. J., & Leighton, D. (1976). Stability of vision with a paralysed eye. *Journal of Physiology, 258*, 65-66.

Burr, D. C., & Morrone, C. (1996). Temporal impulse response functions for luminance and colour during saccades. *Vision Research, 36*(14), 2069-2078.

Burr, D. C., & Morrone, M. C. (2003). Visual perception during saccades. In L. M. Chalupa & J. S. Werner (Eds.), *The Visual Neurosciences* (Vol. 2, pp. 1391-1401). Cambridge, MA: The MIT Press.

Burr, D. C., Morrone, M. C., & Ross, J. (1994). Selective suppression of the magnocellular visual pathway during saccadic eye movements. *Nature, 371*(6497), 511-513.

Cai, R. H., Pouget, A., Schlag Ray, M., & Schlag, J. (1997). Perceived geometrical relationships affected by eye-movement signals. *Nature, 386*(6625), 601-604.

Campbell, F. W., & Wurtz, R. H. (1978). Saccadic omission: Why we do not see a grey-out during a saccadic eye movement. *Vision Research, 18*(1297-1303).

Castet, E., Sebastien, J., & Masson, G. S. (2001). "Saccadic suppression"--no need for an active extra-retinal mechanism. *Trends in Neurosciences, 24*(6), 316-317.

Dassonville, P., Schlag, J., & Schlag Rey, M. (1992). Oculomotor localization relies on a damped representation of saccadic eye displacement in human and nonhuman primates. *Visual Neuroscience, 9*(3-4), 261-269.

Deubel, H., Schneider, W. X., & Bridgeman, B. (1996). Postsaccadic target blanking prevents saccadic suppression of image displacement. *Vision Research, 36*(7), 985-996.

Deubel, H., Schneider, W. X., & Bridgeman, B. (2002). Transsaccadic memory of position and form. In *Brain's Eye: Neurobiological and Clinical Aspects of Oculomotor Research* (Vol. 140, pp. 165-180).

Diamond, M. R., Ross, J., & Morrone, M. C. (2000). Extraretinal control of saccadic suppression. *Journal of Neuroscience, 20*(9), 3449-3455.

Dodge, R. (1900). Visual perception during eye movement. *Psychological Review, 2*, 193-199.

Dodge, R. (1905). The illusion of clear vision during eye movement. *Psychological Bulletin, 2*(6), 193-199.

Dodge, R., & Cline, T. S. (1901). The angle velocity of eye movements. *Psychological Review, 8*, 145-157.

Donaldson, I. M. L. (2000). The functions of the proprioceptors of the eye muscles. *Philosophical Transactions of the Royal Society of London Series B-Biological Sciences, 355*(1404), 1685-1754.

Donkelaar, P., & Muri, R. (2001). Craniotopic updating of visual space across saccades in the human posterior parietal cortex. *Proceedings of the Royal Society, 269*, 735-739.

Driver, J., Vuilleumier, P., & Husain, M. (2004). Spatial neglect and extinction. In M. S. Gazzaniga (Ed.), *The cognitive neurosciences* (III ed.). Cambridge, MA: The MIT Press.

Duhamel, J.-R., Colby, C. L., & Goldberg, M. E. (1992). The updating of the representation of visual space in parietal cortex by intended eye movemments.

*Science, 225*, 90-92.

Duhamel, J.-R., Goldberg, M. E., & Fitzgibbon, E. J. (1992). Saccadic dysmetria in a patient with a right frontoparietal lesion. *Brain, 115*, 1387-1402.

Enright, J. T. (1994a). Voluntary oscillopsia - watching the world go round. *Behavioral and Brain Sciences, 17*(2), 260-262.

Enright, J. T. (1994b). Voluntary, rotatory eye movements, with saccade-like velocities, which evoke oscillopsia. *Investigative Ophthalmology & Visual Science, 35*(4), 1549-1549.

Fierro, B., Brighina, F., Piazza, A., Oliveri, M., & Bisiach, E. (2001). Timing of right parietal and frontal cortex activity in visuo-spatial perception: a TMS study in normal individuals. *Neuroreport, 12*(11), 2605-2607.

Funahashi, S., Bruce, C. J., & Goldman-Rakic, P. S. (1993). Dorsolateral prefrontal lesions and oculomotor delayed-response performance: evidence of "mnemonic" scotomas. *Journal of Neuroscience, 13*, 1479-1497.

Garcia Perez, M. A., & Peli, E. (2001). Intrasaccadic perception. *Journal of Neuroscience, 21*(18), 7313-7322.

Gauthier, G. M., Nommay, D., & Vercher, J. L. (1990). The role of ocular muscle proprioception in visual localization of targets. *Science, 249*(4964), 58-61.

Gaymard, B., Rivaud, S., & Pierrotdeseilligny, C. (1994). Impairment of extraretinal eye position signals after central thalamic lesions in Humans. *Experimental Brain Research, 102*(1), 1-9.

Gibson, J. J. (1966). *The senses considered as perceptual systems*. Boston: Houghton Mifflin.

Gilmore, R. O., & Johnson, M. H. (1997a). Body-centered representations for visually-guided action emerge during early infancy. *Cognition, 65*(1), B1-B9.

Gilmore, R. O., & Johnson, M. H. (1997b). Egocentric action in early infancy: Spatial frames of reference for saccades. *Psychological Science, 8*(3), 224-230.

Goldberg, M. E., & Bruce, C. J. (1990). Primate frontal eye fields. III. Maintenance of a spatially accurate saccade signal. *Journal of Neurophysiology, 64*, 489-508.

Goldberg, M. E., Colby, C. L., & Duhamel, J.-R. (1990). Representation of visuomotor space in the parietal lobe of the monkey. *Cold Spring Harbor Symp, 55*, 729-739.

Haarmeier, T., Thier, P., Repnow, M., & Petersen, D. (1997). False perception of motion in a patient who cannot compensate for eye movements. *Nature, 389*(6653), 849-852.

Haggard, P., Clark, S., & Kalogeras, J. (2002). Voluntary action and conscious awareness. *Nature Neuroscience, 5*(4), 382-385.

Hallett, P. E., & Lightstone, A. D. (1976). Saccadic eye movements towards stimuli triggered by prior saccades. *Vision Research, 16*(1), 99-106.

Hansen, R. M., & Skavenski, A. A. (1985). Accuracy of spatial localizations near the time of saccadic eye movements. *Vision Research, 25*(8), 1077-1082.

Heide, W., Blankenburg, M., Zimmermann, E., & Kompf, D. (1995). Cortical control of double-step saccades - implications for spatial orientation. *Annals of Neurology, 38*(5), 739-748.

Heide, W., & Kompf, D. (1998). Combined deficits of saccades and visuo-spatial orientation after cortical lesions. *Experimental Brain Research, 123*, 164-171.

Helmholtz, H. v. (1925). *Helmholtz's treatise on physiological optics* (J. P. C. Southall, Trans. III ed. Vol. III). New York: The Optical Society of America.

Heywood, S., & Churcher, J. (1981). Direction-specific and position-specific effects upon detection of displacements during saccadic eye movements. *Vision Research, 21*(2), 255-261.

Hogg, R. V., & Craig, A. T. (1995). *Introduction to Mathematical Statistics* (5 ed.). Englewood Cliffs, N.J.: Prentice Hall.

Holt, E. B. (1903). Eye-movement and central anaesthesia. *Psychological Monographs, 4*(1), 1-45.

Honda, H. (1989). Perceptual localization of visual stimuli flashed during saccades. *Perception and Psychophysics, 45*(2), 162-174.

Honda, H. (1991a). Position constancy and eye position information. *Japanese Psychological Review, 34*(1), 17-36.

Honda, H. (1991b). The time course of visual mislocalization and of extraretinal eye position signals at the time of vertical saccades. *Vision Research, 31*, 1915-1921.

Honda, H. (1993). Saccade-contingent displacement of the apparent position of visual stimuli flashed on a dimly illuminated structured background. *Vision Research, 33*(5-6), 709-716.

Honda, H. (1995). Visual mislocalization produced by a rapid image displacement on the retina: Examination by means of dichoptic presentation of a target and its background scene. *Vision Research, 35*(21), 3015-3020.

Honda, H. (1997). Interaction of extraretinal eye position signals in a double-step saccade task: Psychophysical estimation. *Experimental Brain Research, 113*(2), 327-336.

Honda, H. (1999). Modification of saccade-contingent visual mislocalization by the presence of a visual frame of reference. *Vision Research, 39*(1), 51-57.

Inghilleri, M., Berardelli, A., Cruccu, G., & Manfredi, M. (1993). Silent period evoked by transcranial stimulation of the human cortex and cervicomedullary junction. *Journal*

*of Physiology, 466*, 521-534.

James, W. (1950). *The principles of psychology* (Vol. 2). New York: Dover.

Kaiser, M., & Lappe, M. (2004). Perisaccadic mislocalization orthogonal to saccade direction. *Neuron, 41*(2), 293-300.

Kelly, D. H. (1979). Motion and vision .2. stabilized spatio-temporal threshold surface. *Journal of the Optical Society of America, 69*(10), 1340-1349.

King Smith, P. E., Grigsby, S. S., Vingrys, A. J., & Benes, S. C. (1994). Efficient and unbiased modifications of the QUEST threshold method: Theory, simulations, experimental evaluation and practical implementation. *Vision Research, 34*(7), 885-912.

Kleiser, R., & Skrandies, W. (2000). Neural correlates of reafference: evoked brain activity during motion perception and saccadic eye movements. *Experimental Brain Research, 133*(3), 312-320.

Krekelberg, B., Kubischik, M., Hoffmann, K. P., & Bremmer, F. (2003). Neural correlates of visual localization and perisaccadic mislocalization. *Neuron, 37*(3), 537-545.

Kusunoki, M., Colby, C. L., Duhamel, J. R., & Goldberg, M. E. (1997). The role of the lateral intraparietal area in the control of visuospatial attention. In H. Sakata, A. Mikami & J. M. Fuster (Eds.), *In The Assoication Cortex: Structure and Function* (pp. 191-206). New York: Academic Press.

Kusunoki, M., & Goldberg, M. E. (2003). The time course of perisaccadic receptive field shifts in the lateral intraparietal area of the monkey. *Journal of Neurophysiology, 89*, 1519-1527.

Lappe, M., Awater, H., & Krekelberg, B. (2000). Postsaccadic visual references generate presaccadic compression of space. *Nature, 403*(6772), 892-895.

Latour, P. L. (1962). Visual threshold during eye movements. *Vision Research, 2*, 261-262.

Li, W., & Matin, L. (1990a). The influence of saccade length on the saccadic suppression of displacement detection. *Perception and Psychophysics, 48*(5), 453-458.

Li, W., & Matin, L. (1990b). Saccadic suppression of displacement: Influence of postsaccadic exposure duration and of saccadic stimulus elimination. *Vision Research, 30*(6), 945-955.

Li, W., & Matin, L. (1997). Saccadic suppression of displacement: Separate influences of saccade size and of target retinal eccentricity. *Vision Research, 37*(13), 1779-1797.

Lynch, J. C., Graybiel, A. M., & Lobeck, L. J. (1985). The differential projection of two cytoarchitectonic subregions of the inferior parietal lobule of macaque upon the deep layers of the superior colliculus. *Journal of Comparative Neurology, 235*(2),

241-254.

MacAskill, M. R., Jones, R. D., & Anderson, T. J. (2003). Saccadic suppression of displacement: Effects of illumination and background manipulation. *Perception, 32*(4), 463-474.

MacAskill, M. R., Muir, S. R., & Anderson, T. J. (1999). Saccadic suppression and adaptation: Revisiting the methodology. In W. Becker, H. Deubel & T. Mergner (Eds.), *Current oculomotor research* (pp. 93-95). New York: Plenum Press.

Mack, A. (1970). An investigation of the relationship between eye and retinal image movement in the perception of movement. *Perception and Psychophysics, 8*, 291-298.

Mack, A., Fendrich, R., & Pleune, J. (1978). Adaptation to an altered relation between retinal image displacements and saccadic eye movements. *Vision Research, 18*, 1321-1327.

Mackay, D. M. (1970). Elevation of visual threshold by displacement of retinal image. *Nature, 225*, 90-92.

Mackay, D. M. (1973). Visual stability and voluntary eye movements. In R. Jung (Ed.), *Handbook of sensory physiology.* Berlin: Springer.

Macknik, S. L., Fisher, B. D., & Bridgeman, B. (1991). Flicker distorts visual space constancy. *Vision Research, 31*(2057-2064).

Manning, K. A., & Riggs, L. A. (1984). Vergence eye movements and visual suppression. *Vision Research, 24*(6), 521-526.

Mapp, A. P., Barbeito, R., Bedell, H. E., & Ono, H. (1989). Visual localization of briefly presented peripheral targets. *Biological Cybernetics, 60*(4), 261-265.

Martinez-Trujillo, J. C., & Treue, S. (2002). Attentional modulation strength in cortical area MT depends on stimulus contrast. *Neuron, 35*(2), 365-370.

Mateeff, S., & Gourevich, A. (1983). Peripheral vision and perceived visual direction. *Biological Cybernetics, 49*(2), 111-118.

Matin, E. (1974). Saccadic suppression: A review and an analysis. *Psychological Bulletin, 81*(12), 899-917.

Matin, E. (1982a). Saccadic suppression and the dual mechanism theory of direction constancy. *Vision Research, 22*(2), 335-336.

Matin, E. (1986). Visual localization and eye movements. In K. R. Boff, L. Kaufman & J. P. Thomas (Eds.), *Handbook of perception and human performance* (Vol. 2). New York: Wiley.

Matin, E., Clymer, A., & Matin, L. (1972). Metacontrast and saccadic suppression. *Science, 178*, 179-182.

Matin, L. (1965). Visual perception of direction for stimuli flashed during voluntary saccadic eye movements. *Science, 148*, 1485-1487.

Matin, L. (1982b). Visual localization and eye mvoements. In A. Wertheim, W. A. Wagenaar & H. Leibowitz (Eds.), *Tutorials on motion perception* (pp. 101-156). New York: Plenum.

Matin, L., & Bowen, R. W. (1976). Measuring the duration of perception. *Perception and Psychophysics, 20*(1), 66-76.

Matin, L., Matin, E., & Pearce, D. G. (1969). Visual perception of direction when voluntary saccades occur: I. Relation of visual direction of a fixation target extinguished before a saccade to a flash presented during the saccade. *Perception and Psychophysics, 5*(2), 65-80.

Matin, L., Matin, E., & Pola, J. (1970). Visual perception of direction when voluntary saccades occur: II. Relation of visual direction of a fixation target extinguished before a saccade to a subsequent test flash presented before the saccade. *Perception and Psychophysics, 8*(1), 9-14.

Matsumiya, K., & Uchikawa, K. (2003). The role of presaccadic compression of visual space in spatial remapping across saccadic eye movements. *Vision Research, 43*(18), 1969-1981.

Mays, L. E., & Sparks, D. L. (1980). Dissociation of visual and saccade-related responses in superior colliculus neurons. *Journal of Neurophysiology, 43*, 207-232.

McConkie, G. W., & Currie, C. B. (1996). Visual stability across saccades while viewing complex pictures. *Journal of Experimental Psychology: Human Perception and Performance, 22*(3), 563-581.

McGraw, P. V., Walsh, V., & Barrett, B. T. (2004). Motion-sensitive neurones in V5/MT modulate perceived spatial position. *Current Biology, 14*(12), 1090-1093.

Michels, L., & Lappe, M. (2004). Contrast dependency of sacadic compression and suppression. *Vision Research, 44*(20), 2327-2336.

Miller, J. M. (1996). Egocentric localization of a perisaccadic flash by manual pointing. *Vision Research, 36*(6), 837-851.

Morrone, M. C., Ross, J., & Burr, D. C. (1997). Apparent position of visual targets during real and simulated saccadic eye movements. *Journal of Neuroscience, 17*(20), 7941-7953.

Muesseler, J., Van Der Heijden, A. H. C., Mahmud, S. H., Deubel, H., & Ertsey, S. (1999). Relative mislocalization of briefly presented stimuli in the retinal periphery. *Perception and Psychophysics, 61*(8), 1646-1661.

Muri, R. M., Buhler, R., Heinemann, D., Mosimann, U. P., Felblinger, J., Schlaepfer, T. E.,

et al. (2002). Hemispheric asymmetry in visuospatial attention assessed with transcranial magnetic stimulation. *Experimental Brain Research, 143*(4), 426-430.

Nakamura, K., & Colby, C. L. (2002). Updating of the visual representation in monkey striate and extrastriate cortex during saccades. *Proceedings of the National Academy of Sciences of the United States of America, 99*(6), 4026-4031.

Niemeier, M., Crawford, J. D., & Tweed, D. B. (2003). Optimal transsaccadic integration explains distorted spatial perception. *Nature, 422*(6927), 76-80.

Ono, H., & Nakamizo, S. (1977). Saccadic eye movements during changes in fixation to stimuli at different distances. *Vision Research, 17*, 223-238.

O'Regan, J. K. (1984). Retinal versus extraretinal Influences in flash Localization during saccadic eye movements in the presence of a visible background. *Perception & Psychophysics, 36*(1), 1-14.

Pierrot-Deseilligny, C., Ploner, C. J., Muri, R. M., Gaymard, B., & Rivaud-Pechoux, S. (2002). Effects of cortical lesions on saccadic eye movements in humans. In *Neurobiology of Eye Movements: From Molecules to Behavior* (Vol. 956, pp. 216-229).

Pola, J. (2004). Models of the mechanism underlying perceived location of a perisaccadic flash. *Vision Research, 44*(24), 2799-2813.

Pola, J., & Wyatt, H. (2002). Visual Perception of Direction During a Saccade May Involve an Extravisual Signal that Changes as Rapidly as the Saccade. *Investigative Ophthalmology and Vision Science, 43*(12), 2651-.

Pourtois, G., Vandermeeren, Y., Olivier, E., & de Gelder, B. (2001). Event-related TMS over the right posterior parietal cortex induces ipsilateral visuospatial interference. *Neuroreport, 12*(11), 2369-2374.

Reppas, J. B., Usrey, W. M., & Reid, R. C. (2002). Saccadic eye movements modulate visual responses in the lateral geniculate nucleus. *Neuron, 35*(5), 961-974.

Riggs, L. A., Merton, P. A., & Morton, H. B. (1974). Suppression of visual phosphenes during saccadic eye movements. *Vision Research, 14*(10), 997-1011.

Ro, T., Farne, A., & Chang, E. (2002). Locating the human frontal eye field with transcranial magnetic stimulation. *Journal of Clinical and Experimental Neuropsychology, 24*(7), 926-936.

Robertson, E. M., Theoret, H., & Pascual-Leone, A. (2003). Studies in cognition: The problems solved and created by transcranial magnetic stimulation. *Journal of Cognitive Neuroscience, 15*(7), 948-960.

Robinson, D. A. (1964). The mechanics of human saccadic eye movements. *Journal of Physiology (London), 180*, 569-591.

Rorden, C. (2004a). *MRICro*. Retrieved September 13, 2004, from http://www.psychology.nottingham.ac.uk/staff/cr1/mricro.html

Rorden, C. (2004b). *MRIreg: MRI-to-miniBird registration*. Retrieved September 13, from http://www.psychology.nottingham.ac.uk/staff/cr1/mrireg.html

Rorden, C., & Brett, M. (2000). Stereotaxic display of brain lesions. *Behavioural Neurology, 12*, 191-200.

Ross, J., Morrone, M. C., & Burr, D. C. (1997). Compression of visual space before saccades. *Nature, 386*(6625), 598-601.

Ross, J., Morrone, M. C., Goldberg, M. E., & Burr, D. C. (2001a). Changes in visual perception at the time of saccades. *Trends in Neurosciences, 24*(2), 113-121.

Ross, J., Morrone, M. C., Goldberg, M. E., & Burr, D. C. (2001b). "Saccadic suppression"--no need for an active extra-retinal mechanism: Response. *Trends in Neurosciences, 24*(6), 317-318.

Schiller, P. H., & Tehovnik, E. J. (2001). Look and see: how the brain moves your eyes about. In *Vision: From Neurons to Cognition* (Vol. 134, pp. 127-142).

Schlag, J., Schlag-Rey, M., & Pigarev, I. (1990). Supplementary eye field-influence of eye position on neural signals of fixation. *Experimental Brain Research, 90*, 302-306.

Sherrington, C. S. (1918). Observations on the sensual role of the proprioceptive nerve-supply of the extrinsic ocular muscles. *Brain, 41*, 323-343.

Sheth, B. R., & Shimojo, S. (2001). Compression of space in visual memory. *Vision Research, 41*(3), 329-341.

Snodderly, D. M., Kagan, I., & Gur, M. (2001). Selective activation of visual cortex neurons by fixational eye movements: Implications for neural coding. *Visual Neuroscience, 18*(2), 259-277.

Sommer, M. A., & Wurtz, R. H. (2002). A pathway in primate brain for internal monitoring of movements. *Science, 296*(5572), 1480-1482.

Sperry, R. W. (1950). Neural basis of the spontaneous optokinetic response produced by visual inversion. *Journal of Comparative and Physiological Psychology, 43*, 482-489.

Stark, L. (1976). Saccadic suppression of image displacement. *Vision Research, 16*(10), 1185-1187.

Stevens, J. K., Emerson, R. C., Gerstein, G. L., Kallos, T., Neufeld, G. R., Nichols, C. W., et al. (1976). Paralysis of the awake human: Visual perceptions. *Vision Research, 16*(93-98).

Terao, Y., Fukuda, H., Ugawa, Y., Hikosaka, O., Hanajima, R., Furubayashi, T., et al.

(1998). Visualization of the information flow through human oculomotor cortical regions by transcranial magnetic stimulation. *Journal of Neurophysiology, 80*(2), 936-946.

Theoret, H., Kobayashi, M., Ganis, G., Di Capua, P., & Pascual-Leone, A. (2002). Repetitive transcranial magnetic stimulation of human area MT/V5 disrupts perception and storage of the motion aftereffect. *Neuropsychologia, 40*(13), 2280-2287.

Thiele, A., Henning, P., Kubischik, M., & Hoffmann, K. P. (2002). Neural mechanisms of saccadic suppression. *Science, 295*(5564), 2460-2462.

Thier, P., & Karnath, H. O. (Eds.). (1997). *Parietal lobe contributions to orientation in 3D space.* Berlin, Germany: Springer-Verlag.

Thilo, K. V., Santoro, L., Walsh, V., & Blakemore, C. (2004). The site of saccadic suppression. *Nat Neurosci, 7*(1), 13-14.

Tomas, P. (1995). Extraretinal modulaton of cerebral blood flow in the human visual cortex: implication for saccadic suppression. *Journal of Neurophysiology, 74*, 2179-2183.

Umeno, M. M., & Goldberg, M. E. (1997). Spatial processing in the monkey frontal eye field .1. Predictive visual responses. *Journal of Neurophysiology, 78*(3), 1373-1383.

van der Heijden, A. H. C., van der Geest, J. N., de Leeuw, F., Krikke, K., & Musseler, J. (1999). Sources of position-perception error for small isolated targets. *Psychological Research-Psychologische Forschung, 62*(1), 20-35.

Volkmann, F. C. (1962). Vision during voluntary saccadic eye movements. *Journal of the Optical Society of America, 52*, 571-578.

Volkmann, F. C. (1986). Human visual suppression. *Vision Research, 26*(9), 1401-1416.

Volkmann, F. C., Riggs, L. A., White, K. D., & Moore, R. K. (1978). Contrast sensitivity during saccadic eye movements. *Vision Research, 18*(9), 1193-1199.

von Holst, E., & Mittelstaedt, H. (1971). The principle of reafference: interactions between the central nervous system and the peripheral organs. In P. C. Dodwell (Ed.), *Perceptual processing: stimulus equivalence and pattern recognition.* New York: Appleton.

Walker, M. F., Fitzgibbon, E. J., & Goldberg, M. E. (1995). Neurons in the Monkey Superior Colliculus Predict the Visual Result of Impending Saccadic Eye-Movements. *Journal of Neurophysiology, 73*(5), 1988-2003.

Walsh, V., & Cowey, A. (2000). Transcranial magnetic stimulation and cognitive neuroscience. *Nature Reviews Neuroscience, 1*(1), 73-79.

Watson, A. B., & Pelli, D. G. (1983). QUEST: A Bayesian adaptive psychometric method.

*Perception and Psychophysics, 33*(2), 113-120.

Whipple, W., & Wallach, H. (1978). Direction-specific motion thresholds for abnormal image shifts during saccadic eye movement. *Perception and Psychophysics, 24*, 349-355.

Woodworth, R. S. (1906). Vision and localization during eye mvoements. *Psychological Bulletin, 3*, 68-70.

Yosury, T. A., Schmid, U. D., Alkadhi, H., Schmidt, D., Peraud, A., Buettner, A., et al. (1997). Localization of the motor hand area to a knob on the precentral gyrus: A new landmark. *Brain, 120*, 141-157.

Yu, S. X., & Lee, T. S. (2000). What do V1 neurons tell us about saccadic suppression? *Neurocomputing: An International Journal, 32-33*, 271-277.

# APPENDIX A. THE MORRONE ET AL. (1997) MODEL OF THE RELATIONSHIP BETWEEN REAL AND PERCEIVED SPATIAL POSITIONS

Morrone et al.'s (1997) model is composed of two components. The first component, $O$(t), represented the origin of the internal coordinate system that shifts from the initial fixation ($F_0$ ) to the saccadic target ($F_1$). The shift begins before the onset of the saccade and proceeds gradually overtime following a cumulative gaussian function:

$$O(t) = F_0 + \frac{F_1 - F_0}{\sigma_0\sqrt{2\pi}} \int_{-\infty}^{t} e^{\frac{-(\tau-\tau_0)^2}{2\sigma_0^2}} d\tau , \qquad \text{Eq. A1}^{24}$$

where t is the time relative to the saccadic onset, and $\tau_0$ and $\sigma_0$ are free parameters that describe the peak time and spread of the gaussian function.

The second component is a gain function that modulates the metric of the internal space. When the time is too far away from the saccadic onset, the gain is equal to identity. It decreases to nearly zero, however, in the proximity of saccades.

$$\varphi(t) = 1 - a_0 e^{\frac{-(t-t_1)^2}{2\sigma_1^2}} , \qquad \text{Eq. A2}$$

where $t_1$, $a_0$, and $\sigma_1$ are free parameters describing the strength and time course of the compression. The function of perceived position, $P$(x, t), is expressed in the following formula,

$$P(x,t) = sign(\ E(x,t)\ )\left|\ S\ \right| \left| \frac{E\ (x,t)}{S} \right|^{\varphi(t)} + O(\ t\ ) , \qquad \text{Eq. A3}$$

---

[24] In the paper, the gaussian function in formula A1 was missing a factor 2, which was a printing error after proof (Morrone, January, 2004; personal communication).

where E(x, t) is the retinal eccentricity function defined as the difference between the stimulus position and the position of the eye. The *sign* function converts the actual value into the sign (positive or negative) of the variable, and $S = (F_1 - F_0)/2$ is half the amplitude of the saccade. The eye motion was modeled by assuming constant velocity ($v$) for the duration of the saccade ($t_f$), flanked by zero velocity fixations:

$$E(x,t) = x - v\left( \left| t \right| - \left| t - t_f \right| \right), \qquad \text{Eq. A4}$$

Replacing $E(x, t)$ in Eq. A3 with the actual eye scan trace may result in better fit. In Figure 6, the free parameters in the model were: $\tau_0 = -5$, $\sigma_0 = 25$, $t_1 = -7$, $a_0 = 0.93$, and $\sigma_1 = 5$. Duration of the saccade was assumed to be 80 ms, and the average velocity assumed to be 250 deg/s.

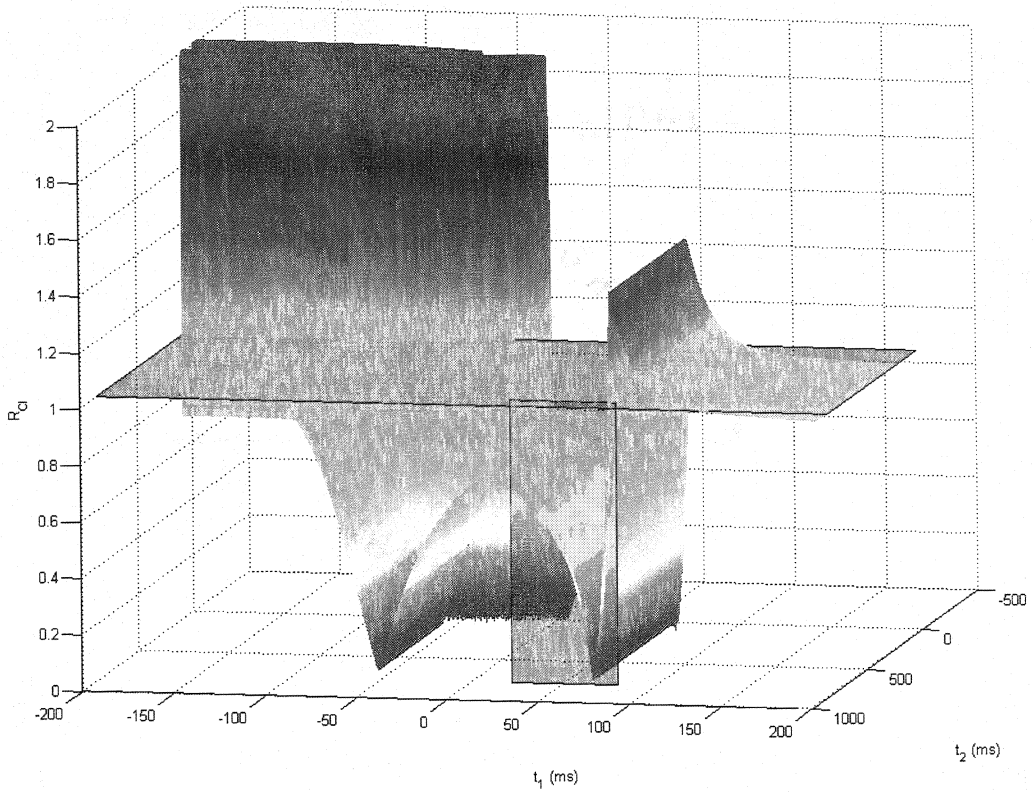


**Figure A1.** Surface plot of the ratio of the perceived size of congruent displacement to incongruent displacement ($R_{CI}$) as a function of the time of registering the initial position ($t_1$) and the final position ($t_2$). The zero on the x- and y-axis is saccade onset. The vertical, red rectangle slices the same temporal parameters as Figure 6 did. The horizontal bluish rectangle represents the level of unity, below which $R_{CI}$ is smaller than one. As can be seen from the figure, when the $t_1$ is between 22 and 80 ms after saccade onset, $R_{CI}$ remains below unity regardless the value of $t_2$.

# APPENDIX B. THE NORMALIZED COORDINATES AND COMPRESSION INDEX FOR PERISACCADIC LOCALIZATION

In Experiment 7 and 8, there were actually two groups of probe positions: one centered on 0 degrees, and the other on 15 or –15 degrees in the allocentric coordinate, depending on the saccade direction. To reduce the number of probe positions in analysis, each group of probe positions was normalized to their respective distance from the saccade target according to the following equation (also see Figure B1),

$$N_{r.pre} = \frac{X_{r.pre} - X_s}{\left|X_p - X_s\right|}, N_{r.peri} = \frac{X_{r.peri} - X_s}{\left|X_p - X_s\right|} \qquad \text{Eq. B1}$$

where $X_{r.pre}$ indicates the horizontal coordinate of localization response to presaccadic probes, $X_{r.peri}$ indicates the horizontal coordinate of localization response to perisaccadic probes, $X_s$ means the physical coordinate of the saccadic target, and $X_p$ means the physical coordinate of the probe. $N_{r.pre}$ and $N_{r.peri}$ indicate the normalized coordinates of responses to presaccadic and perisaccadic probes.

The formal definition of the compression index ($I_c$) is ,

$$I_c = 1 - \left|\overline{N}_{r.peri} / \overline{N}_{r.pre}\right| \qquad \text{Eq. B2}$$

where $\overline{N}$ indicates the averaged normalized coordinates of a condition. $I_c$ should usually vary between 0 and 1, where 0 indicates perisaccadic compression is not different from presaccadic compression, and 1 indicates perisaccadic probe is perceived the same as the

saccade target (complete compression). $I_c$ can be negative if perisaccadic localization of the probe is farther away from saccade target than is the presaccadic localization. $I_c$ can also be infinite if the presaccadic probe location appears to be the same as the saccadic target.

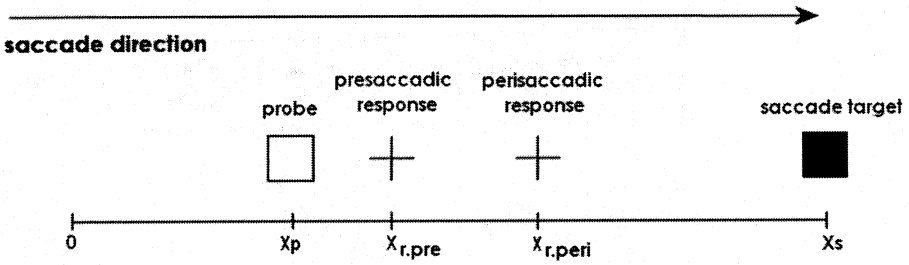


$$N_{r.pre} = \frac{X_{r.pre} - X_s}{|X_p - X_s|}, N_{r.peri} = \frac{X_{r.peri} - X_s}{|X_p - X_s|}$$

$$I_c = 1 - \left| \overline{N}_{r.peri} / \overline{N}_{r.pre} \right|$$

**Figure B1.** Definitions of the normalized distance ($N_r$) and the compression index ($I_c$). This illustration assumes a rightward saccade. $X_p$, $X_{r.pre}$, $X_{r.peri}$, and $X_s$ represent the allocentric coordinates of the probe, the presaccadic localization response, the perisaccadic localization response, and the saccadic target, respectively. $X_s$ is actually 10-degree from straight ahead (0-degree).

# APPENDIX C. THE PRECISION OF THE EYE TRACKER

The *precision* is a fundamental characteristic of any scientific tool. Conceptually, precision means how tightly the results of repeated measurements cluster together. Repeated measurements with a good tool should give average results very tightly clustered around the reference value. Quantitatively precision is characterized by the standard deviation of repeated measurements.

In the operation and service manual of the ASL Model 210 eye tracking system (ASL222-M-961; May 1994), the precision is said to be 0.25° and 1° along the horizontal and vertical dimension, respectively. The manual, however, does not report details of how these specifications were obtained. Therefore, it should informative to measure the precision and accuracy of the ASL 210 tracker used in this project with both ideal settings and settings similar to those in experiments of the current dissertation.

## *C.1. Precision measurement under with a model eye*

The variations in outputs when measuring the movement of a model eye can give one the estimate of internal noise of the eye tracker. To test this, the ASL 210 tracker was fixed in front of a model eye that can be rotated sinusoidally by a galvanometer; the analogue output of the ASL tracker was connected to an oscilloscope. A waveform generator provided voltages signals to the motor. A small mirror was attached to the model eye and reflected a laser beam to a blank field 422 cm away. Any displacement of the model eye position would cause the projection of the laser beam to displace twice as far. When the model eye rotated sinusoidally, the laser beam also move sinusoidally on the blank field. By measuring the distance the laser beam traveled on the field, one can derive the angular distance the model eye moved.

When the model eye remained static, the peak-to-peak magnitude of the tracker's output was 16 mV. That is to say, the internal noise of the eye tracker is 16 mV. The output during measurement of eye movements has to exceed the internal noise to be meaningful. Table B1 shows the outputs of the eye tracker at three different angular distances of model eye rotation. Note that only the horizontal output of the eye tracker was measured.

**Table C1**. The Output of the ASL 210 tracker and its Corresponding Values of Model Eye. Angular Rotation ($O_{ASL}$ = ASL out put; $D_L$ = Laser Beam Traveling Distance; $D_R$ = Angular Distance of Model Eye Rotation).

| $O_{ASL}$ (mV) | $D_L$ (mm) | $D_R$ (min) |
|---|---|---|
| 8 | 4 | 1.63 |
| 20 | 7.3 | 2.97 |
| 40 | 15 | 6.11 |

The relationship between the output of the tracker and the distance of model eye movement can be nicely fit by a linear function,

$$D_R = 0.1417O_{ASL} + 0.3573. \qquad \text{Eq. B1}$$

Thus, the 16 mV internal noise of the tracker is equivalent to 2.62 min eye movement. In other words, with the analogue output one can only discriminate a true eye movement from the noise when the size of eye movement exceeds 2.62 min, which can be regarded as the spatial precision of the eye tracker. Of course, this is the ideal case when everything is totally stable. The variation in output of the eye tracker will be larger under

practical conditions.

*C.2. Precision measurement under experimental settings*

Precision of the ASL tracker under conditions similar to experiments in this study was measured by having three participants fixate on black squares (1 x 1 deg) located at 10-degree eccentricity either in the left or right visual fields (or upper or lower visual fields in the case of measuring precision along the vertical dimension). Before the measurement started, a three-point calibration procedure was performed to ensure the digital output was 87 units when the participant was fixating at 10-degree eccentricity.

Each participant performed 100 trials with 50 for each fixation location. In each trial, a central cross was presented at the beginning where the initial gaze was directed. After 1500 ms, the black square was presented randomly at one of the two peripheral locations. Participants pressed a mouse button to indicate that they had fixated the black square, and the digital output of the eye tracker was recorded immediately. The horizontal and vertical precision was measured in different blocks.

The results for three participants were shown in Table C2. The precision was defined as the standard deviation (in degree) of the distance between eye position and the target eccentricity for the 50 trials of each fixation location. For all of the participants, the precision of the measurement was not as good as reported in the ASL technical manual. The precision was approximately 1 degree on the average. Surprisingly, the precision along the vertical dimension seemed to be better than that along the horizontal dimension, though the difference did not reach statistical significance with just 3 participants.

Table C3 shows the mean locations where the participants' eyes landed. Except for subject EC in the upper visual field condition, each subject's gaze landed very close to

the target (±10 degree). Thus, the variation in the eye positions measured by the eye tracker should not be a consequence of the participants not looking where they were supposed to look but landed their gaze at random locations. One potential source of the variation could be small head movements because the participant was not constrained with a bite bar. Changes in the head pitch could have modulated the gain of the sensor and increased the variability in the recording of eye position.

**Table C2**. The Standard Deviation of Eye Position at Four Different Fixation Location.

| Subject | $P_{LVF}$ | $P_{RVF}$ | $P_{UVF}$ | $P_{DVF}$ |
|---|---|---|---|---|
| **NM** | 0.65 | 0.75 | 0.72 | 0.68 |
| **EC** | 1.00 | 2.00 | 1.14 | 0.71 |
| **AF** | 1.85 | 1.30 | 0.95 | 0.82 |
| **Mean** | 0.83 | 1.38 | 0.94 | 0.74 |

Note. Each cell was calculated from 50 trials. $P_{LVF}$: precision of left visual field; $P_{RVF}$: precision of right visual field; $P_{UVF}$: precision of upper visual field; $P_{DVF}$: precision of lower visual field.

**Table C3**. The Mean of Eye Position at Four Different Fixation Locations.

| Subject | $M_{LVF}$ | $M_{RVF}$ | $M_{UVF}$ | $M_{DVF}$ |
|---|---|---|---|---|
| **NM** | -9.86 | 9.95 | 10.04 | -9.77 |
| **EC** | -9.89 | 9.87 | 8.73 | -10.31 |
| **AF** | -9.87 | 10.22 | 10.03 | -10.62 |
| **Mean** | -9.87 | 10.01 | 9.6 | -10.23 |

*C.3. The Temporal Frequency Response and the Delay of the Eye Tracker*

The temporal frequency characteristic of the eye tracker has the form of a low-pass filter. Typically the filter would be characterized by the TF at which the gain ($g$) falls to 0.5. Assuming that the filter is first order, there is a mathematical relationship between the filter characteristic (cut-off frequency: $f$) and the delay ($t$) that the filter imposes on a ramp input signal, which is an approximation to a saccade:

$$g = \frac{1}{\sqrt{1 + t^2 (2\pi f)^2}} \qquad \text{Eq. C1}$$

Solving Eq. C1 for $t$, one gets:

$$t = \frac{\sqrt{g^{-2} - 1}}{2\pi f} \qquad \text{Eq. C2}$$

To obtain the cut-off value of the temporal frequency response with a gain of 0.5, the eye tracker was mounted in front of the model eye, and the frequency of the model eye's periodic movement was varied from 2 Hz to 120 Hz. For each frequency, the output from the eye tracker and the input from the model eye were measured with an oscilloscope, and the gain of the eye tracker at each frequency was normalized to the gain at 2 Hz. Figure C1 shows the semi-log plot of the results. The solid line represents a linear fit of the data.

The temporal frequency response function has a gain of 0.5 at 72 Hz. According the Eq. C2, the delay is thus 3.8 ms. This is pretty close to the 4 ms delay specified in the

ASL manual.

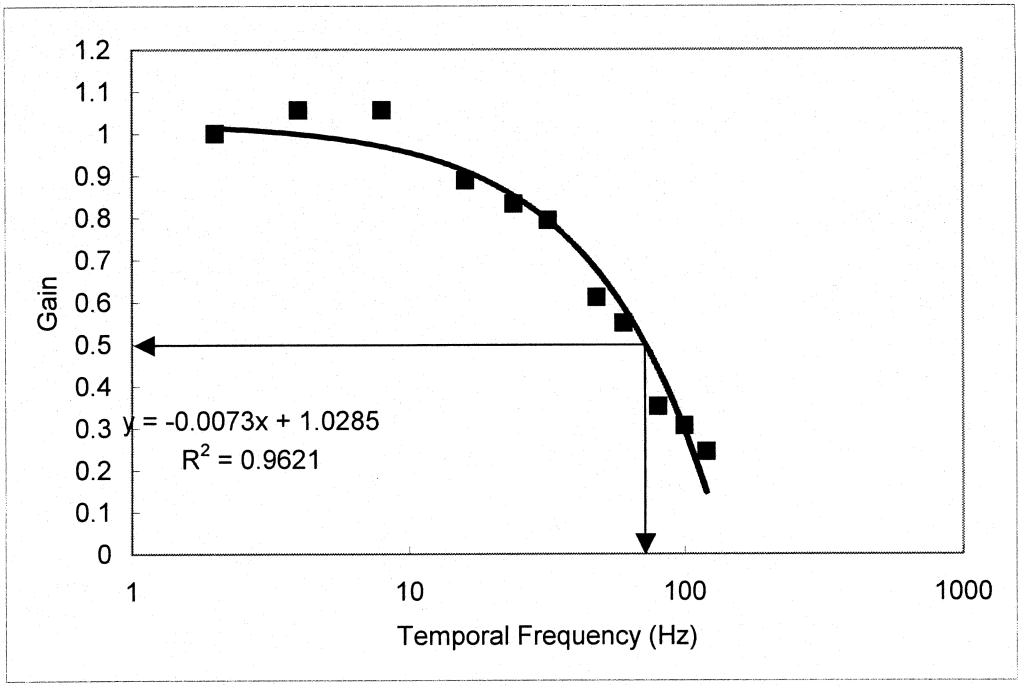


**Figure C1**. Temporal response function of the ASL ET210 tracker. The abscissa represents the frequency of periodic rotation of the model eye. The ordinate represents the ratio of eye tracker output to model eye output.

# APPENDIX D. MEAN HIT RATES AND FALSE ALARM RATES IN EACH CONDITION OF SERIES 1 AND 2

The repeated-measures ANOVAs in Series 1 and 2 were conducted on the arcsine-square-root transformed hit rates, which were also corrected by subtracting the transformed corrected false alarms (see Section 3.1.4, note 9). Table D1 to D8 provide the mean hit rates and false alarms in each condition, in both corrected and uncorrected formats, for readers who would also like to see these data.

**Table D1**. Mean Hit Rates and False Alarms in Each Condition of Experiment 1.

| DIR | SIZE | TIME | HIT | F.A. | C. HIT |
|---|---|---|---|---|---|
| CON | 1 | 22 | 0.20 (0.05) | 0.16 (0.14) | 0.05 (0.20) |
| | | 56 | 0.20 (0.05) | 0.18 (0.09) | 0.03 (0.12) |
| | | 106 | 0.69 (0.10) | 0.15 (0.10) | 0.50 (0.33) |
| | 2 | 22 | 0.45 (0.08) | 0.16 (0.14) | 0.28 (0.27) |
| | | 56 | 0.48 (0.06) | 0.18 (0.09) | 0.32 (0.19) |
| | | 106 | 0.85 (0.06) | 0.15 (0.10) | 0.67 (0.24) |
| INC | 1 | 22 | 0.26 (0.05) | 0.16 (0.14) | 0.09 (0.18) |
| | | 56 | 0.35 (0.07) | 0.18 (0.09) | 0.22 (0.22) |
| | | 106 | 0.65 (0.09) | 0.15 (0.10) | 0.46 (0.35) |
| | 2 | 22 | 0.53 (0.09) | 0.16 (0.14) | 0.38 (0.35) |
| | | 56 | 0.53 (0.09) | 0.18 (0.09) | 0.36 (0.27) |
| | | 106 | 0.72 (0.06) | 0.15 (0.10) | 0.55 (0.23) |

Note. DIR: direction of displacement (CON: congruent; INC: incongruent); SIZE: displacement size (1 or 2 degree[s]); TIME: displacement time (22, 56, or 106 ms after saccade onset); HIT: the mean hit rate in each condition; F.A.: the mean false alarms in each condition. The false alarms are the same for conditions with the same displacement time. C. HIT: mean corrected hit rates (subtracting F.A. from HIT). Data in the parentheses indicate standard deviation of hit rates or false alarms, respectively, across 10 participants.

**Table D2**. Mean Hit Rates and False Alarms in Each Condition of Experiment 2.

| DIR | HIT | F.A. | C. HIT |
|---|---|---|---|
| CON | 0.46 (0.29) | 0.43 (0.28) | 0.04 (0.28) |
| INC | 0.85 (0.19) | 0.43 (0.28) | 0.43 (0.31) |

Note. Abbreviations have the same definitions as Table D1.

**Table D3**. Mean Hit Rates and False Alarms in Each Condition of Experiment 3.

A. Horizontal Saccades/Vertical displacements

| POSITION | DISP | SIZE | HIT | F.A. | C. HIT |
|---|---|---|---|---|---|
| UP | UP | 0.5 | 0.27 (0.20) | 0.02 (0.03) | 0.25 (0.20) |
| | | 1 | 0.46 (0.23) | 0.02 (0.03) | 0.44 (0.24) |
| | | 2 | 0.96 (0.07) | 0.02 (0.03) | 0.94 (0.07) |
| | DOWN | 0.5 | 0.10 (0.14) | 0.02 (0.03) | 0.08 (0.14) |
| | | 1 | 0.38 (0.11) | 0.02 (0.03) | 0.36 (0.10) |
| | | 2 | 0.96 (0.06) | 0.02 (0.03) | 0.94 (0.06) |
| MID | UP | 0.5 | 0.22 (0.19) | 0.02 (0.03) | 0.20 (0.18) |
| | | 1 | 0.77 (0.17) | 0.02 (0.03) | 0.75 (0.16) |
| | | 2 | 1.00 (0.00) | 0.02 (0.03) | 0.98 (0.03) |
| | DOWN | 0.5 | 0.17 (0.11) | 0.02 (0.03) | 0.15 (0.10) |
| | | 1 | 0.55 (0.23) | 0.02 (0.03) | 0.53 (0.21) |
| | | 2 | 0.94 (0.09) | 0.02 (0.03) | 0.92 (0.09) |
| DOWN | UP | 0.5 | 0.08 (0.12) | 0.06 (0.07) | 0.02 (0.10) |
| | | 1 | 0.30 (0.29) | 0.06 (0.07) | 0.24 (0.28) |
| | | 2 | 0.95 (0.08) | 0.06 (0.07) | 0.89 (0.07) |
| | DOWN | 0.5 | 0.25 (0.26) | 0.06 (0.07) | 0.19 (0.26) |
| | | 1 | 0.50 (0.25) | 0.06 (0.07) | 0.44 (0.25) |
| | | 2 | 0.86 (0.22) | 0.06 (0.07) | 0.80 (0.24) |

Note. POSITION: initial probe positions along the vertical meridian (2-degree above the center [UP], at the center [MID], and 2-degree below the center [DOWN]). DISP: displacement direction (**UP**wards or **DOWN**wards). Other abbreviations have the same definition as Table D1.

B. Vertical Saccades/Horizontal displacements

| POSITION | DISP | SIZE | HIT | F.A. | C. HIT |
|---|---|---|---|---|---|
| LEFT | LEFT | 0.5 | 0.20 (0.24) | 0.08 (0.10) | 0.11 (0.20) |
| | | 1 | 0.38 (0.33) | 0.08 (0.10) | 0.29 (0.33) |
| | | 2 | 0.72 (0.32) | 0.08 (0.10) | 0.64 (0.28) |
| | RIGHT | 0.5 | 0.07 (0.08) | 0.08 (0.10) | -0.01 (0.12) |
| | | 1 | 0.27 (0.29) | 0.08 (0.10) | 0.19 (0.30) |
| | | 2 | 0.79 (0.26) | 0.08 (0.10) | 0.70 (0.24) |
| MID | LEFT | 0.5 | 0.12 (0.17) | 0.06 (0.07) | 0.06 (0.19) |
| | | 1 | 0.41 (0.35) | 0.06 (0.07) | 0.35 (0.33) |
| | | 2 | 0.87 (0.25) | 0.06 (0.07) | 0.81 (0.25) |
| | RIGHT | 0.5 | 0.05 (0.09) | 0.06 (0.07) | 0.00 (0.07) |
| | | 1 | 0.31 (0.23) | 0.06 (0.07) | 0.25 (0.21) |
| | | 2 | 0.81 (0.25) | 0.06 (0.07) | 0.76 (0.22) |
| RIGHT | LEFT | 0.5 | 0.08 (0.12) | 0.11 (0.13) | -0.03 (0.13) |
| | | 1 | 0.21 (0.26) | 0.11 (0.13) | 0.10 (0.24) |
| | | 2 | 0.67 (0.31) | 0.11 (0.13) | 0.55 (0.30) |
| | RIGHT | 0.5 | 0.15 (0.20) | 0.11 (0.13) | 0.04 (0.20) |
| | | 1 | 0.28 (0.26) | 0.11 (0.13) | 0.17 (0.23) |
| | | 2 | 0.76 (0.29) | 0.11 (0.13) | 0.65 (025) |

Note. POSITION: initial probe positions along the horizontal meridian (2-degree to the left of the center [LEFT], at the center [MID], and 2-degree to the right of the center [RIGHT]). DISP: displacement direction (**LEFT**wards or **RIGHT**wards). Other abbreviations have the same definition as Table D1.

**Table D4**. Mean Hit Rates and False Alarms in Each Condition of Experiment 4.

| CX | TMS | SAC | DISP | HIT | F.A. | C. HIT |
|---|---|---|---|---|---|---|
| Frontal | NO TMS | L | CON | 0.42 (0.29) | 0.27 (0.13) | 0.12 (0.38) |
| | | | INC | 0.70 (0.25) | 0.27 (0.13) | 0.40 (0.25) |
| | | R | CON | 0.42 (0.35) | 0.18 (0.11) | 0.44 (0.31) |
| | | | INC | 0.67 (0.28) | 0.18 (0.11) | 0.56 (0.30) |
| | 50 ms | L | CON | 0.47 (0.28) | 0.24 (0.21) | 0.11 (0.37) |
| | | | INC | 0.76 (0.32) | 0.24 (0.21) | 0.45 (0.28) |
| | | R | CON | 0.43 (0.38) | 0.21 (0.11) | 0.32 (0.43) |
| | | | INC | 0.66 (0.30) | 0.21 (0.11) | 0.45 (0.28) |
| | 100 ms | L | CON | 0.41 (0.32) | 0.33 (0.24) | 0.14 (0.29) |
| | | | INC | 0.79 (0.24) | 0.33 (0.24) | 0.45 (0.23) |
| | | R | CON | 0.48 (0.35) | 0.21 (0.12) | 0.27 (0.41) |
| | | | INC | 0.70 (0.30) | 0.21 (0.12) | 0.43 (0.33) |
| | 150 ms | L | CON | 0.42 (0.33) | 0.36 (0.30) | 0.11 (0.40) |
| | | | INC | 0.71 (0.28) | 0.36 (0.30) | 0.46 (0.30) |
| | | R | CON | 0.56 (0.28) | 0.19 (0.17) | 0.30 (0.44) |
| | | | INC | 0.80 (0.22) | 0.19 (0.17) | 0.45 (0.29) |
| Parietal | NO TMS | L | CON | 0.38 (0.31) | 0.27 (0.22) | 0.15 (0.29) |
| | | | INC | 0.66 (0.29) | 0.27 (0.22) | 0.44 (0.23) |
| | | R | CON | 0.53 (0.33) | 0.08 (0.10) | 0.24 (0.29) |
| | | | INC | 0.65 (0.30) | 0.08 (0.10) | 0.49 (0.28) |
| | 50 ms | L | CON | 0.41 (0.33) | 0.30 (0.22) | 0.24 (0.33) |
| | | | INC | 0.74 (0.32) | 0.30 (0.22) | 0.52 (0.32) |
| | | R | CON | 0.45 (0.37) | 0.13 (0.11) | 0.22 (0.43) |
| | | | INC | 0.58 (0.33) | 0.13 (0.11) | 0.45 (0.32) |
| | 100 ms | L | CON | 0.41 (0.30) | 0.26 (0.18) | 0.08 (0.35) |
| | | | INC | 0.71 (0.29) | 0.26 (0.18) | 0.46 (0.27) |
| | | R | CON | 0.48 (0.34) | 0.21 (0.20) | 0.27 (0.43) |
| | | | INC | 0.65 (0.34) | 0.21 (0.20) | 0.49 (0.28) |
| | 150 ms | L | CON | 0.38 (0.28) | 0.27 (0.28) | 0.07 (0.38) |
| | | | INC | 0.73 (0.30) | 0.27 (0.28) | 0.35 (0.30) |
| | | R | CON | 0.51 (0.39) | 0.22 (0.22) | 0.37 (0.37) |
| | | | INC | 0.66 (0.34) | 0.22 (0.22) | 0.60 (0.21) |

Note. CX: TMS site on the cortex (Parietal or Frontal); TMS: tms onset (No TMS, 50 ms, 100 ms, or 150 ms after onset of the saccade target); SAC: saccade direction (Left or Right); DISP: displacement direction (congruent or incongruent). Other abbreviations have the same definition as Table D1.

# APPENDIX E. MEAN COORDINATES OF LOCALIZATION AND COMPRESSION INDEX IN SERIES 3 AND 4

**Table E1**. Mean Coordinates of Perisaccadic Localization in Each Condition of Experiment 6 for Every Participant.

A. Horizontal Saccades

| | LEFT | | | | | RIGHT | | | | |
|---|---|---|---|---|---|---|---|---|---|---|
| **SUBJ** | **-15** | **-5** | **0** | **5** | **15** | **-15** | **-5** | **0** | **5** | **15** |
| **1** | -11.94 | -6.73 | 0.13 | 7.39 | 10.85 | -12.37 | -6.95 | -0.13 | 7.70 | 12.62 |
| **2** | -10.73 | -5.25 | -0.91 | 4.47 | 11.46 | -11.50 | -4.78 | -0.42 | 5.50 | 11.60 |
| **3** | -9.16 | -4.30 | 0.38 | 4.13 | 10.21 | -11.13 | -3.82 | -0.55 | 4.48 | 10.26 |
| **4** | -10.29 | -5.65 | -0.04 | 6.69 | 9.52 | -11.87 | -7.33 | -0.23 | 6.61 | 12.20 |
| **5** | -10.50 | -3.72 | 0.99 | 4.98 | 8.80 | -11.24 | -4.62 | -0.78 | 5.24 | 11.43 |
| **6** | -13.10 | -5.78 | 0.27 | 5.61 | 13.14 | -12.84 | -6.32 | 0.80 | 5.25 | 12.26 |
| **7** | -9.91 | -6.30 | 0.78 | 7.05 | 10.24 | -11.59 | -6.58 | -1.10 | 6.45 | 10.63 |
| **8** | -14.03 | -5.90 | 0.10 | 5.85 | 13.30 | -13.36 | -5.74 | -0.71 | 5.63 | 13.48 |
| **mean** | -11.21 | -5.45 | 0.21 | 5.77 | 10.94 | -11.99 | -5.77 | -0.39 | 5.86 | 11.81 |

Note. Coordinates for locations and responses during leftward saccades were reversed in sign so that for both saccade directions, -15 is closer to the initial fixation and +15 is closer to the saccade target.

B. Vertical Saccades

| | UP | | | | | DOWN | | | | |
|---|---|---|---|---|---|---|---|---|---|---|
| **SUBJ** | **-15** | **-5** | **0** | **5** | **15** | **-15** | **-5** | **0** | **5** | **15** |
| **1** | -12.45 | -6.20 | -0.10 | 5.72 | 12.15 | -10.10 | -5.51 | -0.11 | 5.12 | 11.19 |
| **2** | -12.39 | -3.98 | -0.94 | 5.77 | 11.57 | -11.14 | -3.63 | -0.34 | 3.15 | 11.83 |
| **3** | -11.23 | -6.37 | 1.15 | 6.36 | 13.44 | -13.01 | -5.39 | 0.42 | 4.05 | 12.08 |
| **4** | -9.23 | -4.66 | 0.81 | 4.18 | 7.77 | -5.51 | -4.12 | 0.20 | 1.86 | 6.76 |
| **5** | -10.31 | -7.54 | -0.01 | 7.75 | 10.16 | -11.40 | -7.60 | -1.88 | 7.90 | 10.95 |
| **6** | -13.24 | -7.37 | 0.16 | 7.91 | 12.82 | -13.02 | -6.72 | -0.50 | 6.88 | 13.61 |
| **7** | -9.40 | -6.16 | -0.05 | 6.09 | 10.35 | -10.59 | -6.05 | 0.22 | 5.91 | 10.72 |
| **8** | -14.96 | -6.50 | -0.62 | 6.04 | 14.65 | -13.86 | -9.64 | -2.05 | 6.47 | 14.04 |
| **mean** | -11.65 | -6.10 | 0.05 | 6.23 | 11.61 | -11.08 | -6.08 | -0.50 | 5.17 | 11.40 |

Note. Coordinates for locations responses during downward saccades were reversed in sign so that for both saccade directions, -15 is closer to the initial fixation and +15 is closer to the saccade target.

**Table E2**. Standard Deviation of Coordinates in Each Condition of Experiment 6 for Every Participant.

A. Horizontal Saccades.

| | LEFT | | | | | RIGHT | | | | |
|---|---|---|---|---|---|---|---|---|---|---|
| **SUBJ** | **-15** | **-5** | **0** | **5** | **15** | **-15** | **-5** | **0** | **5** | **15** |
| **1** | 1.85 | 0.95 | 3.23 | 1.56 | 0.96 | 2.56 | 2.04 | 2.72 | 2.28 | 3.52 |
| **2** | 2.56 | 1.19 | 3.19 | 1.58 | 2.09 | 2.85 | 1.57 | 1.22 | 0.93 | 2.47 |
| **3** | 2.15 | 1.45 | 1.28 | 1.54 | 2.27 | 3.15 | 1.41 | 1.40 | 1.50 | 2.12 |
| **4** | 2.76 | 2.16 | 2.14 | 1.81 | 2.18 | 2.72 | 2.12 | 2.03 | 1.24 | 2.04 |
| **5** | 3.90 | 6.36 | 3.85 | 3.94 | 4.96 | 4.26 | 7.37 | 5.88 | 5.56 | 4.37 |
| **6** | 1.92 | 2.41 | 3.24 | 1.65 | 3.10 | 1.12 | 1.02 | 1.53 | 1.45 | 1.52 |
| **7** | 3.41 | 1.45 | 2.03 | 1.75 | 3.13 | 1.85 | 2.39 | 5.13 | 2.36 | 1.10 |
| **8** | 1.11 | 1.07 | 1.60 | 0.64 | 1.20 | 0.78 | 1.12 | 3.35 | 1.09 | 1.30 |
| **mean** | 2.46 | 2.13 | 2.57 | 1.81 | 2.49 | 2.41 | 2.38 | 2.91 | 2.05 | 2.31 |
| **s.d.** | 1.67 | 1.01 | 0.57 | 1.20 | 1.62 | 0.80 | 1.25 | 0.57 | 1.01 | 1.05 |

B. Vertical Saccades.

| | UP | | | | | DOWN | | | | |
|---|---|---|---|---|---|---|---|---|---|---|
| **SUBJ** | **-15** | **-5** | **0** | **5** | **15** | **-15** | **-5** | **0** | **5** | **15** |
| **1** | 2.44 | 1.58 | 2.95 | 1.36 | 2.52 | 1.93 | 1.00 | 1.90 | 0.98 | 1.65 |
| **2** | 1.62 | 2.36 | 1.56 | 1.65 | 1.94 | 1.93 | 2.01 | 1.86 | 2.24 | 1.21 |
| **3** | 4.18 | 1.38 | 1.34 | 1.98 | 4.66 | 1.22 | 4.78 | 5.97 | 4.98 | 1.42 |
| **4** | 2.02 | 2.00 | 1.77 | 2.39 | 3.78 | 2.08 | 2.23 | 3.10 | 2.53 | 3.48 |
| **5** | 4.74 | 4.41 | 5.26 | 4.31 | 4.72 | 2.69 | 2.81 | 4.76 | 1.86 | 2.71 |
| **6** | 1.41 | 1.43 | 3.68 | 2.31 | 1.41 | 1.10 | 1.53 | 3.36 | 1.54 | 0.93 |
| **7** | 2.69 | 1.42 | 1.97 | 1.23 | 2.72 | 1.13 | 0.85 | 2.22 | 1.40 | 1.98 |
| **8** | 0.89 | 1.59 | 1.13 | 1.13 | 0.81 | 1.59 | 2.64 | 3.29 | 1.11 | 0.72 |
| **mean** | 2.50 | 2.02 | 2.46 | 2.04 | 2.82 | 1.71 | 2.23 | 3.31 | 2.08 | 1.76 |
| **s.d.** | 1.98 | 1.23 | 0.68 | 1.19 | 2.17 | 2.61 | 1.93 | 0.95 | 2.03 | 2.23 |

Note. This table shows the spread of localization response for each participant.

**Table E3.** Mean Compression Index in Each Condition of Experiment 6 for Every Participant.

A. Horizontal Saccades

| SAC | LEFT | | | | | RIGHT | | | | |
|---|---|---|---|---|---|---|---|---|---|---|
| POSI / SUBJ | -15 | -5 | 0 | 5 | 15 | -15 | -5 | 0 | 5 | 15 |
| 1 | 0.15 | -0.11 | 0.07 | 0.42 | 0.81 | 0.10 | -0.10 | 0.06 | 0.59 | 0.60 |
| 2 | 0.14 | 0.01 | -0.14 | -0.11 | 0.61 | 0.13 | 0.00 | -0.05 | 0.06 | 0.64 |
| 3 | 0.25 | 0.05 | 0.02 | -0.15 | 0.68 | 0.15 | 0.05 | -0.05 | -0.11 | 0.78 |
| 4 | 0.20 | -0.04 | 0.00 | 0.34 | 0.72 | 0.15 | -0.14 | -0.02 | 0.30 | 0.59 |
| 5 | 0.19 | 0.07 | 0.19 | -0.15 | 0.49 | 0.17 | -0.06 | -0.01 | 0.05 | 0.39 |
| 6 | 0.07 | -0.06 | 0.01 | 0.09 | 0.40 | 0.09 | -0.07 | 0.07 | 0.09 | 0.50 |
| 7 | 0.16 | -0.08 | 0.02 | 0.47 | 0.46 | 0.13 | -0.14 | -0.38 | 0.35 | 0.81 |
| 8 | 0.04 | -0.09 | -0.02 | 0.17 | 0.33 | 0.06 | -0.03 | -0.14 | 0.13 | 0.33 |
| **mean** | *0.15* | *-0.03* | *0.02* | *0.14* | *0.56* | *0.12* | *-0.06* | *-0.07* | *0.18* | *0.58* |
| **s.d.** | *0.07* | *0.07* | *0.09* | *0.26* | *0.17* | *0.04* | *0.07* | *0.14* | *0.22* | *0.17* |

B. Vertical Saccades

| SAC | UP | | | | | DOWN | | | | |
|---|---|---|---|---|---|---|---|---|---|---|
| POSI / SUBJ | -15 | -5 | 0 | 5 | 15 | -15 | -5 | 0 | 5 | 15 |
| 1 | 0.11 | -0.05 | 0.01 | 0.24 | 0.49 | 0.15 | -0.01 | 0.01 | 0.10 | 0.74 |
| 2 | 0.14 | -0.05 | 0.09 | -0.20 | 0.51 | 0.13 | 0.12 | 0.03 | -0.27 | 0.61 |
| 3 | 0.06 | -0.09 | -0.11 | 0.27 | 0.28 | 0.12 | 0.06 | -0.04 | 0.01 | 0.40 |
| 4 | 0.29 | 0.05 | -0.08 | -0.07 | 0.67 | 0.33 | 0.21 | -0.02 | -0.18 | 0.10 |
| 5 | 0.19 | -0.18 | 0.00 | 0.16 | 0.22 | 0.16 | -0.19 | 0.19 | 0.38 | 0.59 |
| 6 | 0.09 | -0.19 | -0.02 | 0.47 | 0.35 | 0.06 | -0.13 | 0.05 | 0.34 | 0.40 |
| 7 | 0.19 | -0.07 | 0.00 | 0.23 | 0.50 | 0.17 | -0.06 | -0.02 | 0.21 | 0.79 |
| 8 | 0.01 | -0.07 | 0.06 | 0.30 | 0.01 | 0.04 | -0.10 | 0.20 | 0.54 | 0.22 |
| **mean** | *0.14* | *-0.08* | *0.00* | *0.18* | *0.38* | *0.14* | *-0.01* | *0.05* | *0.14* | *0.48* |
| **s.d.** | *0.09* | *0.08* | *0.07* | *0.22* | *0.21* | *0.09* | *0.14* | *0.10* | *0.28* | *0.25* |

Note. See Appendix B for the definition of the compression index.

**Table E4**. Mean Coordinates of Perisaccadic Localization in Each Condition of Experiment 7 for Every Participant.

| POSI | 0 | | | | 15 | | | |
|---|---|---|---|---|---|---|---|---|
| LUM | LOW | | HIGH | | LOW | | HIGH | |
| TIME / SUBJ | peri | pre | peri | pre | peri | pre | peri | pre |
| 1 | -6.12 | -0.08 | -2.76 | 0.34 | 10.58 | 12.94 | 10.83 | 13.80 |
| 2 | -3.78 | -0.07 | -2.77 | 0.23 | 12.42 | 14.05 | 12.87 | 14.55 |
| 3 | -1.56 | -0.08 | -1.36 | -0.75 | 10.01 | 12.54 | 9.97 | 13.53 |
| 4 | 1.04 | -0.50 | -1.06 | -0.77 | 5.37 | 16.03 | 12.92 | 16.46 |
| 5 | 5.65 | -1.12 | 0.20 | -0.98 | 9.33 | 13.45 | 10.79 | 13.75 |
| 6 | 0.12 | -1.07 | -1.87 | -1.51 | 11.24 | 14.17 | 12.25 | 14.57 |
| 7 | -2.33 | -3.03 | -1.72 | -4.84 | 5.02 | 13.51 | 8.98 | 13.45 |
| 8 | 3.74 | 0.69 | 0.12 | 0.27 | 4.64 | 14.49 | 7.61 | 12.98 |
| mean | -0.40 | -0.66 | -1.40 | -1.00 | 8.58 | 13.90 | 10.78 | 14.14 |
| s.d. | 3.88 | 1.12 | 1.14 | 1.69 | 3.09 | 1.08 | 1.89 | 1.08 |

**Table E5**. Standard Deviation of Coordinates in Each Condition of Experiment 7 for Every Participant.

| POSI | 0 | | | | 15 | | | |
|---|---|---|---|---|---|---|---|---|
| LUM | LOW | | HIGH | | LOW | | HIGH | |
| TIME / SUBJ | peri | pre | peri | pre | peri | pre | peri | pre |
| 1 | 3.49 | 2.05 | 3.54 | 2.16 | 1.39 | 1.31 | 1.21 | 1.52 |
| 2 | 2.82 | 2.09 | 2.38 | 2.70 | 1.18 | 1.20 | 1.71 | 1.45 |
| 3 | 2.33 | 2.25 | 2.10 | 2.48 | 3.86 | 3.06 | 1.72 | 1.40 |
| 4 | 4.01 | 3.99 | 4.53 | 3.76 | 6.00 | 2.78 | 2.72 | 3.18 |
| 5 | 4.48 | 1.47 | 1.93 | 1.87 | 1.30 | 1.62 | 1.02 | 1.03 |
| 6 | 1.84 | 2.27 | 1.68 | 2.19 | 1.40 | 1.62 | 1.35 | 1.44 |
| 7 | 5.28 | 3.76 | 3.18 | 3.20 | 5.22 | 1.53 | 1.64 | 2.06 |
| 8 | 6.10 | 1.75 | 2.78 | 1.25 | 3.31 | 1.75 | 1.78 | 1.78 |
| mean | 3.79 | 2.45 | 2.76 | 2.45 | 2.96 | 1.86 | 1.64 | 1.73 |
| s.d. | 1.46 | 0.92 | 0.95 | 0.78 | 1.93 | 0.68 | 0.51 | 0.66 |

**Table E6**. Mean Compression Index in Each Condition of Experiment 7 for Every Participant.

| | LOW | | HIGH | |
|---|---|---|---|---|
| **SUBJ** | **0** | **15** | **0** | **15** |
| **1** | 0.69 | 0.89 | 0.11 | 0.69 |
| **2** | 0.3 | 0.47 | 0.01 | 0.39 |
| **3** | 0.02 | 0.65 | 0.03 | 0.98 |
| **4** | -0.08 | 0.42 | 0.03 | 0.57 |
| **5** | 0.56 | 0.74 | 0.09 | 0.74 |
| **6** | 0.02 | 0.69 | 0 | 0.53 |
| **7** | 0.11 | 0.11 | -0.96 | 0.59 |
| **8** | 0.17 | -0.51 | 0.08 | 0.29 |
| **mean** | *0.22* | *0.43* | *-0.08* | *0.6* |
| **s.d.** | *0.27* | *0.45* | *0.36* | *0.21* |

Note. See Appendix B for the definition of the compression index.

**Table E7**. Mean Response Coordinates of Perisaccadic Localization in Each Condition of Experiment 8 for Every Participant.

A. Parietal Site

| TIME | TMS | POSI | SUBJ / SAC | 1 | 2 | 3 | 4 | 5 | mean | s.d. |
|---|---|---|---|---|---|---|---|---|---|---|
| peri | No TMS | 0 | L | -5.70 | -3.09 | -3.64 | -2.93 | -2.07 | *-3.49* | *1.36* |
| | | | R | -2.09 | -0.27 | -1.55 | -2.85 | -2.50 | *-1.85* | *1.01* |
| | | 15 | L | 11.03 | 10.75 | 10.83 | 11.23 | 11.27 | *11.02* | *0.23* |
| | | | R | 9.85 | 10.29 | 9.44 | 10.50 | 8.69 | *9.75* | *0.72* |
| | 100 | 0 | L | -3.91 | 0.30 | 0.49 | -0.89 | 0.08 | *-0.78* | *1.83* |
| | | | R | -3.07 | -1.72 | -3.32 | -4.14 | -3.48 | *-3.15* | *0.89* |
| | | 15 | L | 11.05 | 10.73 | 10.57 | 10.88 | 10.82 | *10.81* | *0.18* |
| | | | R | 10.11 | 10.72 | 10.56 | 10.74 | 10.44 | *10.51* | *0.25* |
| | 150 | 0 | L | -6.05 | -4.31 | -4.88 | -5.08 | -4.11 | *-4.89* | *0.76* |
| | | | R | -3.42 | -0.25 | -1.90 | -3.13 | -3.05 | *-2.35* | *1.31* |
| | | 15 | L | 10.98 | 11.04 | 11.00 | 11.34 | 11.38 | *11.15* | *0.20* |
| | | | R | 9.94 | 10.20 | 9.94 | 10.68 | 10.23 | *10.20* | *0.30* |
| | 200 | 0 | L | -5.27 | -1.94 | -3.51 | -3.70 | -2.31 | *-3.35* | *1.31* |
| | | | R | -1.56 | -1.46 | -3.24 | -3.80 | -3.29 | *-2.67* | *1.08* |
| | | 15 | L | 11.39 | 11.38 | 11.46 | 11.65 | 11.46 | *11.47* | *0.11* |
| | | | R | 10.12 | 10.49 | 9.84 | 10.30 | 9.92 | *10.13* | *0.27* |
| pre | No TMS | 0 | L | 0.63 | 0.85 | 0.40 | 0.02 | -0.35 | *0.31* | *0.48* |
| | | | R | -2.51 | -2.08 | -2.18 | -2.32 | -2.74 | *-2.37* | *0.26* |
| | | 15 | L | 13.98 | 14.25 | 15.07 | 15.24 | 14.97 | *14.70* | *0.55* |
| | | | R | 11.33 | 13.23 | 13.84 | 14.43 | 14.24 | *13.41* | *1.25* |
| | 100 | 0 | L | -0.28 | 1.07 | 0.54 | 0.14 | -0.31 | *0.23* | *0.58* |
| | | | R | -1.55 | -1.15 | -1.52 | -1.56 | -2.11 | *-1.58* | *0.34* |
| | | 15 | L | 13.75 | 14.52 | 14.66 | 15.04 | 14.99 | *14.59* | *0.52* |
| | | | R | 11.38 | 12.85 | 13.05 | 13.96 | 13.58 | *12.96* | *0.99* |
| | 150 | 0 | L | -0.43 | 0.71 | 0.47 | 0.22 | -0.01 | *0.19* | *0.44* |
| | | | R | -2.84 | -1.71 | -2.28 | -1.80 | -2.49 | *-2.22* | *0.47* |
| | | 15 | L | 13.39 | 14.19 | 14.98 | 15.19 | 14.88 | *14.52* | *0.74* |
| | | | R | 12.26 | 13.94 | 14.03 | 14.69 | 14.36 | *13.85* | *0.94* |
| | 200 | 0 | L | 0.69 | 0.64 | 0.98 | 0.51 | -0.21 | *0.52* | *0.45* |
| | | | R | -2.45 | -1.14 | -1.71 | -1.98 | -2.30 | *-1.91* | *0.52* |
| | | 15 | L | 14.14 | 14.86 | 15.28 | 15.39 | 15.20 | *14.97* | *0.50* |
| | | | R | 11.85 | 13.52 | 13.70 | 14.42 | 14.28 | *13.55* | *1.03* |

Note. TIME: onsets of localization probe (**peri**saccadic or **pre**saccadic); TMS: onset of TMS (none, 100 ms, 150 ms, or 200 ms after the onset of saccade target); POSI: probe location (0 degree or 15 degree in the allocentric space). The probe positions and localization responses during leftward saccades are reversed in sign to simplify the comparison between two saccade directions.

B. Frontal Site

| TIME | TMS | POSI | SUBJ / SAC | 1 | 2 | 3 | 4 | 5 | mean | s.d. |
|---|---|---|---|---|---|---|---|---|---|---|
| peri | No TMS | 0 | L | -3.23 | -1.37 | -1.60 | -2.20 | -0.99 | *-1.88* | *0.87* |
| | | | R | -2.15 | -1.24 | -1.84 | -2.31 | -2.28 | *-1.96* | *0.45* |
| | | 15 | L | 11.01 | 10.77 | 10.45 | 10.72 | 10.35 | *10.66* | *0.26* |
| | | | R | 9.60 | 9.89 | 8.83 | 9.44 | 7.99 | *9.15* | *0.76* |
| | 100 | 0 | L | -1.47 | -0.32 | -1.18 | -1.94 | -1.17 | *-1.22* | *0.59* |
| | | | R | -3.26 | -2.49 | -3.31 | -3.89 | -3.49 | *-3.29* | *0.51* |
| | | 15 | L | 10.76 | 10.97 | 10.95 | 11.06 | 11.10 | *10.97* | *0.13* |
| | | | R | 10.20 | 10.25 | 9.50 | 10.11 | 9.64 | *9.94* | *0.34* |
| | 150 | 0 | L | -4.70 | -3.78 | -4.05 | -4.14 | -2.41 | *-3.82* | *0.85* |
| | | | R | -2.85 | -2.06 | -2.77 | -3.05 | -3.14 | *-2.77* | *0.43* |
| | | 15 | L | 11.21 | 11.29 | 11.20 | 11.55 | 11.45 | *11.34* | *0.15* |
| | | | R | 10.03 | 9.90 | 9.80 | 10.07 | 9.27 | *9.81* | *0.32* |
| | 200 | 0 | L | -4.16 | -3.27 | -3.17 | -3.70 | -2.56 | *-3.37* | *0.60* |
| | | | R | -2.73 | -2.06 | -2.71 | -2.78 | -2.27 | *-2.51* | *0.33* |
| | | 15 | L | 11.23 | 11.23 | 10.79 | 11.08 | 10.42 | *10.95* | *0.35* |
| | | | R | 9.75 | 9.73 | 8.94 | 9.35 | 8.93 | *9.34* | *0.40* |
| pre | No TMS | 0 | L | -0.22 | 0.27 | -0.03 | 0.04 | -0.52 | *-0.09* | *0.30* |
| | | | R | -2.43 | -1.59 | -1.60 | -1.58 | -1.91 | *-1.82* | *0.37* |
| | | 15 | L | 14.52 | 14.80 | 15.09 | 15.23 | 14.87 | *14.90* | *0.27* |
| | | | R | 13.43 | 14.01 | 14.06 | 14.34 | 13.96 | *13.96* | *0.33* |
| | 100 | 0 | L | -0.28 | -0.06 | -0.17 | -0.34 | -1.02 | *-0.38* | *0.38* |
| | | | R | -1.88 | -1.08 | -1.33 | -1.29 | -1.89 | *-1.49* | *0.37* |
| | | 15 | L | 14.55 | 14.78 | 15.15 | 15.11 | 14.91 | *14.90* | *0.24* |
| | | | R | 12.77 | 13.36 | 13.51 | 13.77 | 13.55 | *13.39* | *0.38* |
| | 150 | 0 | L | -0.10 | 0.17 | 0.02 | -0.13 | -0.43 | *-0.09* | *0.22* |
| | | | R | -2.16 | -1.22 | -1.43 | -1.68 | -2.26 | *-1.75* | *0.45* |
| | | 15 | L | 14.38 | 14.48 | 14.85 | 14.94 | 14.77 | *14.68* | *0.24* |
| | | | R | 13.63 | 14.06 | 13.93 | 14.33 | 13.92 | *13.97* | *0.25* |
| | 200 | 0 | L | -0.20 | 0.01 | -0.02 | -0.27 | -0.44 | *-0.18* | *0.18* |
| | | | R | -2.26 | -1.52 | -1.70 | -1.82 | -2.47 | *-1.95* | *0.40* |
| | | 15 | L | 14.62 | 14.90 | 15.25 | 15.25 | 14.85 | *14.97* | *0.28* |
| | | | R | 13.56 | 13.89 | 13.93 | 14.21 | 14.01 | *13.92* | *0.24* |

Note. Abbreviations follow the convention of Table E7(A).

**Table E8**. Standard Deviation of Response Coordinates in Each Condition of Experiment 8 for Every Participant.

A. Parietal Site

| TIME | TMS | POSI | SUBJ / SAC | 1 | 2 | 3 | 4 | 5 | mean | s.d. |
|---|---|---|---|---|---|---|---|---|---|---|
| peri | No TMS | 0 | L | 4.74 | 6.40 | 5.96 | 5.72 | 6.29 | *5.82* | *0.66* |
| | | | R | 3.68 | 4.16 | 4.35 | 4.55 | 4.40 | *4.23* | *0.34* |
| | | 15 | L | 1.24 | 2.30 | 2.40 | 2.05 | 2.73 | *2.14* | *0.56* |
| | | | R | 3.02 | 2.26 | 4.26 | 3.78 | 5.21 | *3.71* | *1.13* |
| | 100 | 0 | L | 7.10 | 7.91 | 7.42 | 7.07 | 7.27 | *7.35* | *0.34* |
| | | | R | 3.86 | 4.33 | 4.28 | 4.40 | 4.51 | *4.28* | *0.25* |
| | | 15 | L | 1.07 | 1.18 | 1.25 | 1.34 | 1.57 | *1.28* | *0.19* |
| | | | R | 2.10 | 2.02 | 3.37 | 2.52 | 3.44 | *2.69* | *0.68* |
| | 150 | 0 | L | 4.28 | 5.15 | 4.65 | 4.62 | 6.29 | *5.00* | *0.79* |
| | | | R | 4.82 | 5.29 | 5.19 | 5.22 | 5.06 | *5.12* | *0.19* |
| | | 15 | L | 1.56 | 1.54 | 1.88 | 1.83 | 2.02 | *1.76* | *0.21* |
| | | | R | 2.00 | 2.05 | 2.43 | 2.43 | 3.35 | *2.45* | *0.54* |
| | 200 | 0 | L | 4.71 | 5.73 | 5.41 | 5.08 | 5.77 | *5.34* | *0.45* |
| | | | R | 4.06 | 4.50 | 4.34 | 4.55 | 4.73 | *4.44* | *0.25* |
| | | 15 | L | 1.42 | 1.39 | 1.87 | 1.70 | 2.75 | *1.83* | *0.55* |
| | | | R | 2.30 | 2.23 | 3.59 | 3.20 | 3.66 | *3.00* | *0.69* |
| pre | No TMS | 0 | L | 2.96 | 3.25 | 3.14 | 3.38 | 4.04 | *3.35* | *0.41* |
| | | | R | 2.13 | 2.76 | 2.76 | 2.79 | 2.89 | *2.67* | *0.30* |
| | | 15 | L | 1.85 | 2.01 | 2.06 | 1.96 | 2.13 | *2.00* | *0.11* |
| | | | R | 2.53 | 2.54 | 2.38 | 2.45 | 2.60 | *2.50* | *0.09* |
| | 100 | 0 | L | 3.49 | 3.46 | 3.46 | 3.49 | 3.67 | *3.51* | *0.09* |
| | | | R | 2.22 | 2.86 | 2.60 | 2.88 | 3.03 | *2.72* | *0.32* |
| | | 15 | L | 1.89 | 1.87 | 2.00 | 1.96 | 1.95 | *1.93* | *0.05* |
| | | | R | 2.38 | 2.59 | 2.48 | 2.50 | 2.49 | *2.49* | *0.08* |
| | 150 | 0 | L | 3.01 | 3.11 | 3.05 | 3.17 | 3.29 | *3.13* | *0.11* |
| | | | R | 2.73 | 3.45 | 3.28 | 3.43 | 3.22 | *3.23* | *0.29* |
| | | 15 | L | 1.99 | 2.12 | 2.25 | 2.19 | 2.17 | *2.14* | *0.09* |
| | | | R | 2.63 | 2.65 | 2.40 | 2.60 | 2.64 | *2.58* | *0.10* |
| | 200 | 0 | L | 3.22 | 3.20 | 3.28 | 3.46 | 3.51 | *3.33* | *0.14* |
| | | | R | 2.65 | 3.13 | 3.04 | 3.13 | 3.10 | *3.01* | *0.21* |
| | | 15 | L | 1.78 | 1.75 | 1.89 | 1.86 | 2.07 | *1.87* | *0.12* |
| | | | R | 2.60 | 2.45 | 2.39 | 2.49 | 2.49 | *2.48* | *0.08* |

Note. Abbreviations follow the convention of Table E7(A).

B. Frontal Site

| TIME | TMS | POSI | SAC | 1 | 2 | 3 | 4 | 5 | mean | s.d. |
|---|---|---|---|---|---|---|---|---|---|---|
| peri | No TMS | 0 | L | 4.74 | 6.40 | 5.96 | 5.72 | 6.29 | *5.82* | *0.66* |
| | | | R | 3.68 | 4.16 | 4.35 | 4.55 | 4.40 | *4.23* | *0.34* |
| | | 15 | L | 1.24 | 2.30 | 2.40 | 2.05 | 2.73 | *2.14* | *0.56* |
| | | | R | 3.02 | 2.26 | 4.26 | 3.78 | 5.21 | *3.71* | *1.13* |
| | 100 | 0 | L | 7.10 | 7.91 | 7.42 | 7.07 | 7.27 | *7.35* | *0.34* |
| | | | R | 3.86 | 4.33 | 4.28 | 4.40 | 4.51 | *4.28* | *0.25* |
| | | 15 | L | 1.07 | 1.18 | 1.25 | 1.34 | 1.57 | *1.28* | *0.19* |
| | | | R | 2.10 | 2.02 | 3.37 | 2.52 | 3.44 | *2.69* | *0.68* |
| | 150 | 0 | L | 4.28 | 5.15 | 4.65 | 4.62 | 6.29 | *5.00* | *0.79* |
| | | | R | 4.82 | 5.29 | 5.19 | 5.22 | 5.06 | *5.12* | *0.19* |
| | | 15 | L | 1.56 | 1.54 | 1.88 | 1.83 | 2.02 | *1.76* | *0.21* |
| | | | R | 2.00 | 2.05 | 2.43 | 2.43 | 3.35 | *2.45* | *0.54* |
| | 200 | 0 | L | 4.71 | 5.73 | 5.41 | 5.08 | 5.77 | *5.34* | *0.45* |
| | | | R | 4.06 | 4.50 | 4.34 | 4.55 | 4.73 | *4.44* | *0.25* |
| | | 15 | L | 1.42 | 1.39 | 1.87 | 1.70 | 2.75 | *1.83* | *0.55* |
| | | | R | 2.30 | 2.23 | 3.59 | 3.20 | 3.66 | *3.00* | *0.69* |
| pre | No TMS | 0 | L | 2.96 | 3.25 | 3.14 | 3.38 | 4.04 | *3.35* | *0.41* |
| | | | R | 2.13 | 2.76 | 2.76 | 2.79 | 2.89 | *2.67* | *0.30* |
| | | 15 | L | 1.85 | 2.01 | 2.06 | 1.96 | 2.13 | *2.00* | *0.11* |
| | | | R | 2.53 | 2.54 | 2.38 | 2.45 | 2.60 | *2.50* | *0.09* |
| | 100 | 0 | L | 3.49 | 3.46 | 3.46 | 3.49 | 3.67 | *3.51* | *0.09* |
| | | | R | 2.22 | 2.86 | 2.60 | 2.88 | 3.03 | *2.72* | *0.32* |
| | | 15 | L | 1.89 | 1.87 | 2.00 | 1.96 | 1.95 | *1.93* | *0.05* |
| | | | R | 2.38 | 2.59 | 2.48 | 2.50 | 2.49 | *2.49* | *0.08* |
| | 150 | 0 | L | 3.01 | 3.11 | 3.05 | 3.17 | 3.29 | *3.13* | *0.11* |
| | | | R | 2.73 | 3.45 | 3.28 | 3.43 | 3.22 | *3.23* | *0.29* |
| | | 15 | L | 1.99 | 2.12 | 2.25 | 2.19 | 2.17 | *2.14* | *0.09* |
| | | | R | 2.63 | 2.65 | 2.40 | 2.60 | 2.64 | *2.58* | *0.10* |
| | 200 | 0 | L | 3.22 | 3.20 | 3.28 | 3.46 | 3.51 | *3.33* | *0.14* |
| | | | R | 2.65 | 3.13 | 3.04 | 3.13 | 3.10 | *3.01* | *0.21* |
| | | 15 | L | 1.78 | 1.75 | 1.89 | 1.86 | 2.07 | *1.87* | *0.12* |
| | | | R | 2.60 | 2.45 | 2.39 | 2.49 | 2.49 | *2.48* | *0.08* |

Note. Abbreviations follow the convention of Table E7(A).

**Table E9**. Mean Compression Index in Each Condition of Experiment 8 for Every Participant.

A. Parietal Site

| TMS | POSI | SUBJ / SAC | 1 | 2 | 3 | 4 | 5 | mean | s.d. |
|---|---|---|---|---|---|---|---|---|---|
| No TMS | 0 | L | 0.51 | 0.40 | 0.32 | 0.25 | 0.21 | *0.34* | *0.12* |
| | | R | 0.10 | 0.12 | 0.18 | 0.20 | 0.14 | *0.15* | *0.04* |
| | 15 | L | 0.81 | 0.83 | 0.85 | 0.74 | 0.77 | *0.80* | *0.04* |
| | | R | 0.89 | 0.93 | 0.87 | 0.99 | 0.90 | *0.92* | *0.05* |
| 100 | 0 | L | 0.33 | 0.51 | 0.39 | 0.38 | 0.38 | *0.40* | *0.07* |
| | | R | 0.23 | 0.25 | 0.37 | 0.35 | 0.32 | *0.31* | *0.06* |
| | 15 | L | 0.75 | 0.86 | 0.89 | 0.81 | 0.79 | *0.82* | *0.06* |
| | | R | 0.98 | 0.73 | 0.77 | 0.75 | 0.88 | *0.82* | *0.10* |
| 150 | 0 | L | 0.51 | 0.41 | 0.43 | 0.35 | 0.34 | *0.41* | *0.07* |
| | | R | 0.07 | 0.31 | 0.37 | 0.34 | 0.28 | *0.27* | *0.12* |
| | 15 | L | 0.73 | 0.73 | 0.80 | 0.72 | 0.73 | *0.74* | *0.03* |
| | | R | 0.89 | 0.96 | 0.96 | 0.85 | 0.98 | *0.93* | *0.06* |
| 200 | 0 | L | 0.43 | 0.39 | 0.37 | 0.27 | 0.29 | *0.35* | *0.07* |
| | | R | -0.09 | -0.03 | 0.15 | 0.19 | 0.14 | *0.07* | *0.12* |
| | 15 | L | 0.72 | 0.69 | 0.69 | 0.70 | 0.71 | *0.70* | *0.01* |
| | | R | 1.00 | 0.90 | 0.99 | 0.90 | 0.98 | *0.95* | *0.05* |

B. Frontal Site

| TMS | POSI | SUBJ / SAC | 1 | 2 | 3 | 4 | 5 | mean | s.d. |
|---|---|---|---|---|---|---|---|---|---|
| No TMS | 0 | L | 0.64 | 0.80 | 0.56 | 0.53 | 0.40 | 0.59 | 0.15 |
| | | R | 0.05 | 0.12 | 0.25 | 0.30 | 0.25 | 0.19 | 0.10 |
| | 15 | L | 0.79 | 0.84 | 1.00 | 0.91 | 0.96 | 0.90 | 0.08 |
| | | R | -0.43 | 0.88 | 0.89 | 0.92 | 0.81 | 0.61 | 0.59 |
| 100 | 0 | L | 0.78 | 0.94 | 0.75 | 0.67 | 0.55 | 0.74 | 0.15 |
| | | R | 0.06 | 0.13 | 0.32 | 0.38 | 0.30 | 0.24 | 0.14 |
| | 15 | L | 0.82 | 0.74 | 0.81 | 0.75 | 0.73 | 0.77 | 0.04 |
| | | R | -2.72 | 0.84 | 0.82 | 0.93 | 0.93 | 0.16 | 1.61 |
| 150 | 0 | L | 0.68 | 0.67 | 0.56 | 0.51 | 0.55 | 0.59 | 0.08 |
| | | R | 0.24 | 0.24 | 0.31 | 0.39 | 0.29 | 0.30 | 0.06 |
| | 15 | L | 0.75 | 0.72 | 0.80 | 0.67 | 0.68 | 0.72 | 0.05 |
| | | R | -1.25 | 0.76 | 0.87 | 0.98 | 0.68 | 0.41 | 0.93 |
| 200 | 0 | L | 0.77 | 0.72 | 0.53 | 0.49 | 0.44 | 0.59 | 0.15 |
| | | R | -0.03 | 0.12 | 0.23 | 0.25 | 0.12 | 0.14 | 0.11 |
| | 15 | L | 0.89 | 0.83 | 0.98 | 0.88 | 0.95 | 0.91 | 0.06 |
| | | R | -1.76 | 0.83 | 0.64 | 0.83 | 0.76 | 0.26 | 1.13 |

Note. See Appendix B for the definition of the compression index.